NASA TECHNICAL NOTE

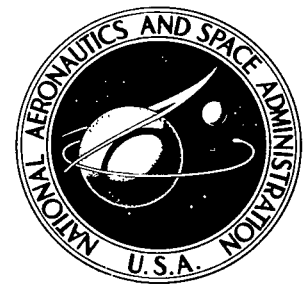

NASA TN D-6684

NASA TN D-6684

AIR-SEA INTERACTION IN THE TROPICAL PACIFIC OCEAN

by Lewis J. Allison, Joseph Steranka, Robert J. Holub, John Hansen, Fredric A. Godshall, and Cuddapah Prabhakara

Goddard Space Flight Center
Greenbelt, Md. 20771

NATIONAL AERONAUTICS AND SPACE ADMINISTRATION • WASHINGTON, D. C. • MAY 1972

1. Report No.	2. Government Accession No.	3. Recipient's Catalog No.
NASA TN D-6684		

4. Title and Subtitle

Air-Sea Interaction in the Tropical Pacific Ocean

5. Report Date: May 1972

6. Performing Organization Code

7. Author(s): Lewis J. Allison, Joseph Steranka, Robert J. Holub, John Hansen, Fredric A. Godshall, Cuddapah Prabhakara

8. Performing Organization Report No.: G-1042

9. Performing Organization Name and Address

Goddard Space Flight Center
Greenbelt, Maryland 20771

10. Work Unit No.

11. Contract or Grant No.

12. Sponsoring Agency Name and Address

National Aeronautics and Space Administration
Washington, D.C. 20546

13. Type of Report and Period Covered: Technical Note

14. Sponsoring Agency Code

15. Supplementary Notes

16. Abstract

Charts of 3-month sea surface temperature (SST) anomalies in the eastern tropical Pacific Ocean were produced for the period 1949 to 1970. The anomalies along the United States and South American west coasts and in the eastern tropical Pacific appeared to be oscillating in phase during this period. Similarly, the satellite-derived cloudiness for each of four quadrants of the Pacific Ocean (130°E to 100°W, 30°N to 25°S) appeared to be oscillating in phase. In addition, a global tropical cloudiness oscillation from 30°N to 30°S was noted from 1965 to 1970, by using J. C. Sadler's monthly satellite television nephanalyses.

The SST anomalies were found to have a good degree of correlation both positive and negative with the following monthly geophysical parameters: (1) satellite-derived cloudiness, (2) strength of the North and South Pacific semipermanent anticyclones, (3) tropical Pacific island rainfall, and (4) Darwin surface pressure. Several strong direct local and crossequatorial relationships were noted. In particular, the high degree of correlation between the tropical island rainfall and the SST anomalies ($r = +0.93$) permitted the derivation of SST's for the tropical Pacific back to 1905. The close occurrence of cold tropical SST and North Pacific 700-mb positive height anomalies with central United States drought conditions was noted.

17. Key Words (Selected by Author(s))
Satellite-Derived Cloudiness
Tropical Pacific Rainfall
Pacific Sea Surface Temperatures
Pacific Air-Sea Interaction
Pacific 700-mb Height Anomalies

18. Distribution Statement: Unclassified-Unlimited

19. Security Classif. (of this report)	20. Security Classif. (of this page)	21. No. of Pages	22. Price
Unclassified	Unclassified	84	$3.00

*For sale by the National Technical Information Service, Springfield, Virginia 22151

CONTENTS

AIR-SEA INTERACTION IN THE TROPICAL PACIFIC OCEAN

by

Lewis J. Allison and Joseph Steranka
Goddard Space Flight Center

Robert Holub, Capt., and John Hansen, Lt. Col.
Air Weather Service
USAF Environmental Technical Applications Center

Fredric A. Godshall
Environmental Data Service
National Oceanic and Atmospheric Administration

and

Cuddapah Prabhakara
Goddard Space Flight Center

INTRODUCTION

An understanding of the interaction of the tropical oceans with the atmosphere is important for the solution of problems concerning the varied time-period changes in the oceans and atmosphere. (Zipser, 1969; U.S. Committee for the GARP, 1969; Rasool and Hogan, 1969). Large-scale oceanographic processes over the tropical Pacific Ocean have been described by eminent researchers (Bjerknes, 1961, 1966a, 1966b, and 1969; Bjerknes et al., 1969; Berlage, 1966; Wyrtki, 1966; Roden and Reid, 1961; Roden, 1962 and 1965; Shell, 1965). These climatological and analytical studies were made in the last decade when there was a shortage of basic oceanographic data over large areas of the Pacific Ocean. Research efforts conducted during the 1960 STEP-I Expedition (Wooster, 1961b), the 1963 to 1965 Trade Wind Zone Oceanography Pilot Study (Seckel, 1970), and the 1967 to 1968 EASTROPAC cruises (U.S. Department of Commerce, 1970a) are relatively recent attempts to fill this serious data gap.

Bjerknes (1969) described the relationship between the increased monthly Canton Island rainfall and the presence of local warm sea surface temperatures (SST's) and suggested that the strong interannual variability of SST's and rainfall observed at Canton Island could be applied to the eastern tropical Pacific Ocean. On the other hand, Krueger and Gray (1969) analyzed 5 years (1962 to

1967) of winter (December to February) SST's over the eastern tropical Pacific. They found decreased tropical cloudiness in the winter of 1966 through the use of satellite data in the presence of anomalously warm SST's. Widespread tropospheric subsidence was suggested as the cause for this suppressed cloudiness. In order to gain a comprehensive insight into these complex air-sea interactions, we will examine long-term variations of satellite-derived tropical cloudiness, SST's, tropical Pacific island rainfall, and also the strength of the semipermanent anticyclones in the northern and southern Pacific Ocean between latitudes 30°N and 40°N and 30°S and 40°S, respectively.

OCEAN-ATMOSPHERE INTERACTION CONSIDERATIONS

The ultimate source of the energy that drives the atmosphere and the oceans is the differential heating of the earth's surface by the sun. The immense amount of heat capacity of the oceans, which constitute about 70 percent of the earth's surface, acts as a huge flywheel for this coupled system. In general, the movement of the major Pacific Ocean current systems [Figure 1 (U.S. Navy, 1966)] are caused by the wind stress on the water, the downslope movement of low-density water (which is dynamically higher than high-density water), the blockage of the currents by land masses, and the earth's rotation (Svedrup, 1947; Malkus, 1962; U.S. Navy, 1962; Stewart, 1969). Since the large North Pacific anticyclone is the major pressure source driving the surface currents in the northeastern temperate and tropical Pacific Ocean, the region 30°N to 40°N, 180° to 130°W was selected for analysis. This area encompasses the range of movement of the anticyclone's central pressure during its yearly trek north and south in synchronization with the sun's seasonal migration. Table 1 (Crutcher and Meserve, 1970) lists the monthly long-term mean central position of the North Pacific anticyclone. Roden and Reid (1961) had noted the importance of the strength of the Aleutian Low in the winter months and its close relation to oceanic SST anomalies. However, for this study, only the climatological variation of the North Pacific High will be examined.

Table 1—Monthly long-term mean central position of the North Pacific anticyclone.

Month	Mean Position	
January	30°N	138°W
February	31°N	137°W
March	35°N	150°W
April	34°N	165°W
May	33°N	155°W
June	33°N	146°W
July	38°N	149°W
August	39°N	151°W
September	34°N	155°W
October	33°N	141°W
November	31°N	136°W
December	30°N	139°W

The sea-level pressure (SLP) and the 700-mb heights over the North Pacific High were collected for the period 1949 to 1970. The monthly surface pressure data from 5° latitude-longitude intersections were obtained from microfilmed Northern Hemisphere surface maps provided by the National Climatic Center, National Oceanic and Atmospheric Administration (NOAA), Asheville, North Carolina. The monthly mean 700-mb height anomalies at the same intersections were obtained from the *Monthly Weather Review* (U.S. Weather Bureau, 1949 to 1970). Figure 2 shows the close pattern similarity between these two levels from 12-month running means during the 22-year period ($r = +0.80$, with zero lag). The symbol r will be used in the paper to represent the correlation coefficient.

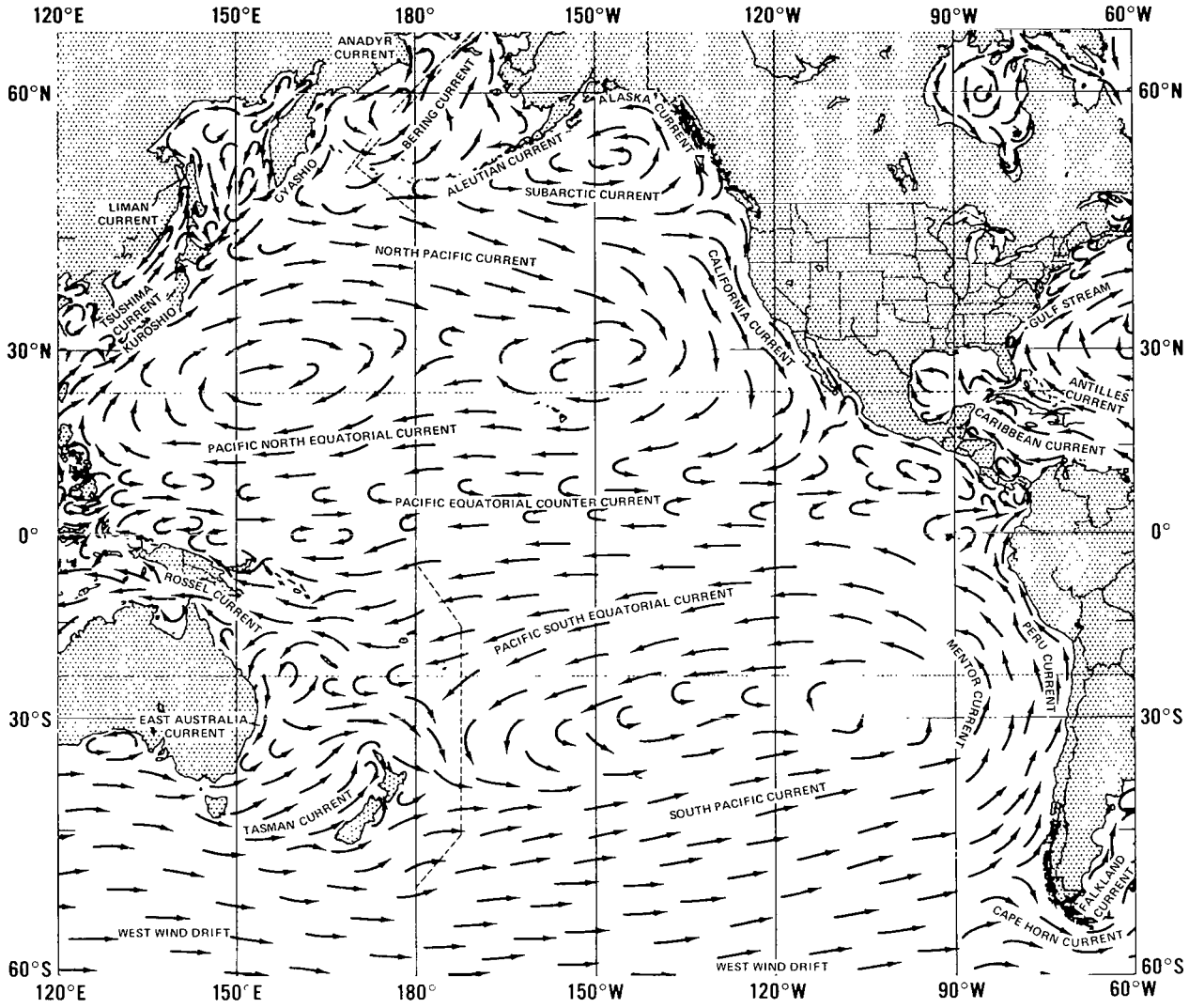

Figure 1—Surface currents of the Pacific Ocean during July (U.S. Navy, 1966).

Roden and Reid (1961) and Reid et al. (1958) had noted that the upwelling and cold-water advection in the California Current (Figure 1) was coupled with the northerly winds, which for the most part are driven by the North Pacific High. In addition, an areal coherence of monthly SST anomalies of the same sign and approximate amplitude occurred almost simultaneously from 40°N to 20°N in the California Current. In order to allow analysis of a longer series of data, monthly SST's were obtained from U.S. Coast and Geodetic Survey records from 1925 to 1970 for the piers and recording sites along the west coast (Figure 3). Long-term means and monthly anomalies were assembled from these data. A single monthly average of all coastal SST anomalies was then made, and 12-month running means were plotted (Figure 4a). Both the monthly surface pressure and the 700-mb height anomalies yielded r of only −0.68, with +6- to +8-month lead time with these coastal SST's (i.e., increases in 700-mb heights preceded the corresponding decreases in SST's by 6 to 8

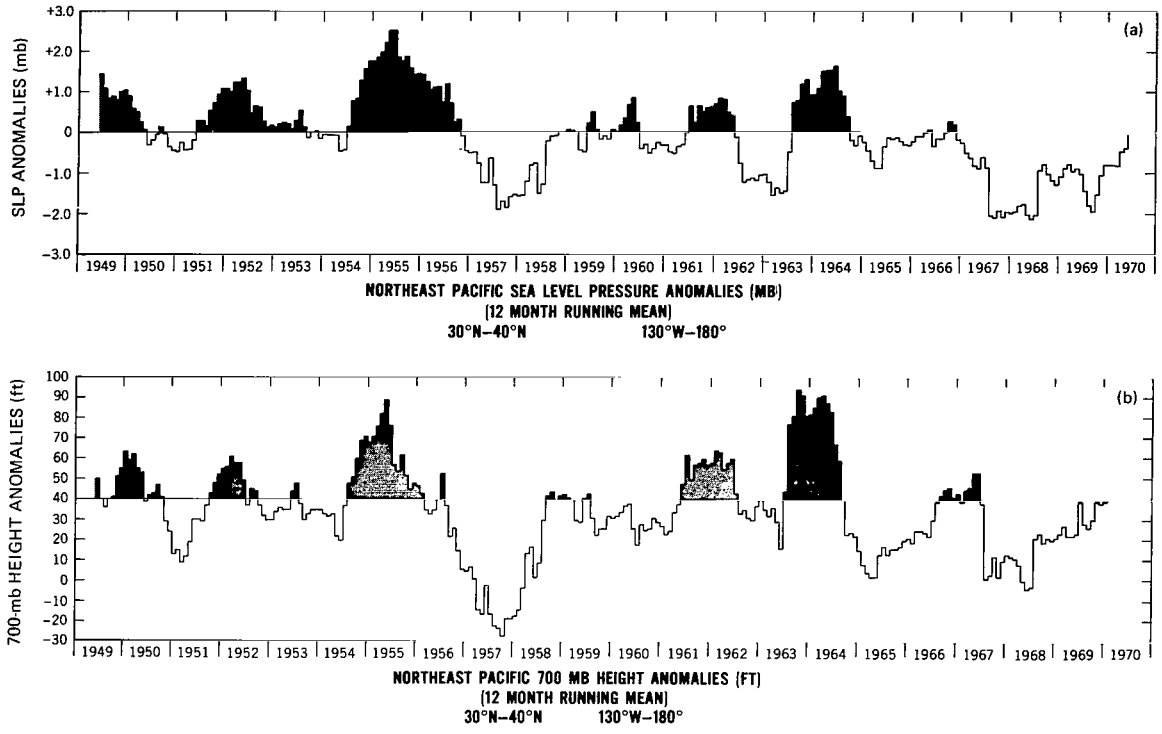

Figure 2—(a) Northeast Pacific (30°N to 40°N, 130°W to 180°) SLP anomalies, 12-month running mean; (b) Northeast Pacific (30°N to 40°N, 130°W to 180°) 700-mb height anomalies, 12-month running mean.

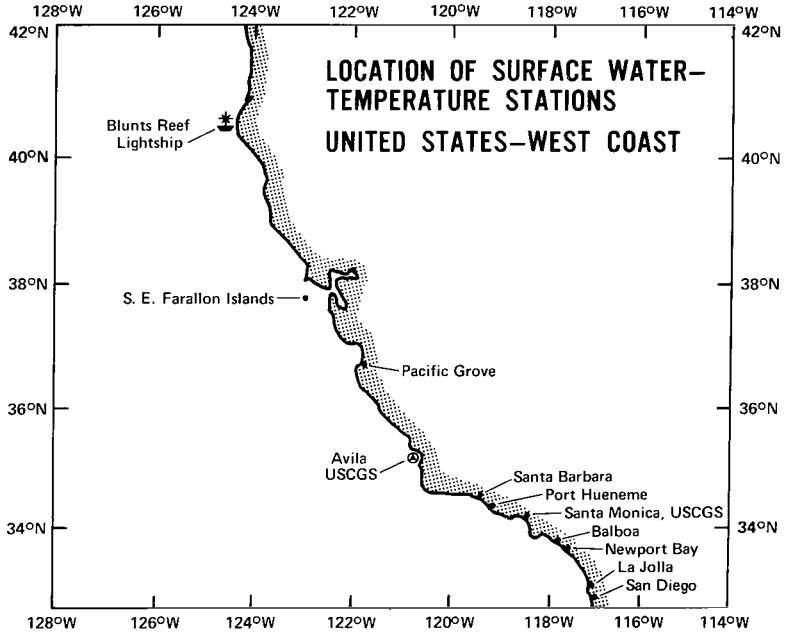

Figure 3—Location of surface water temperature stations along the United States west coast.

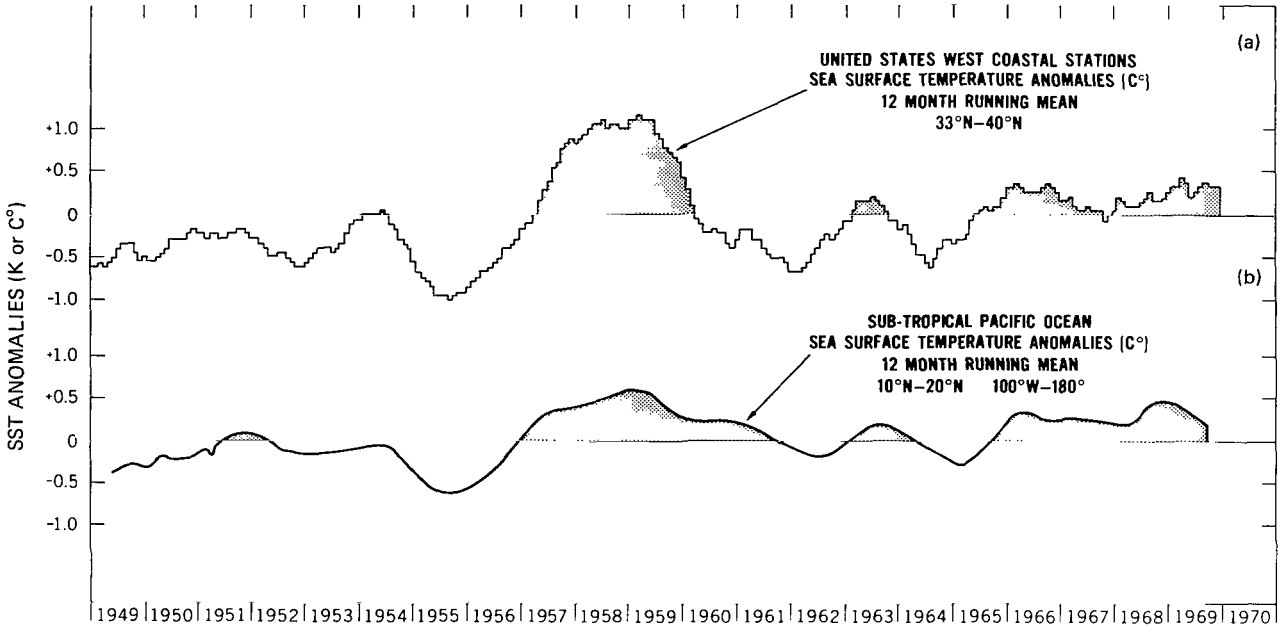

Figure 4—(a) United States west coast station (33°N to 40°N) SST anomalies, 12-month running mean; (b) tropical Pacific Ocean (10°N to 20°N, 100°W to 180°) SST anomalies, 12-month running mean.

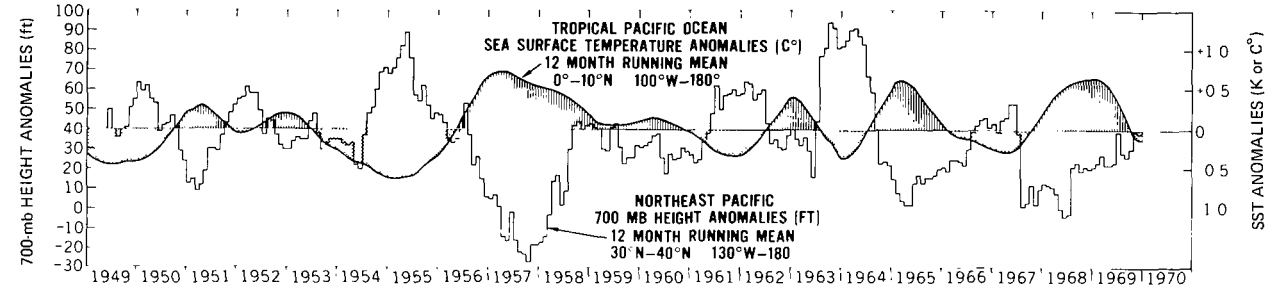

Figure 5—A comparison of 12-month running means of Northeast Pacific (30°N to 40°N, 130°W to 180°) 700-mb height anomalies and tropical Pacific (0° to 10°N, 100°W to 180°) SST anomalies. The SST plot is lagged −6 months on this graph.

months). The plot (Figure 4b) of the 12-monthly mean of the 10°N to 20°N, 100°W to 180° SST anomalies over the extension of the California Current (Figure 1) showed a close correlation, as was expected, with the United States west coast data (r = +0.87, with −1-month lag). The source of the tropical ocean data will be described later.

A comparison was made of the Northeast Pacific 700-mb height anomalies and the SST anomalies from 30°N to 10°S and from 180° to the continental shorelines, and surprisingly good relations [r = −0.70 to −0.74, with +5 to +9-month lead (i.e., increases in 700-mb heights preceded the corresponding decreases in SST's by 5 to 9 months)] were noted. Figure 5 shows this comparison, with the 0°N to 10°N SST anomalies slipped 6 months in time. High pressure was related to cool SST anomalies and low pressure to warm SST anomalies. A more complete discussion of these statistical results will be made later.

A similar analysis was made for the Southern Hemisphere in order to obtain the long-term variation of the Peru Current, a northward-flowing current along the west coast of South America (Figure 1). Historical monthly SST data were obtained from U.S. Coast and Geodetic Survey records from 1950 to 1967 for the South American west coast stations shown in Figure 6. A monthly average of all station SST anomalies was made, and is shown in Figure 7a. Figure 7b shows the 12-month running means of these anomalies and confirms the close coupling ($r = +0.90$, with +1-month lead) that should exist between the Peru Current and its extension from 0° to 10°S, 80°W to 180° (Figure 1) (Wyrtki, 1965).

Because of the sparsity of South Pacific SLP and 700-mb data, the long period of SLP records for Juan Fernandez Island was utilized to investigate the South Pacific anticyclone. The data for Juan Fernandez Island (34°S, 80°W) are not completely representative of the South Pacific High during June to August, a period when the area is affected by disturbances in the extratropical westerlies (Bjerknes, 1966b). Table 2 lists the monthly long-term mean central position of the South Pacific High (Taljaard et al., 1969).

Figure 8 shows the agreement between the SST data for the extension of the Peru Current 0° to 10°S, 180° to 100°W and the Juan Fernandez Island SLP data ($r = -0.63$, with −2-month lag). Note the drop in Juan Fernandez Island surface pressure, which relates the abnormal weakening in the trade-wind circulation and the resultant anomalous SST warming during 1951, 1953, 1957 to 1961, 1963, 1965, and 1968 to 1969. The work of Bjerknes (1961) and Wooster (1961a) tends to support this interpre-

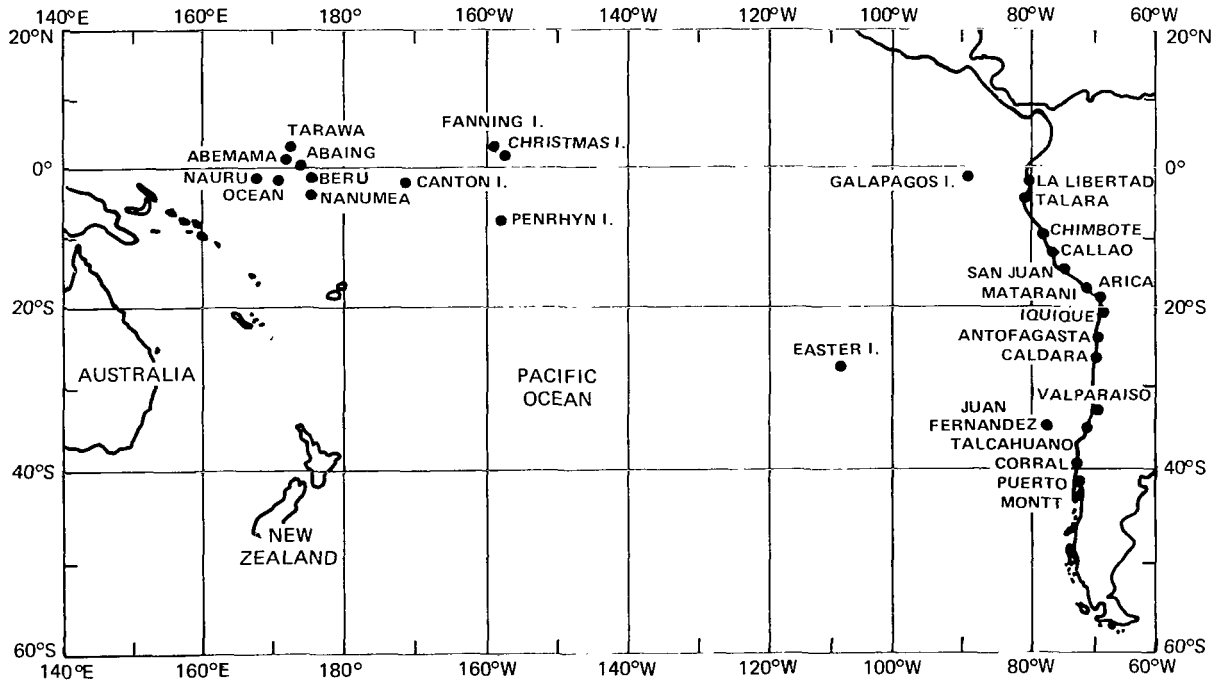

Figure 6—Location of South American west coast SST recording stations and the tropical Pacific island rainfall recording network.

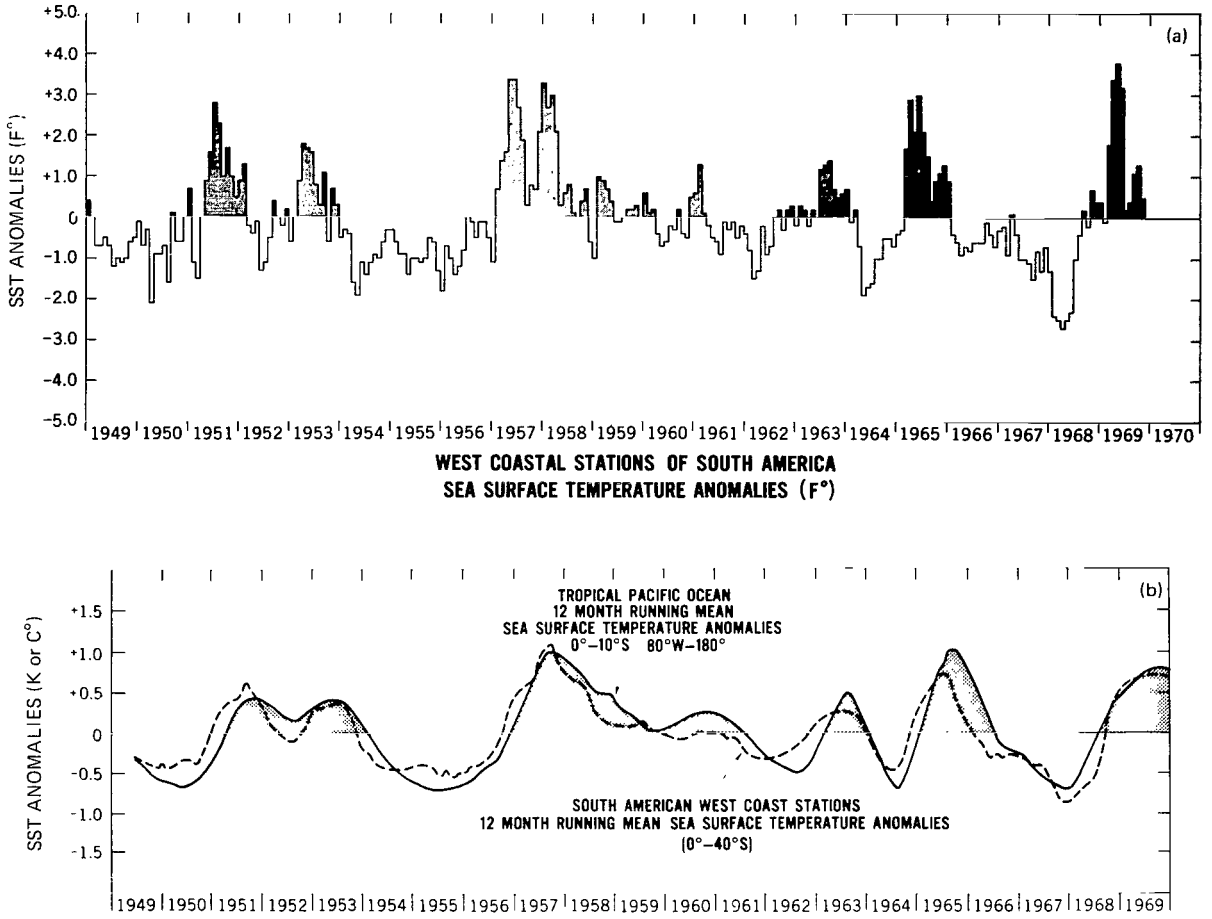

Figure 7—(a) South American west coast station (0° to 40°S) SST anomalies (monthly mean); (b) a comparison of 12-month running means of South American west coast station (0° to 40°S) and tropical Pacific Ocean (0° to 10°S, 80°W to 180°) SST anomalies.

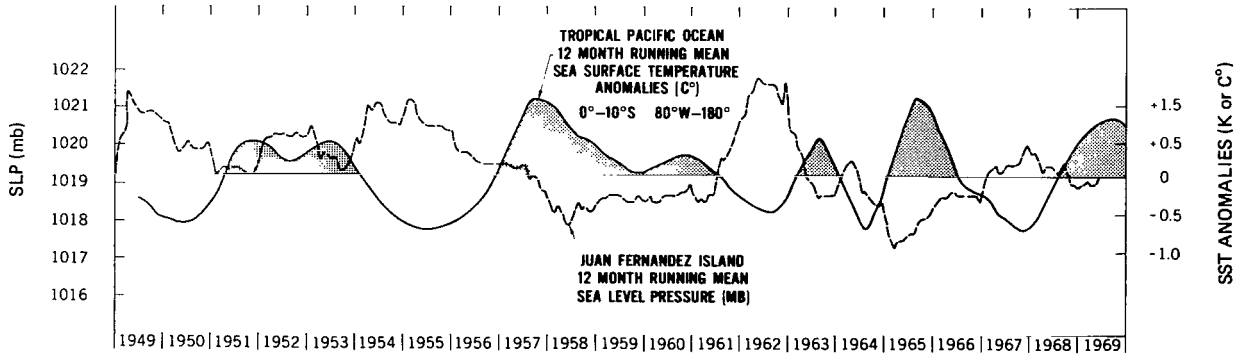

Figure 8—A comparison of 12-month running means of tropical Pacific Ocean (0° to 10°S, 80°W to 180°) SST anomalies and Juan Fernandez Island SLP.

Table 2—Monthly long-term mean central position of the South Pacific High.

Month	Mean Position	
January	31°S	89°W
February	31°S	90°W
March	30°S	90°W
April	30°S	88°W
May	27°S	85°W
June	25°S	90°W
July	26°S	90°W
August	27°S	88°W
September	28°S	89°W
October	29°S	88°W
November	30°S	89°W
December	30°S	89°W

tation between the strength of the trade winds and equatorial upwelling in the central tropical Pacific Ocean. Berlage (1966) noted that SLP differences between Juan Fernandez Island and Santiago appear to relate more completely to changes in the Peru Current. This premise will be tested in a later study.

SATELLITE-DERIVED CLOUDINESS AND SEA SURFACE TEMPERATURE DATA

With the launching of the TIROS, ESSA, Nimbus, ITOS, and ATS meteorological satellites in the last decade, it is now possible to view tropical cloudiness on a day-to-day, weekly, monthly, seasonal, and yearly basis over vast oceanic regions of the world* ** (Atkinson and Sadler, 1970; Leese et al., 1970; Miller, 1971; U.S. Department of Commerce, 1970b; Allison et al., 1969; Allison, 1971; Bjerknes et al., 1969; Sadler, 1968; Sherr et al., 1968; Taylor et al., 1968; Wallace, 1970; Anderson et al., 1969; Suomi and Vonder Haar, 1970).

Only recently has the time span of satellite data become extensive enough to allow satisfactory viewing of the longer-term variations in cloud amounts over the tropical Pacific Ocean. Figure 9 shows the monthly variation in cloud cover (in percent of area covered by $\geq 6/10$ cloudiness) derived from satellite television analyses over the eastern tropical Pacific from 0° to 30°N, 180° to 100°W from August 1962 to October 1970 (only the January, April, August, and October monthly cloudiness amounts were computed). Examples of monthly cloudiness minimum and maximum periods, April

*V. V. Salomonson, "Cloud Statistics in Earth Resources Technology Satellite (ERTS) Mission Planning", GSFC Document X-622-69-386. August 1969.

**J. Kornfield and A. Hasler, "Photographic Cloud Averages", *Weather Motions From Space,* University of Wisconsin, Madison, Wisconsin, in press.

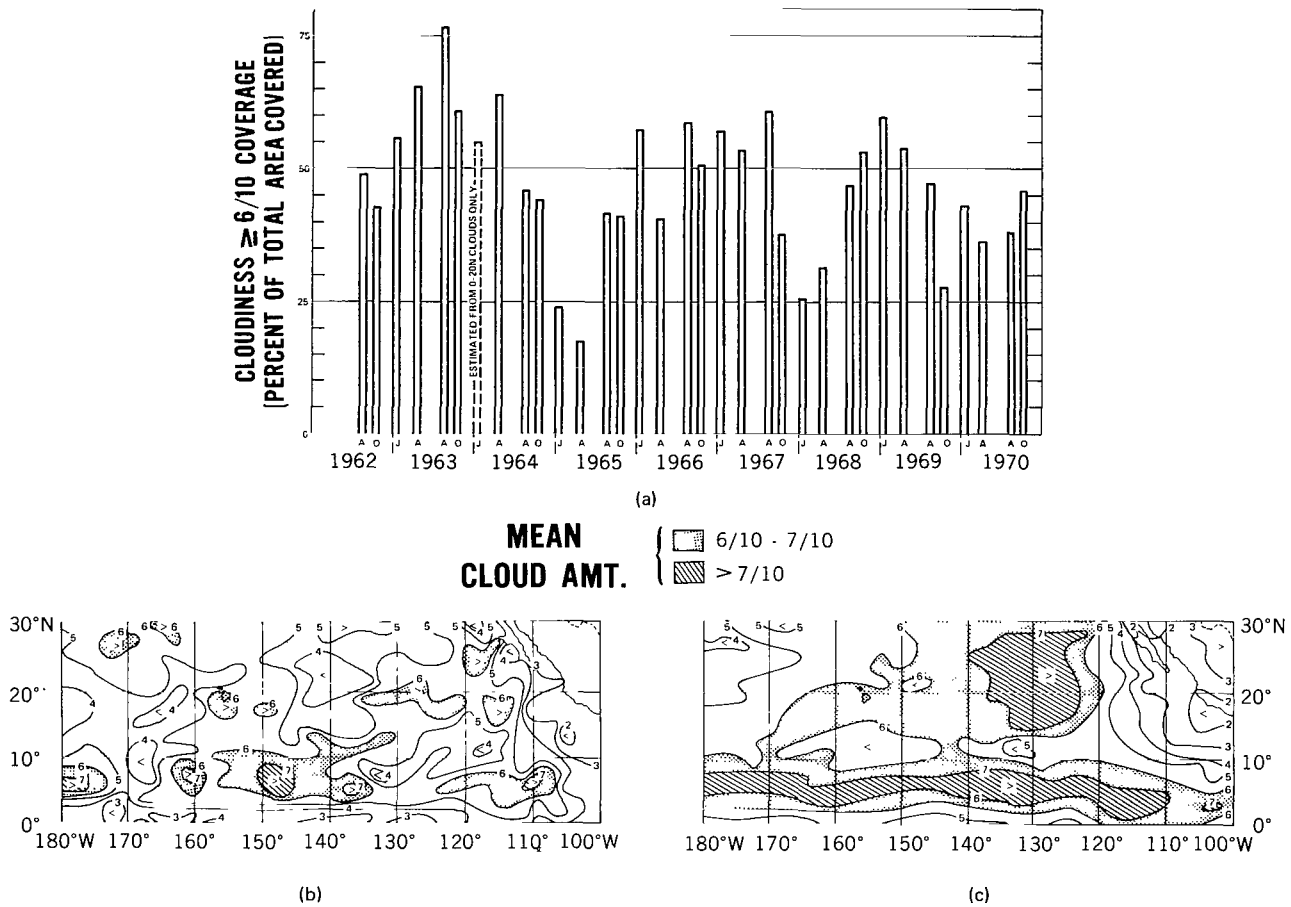

Figure 9—(a) A histogram of satellite-derived cloudiness (percent of area covered by $\geq$ 6/10 cloudiness) from 0° to 30°N, 100°W to 180°, from 1962 to 1970; (b) mean cloud amount (in tenths) derived from TIROS 9 nephanalysis, April 1965; (c) mean cloud amount (in tenths) derived from ESSA 7 and 9 nephanalysis, April 1969.

1965 and 1969, respectively, are shown in parts (b) and (c) of this figure. These cloudiness amounts were derived from daily television nephanalyses, which were produced by the National Environmental Satellite Service of NOAA. The daily charts were composited from TIROS, ESSA, and ITOS television data for four to five orbits. Cloud amounts, in tenths, were weighted and hand plotted in 2° latitude-longitude squares and averaged to produce monthly cloud values (Godshall, 1968; Godshall et al., 1969).

In order to determine the relationship that could exist between tropical cloudiness and SST's, it was decided to study the monthly SST data for the tropical Pacific Ocean, published by the renamed National Marine Fisheries Services, NOAA (Renner, 1962 to 1970). Since ship SST data were sparse in the tropical ocean, 3-month means of the data were produced with the technique described by Krueger and Gray (1969). Long-term means, obtained from the U.S. Naval Oceanographic Office (1969) were used for the anomaly data base at the center of the 5° latitude-longitude squares from 20°N to 10°S,

180° to 80°W. Charts showing these 3-month SST anomalies (in K) from 1962 to 1970 are given in Appendix A. The area covered by a positive SST anomaly was planimetered and weighted by the mean SST anomaly for each latitude band. Histograms of the monthly cloud cover and 3-month SST variations are given in Appendix B.

In order to extend our SST data base back prior to 1962, an atlas of monthly SST's (Eber et al., 1968) was processed by the technique described previously and reduced to 3-month SST anomalies for the period 1949 to 1962. A complete atlas of these anomaly charts is given in Appendix A.

Figures 10 and 11, which summarize the results of this atlas, show the seasonal SST anomalies from 1949 to 1970 for 10°N to 20°N, 0° to 10°N, 0° to 10°S, 5°N to 15°N, and 5°N to 5°S obtained from all available data. The 5°N to 15°N band covers the Intertropical Zone of Convergence, the Equatorial Counter Current, and the California Current extension, and the 5°N to 5°S band covers the Peru Current extension (Wyrtki, 1965). Note the warm periods for the regions within 20°N and 10°S: 1951, 1953, 1957 to 59, 1960 to 61, 1963, 1965, 1968 to 69. Note also the gross similarity with the yearly SST anomaly for the 20°N to 30°N band across the entire Pacific Ocean (Namias, 1970). Figures 12 and 13 show the percent of area covered by a positive anomaly for regions within 20°N and 10°S. A good relationship was noted between these two types of SST analyses (i.e., Figures 10 through 13).

In previous studies, Bjerknes (1966a, 1969, and 1970) had noted the importance of the Canton Island SST's: They should relate strongly to the eastern tropical Pacific Ocean circulation. Figure 14 confirms the fact that Canton Island SST anomalies are in good agreement with and very representative of the SST features of the eastern half of the South Equatorial Current (5°N to 5°S, 80°W to 180°). In addition, the island rainfall and SST relationship previously reported by Bjerknes (1969) also show good qualitative agreement with the 5°N to 5°S SST anomalies (Figure 15). Conventional monthly surface cloud amounts observed at Canton Island (Figure 15) and satellite-derived monthly cloudiness (Figure 16) over the tropical Pacific islands (170°E to 160°W) also show a fair relationship with the 5°N to 5°S SST anomalies; i.e., heavier cloud cover and rainfall generally occur with warmer SST's.

In order to study the apparent oscillations in the general atmospheric circulation shown by changes in cloud cover in periods prior to 1962, monthly rainfall data were analyzed for eleven Central Pacific islands (Quinn and Burt, 1970). These rainfall data, which were studied statistically by Doberitz (1968a and 1968b) for the islands located in Figure 6, had shown a definite coherence in periodicity. Apparently, the rainfall over the tropical Pacific islands responded to the SST pulsations in the South Equatorial Current during their long period of record. Twelve-month running means were made from all coincident monthly averaged rainfall records from 1949 to 1970. A strong pattern similarity (Figure 17) was noted between the tropical island rainfall and SST anomalies for 5°N to 5°S, 180° to 80°W. The results of a statistical comparison of these two parameters for six oceanographic regions are shown in Table 3. The high correlation coefficients (> +0.90) show that the variation in SST is an excellent indication of tropical rainfall and cloudiness. In the 5°N to 5°S region, for example, increases in rainfall followed the corresponding increases in SST by 1 month.*

*P. R. Rowntree, "The Influence of Tropical East Pacific Ocean Temperatures on the Atmosphere", Meteorological Office, Bracknell, United Kingdom, unpublished article, April 1971.

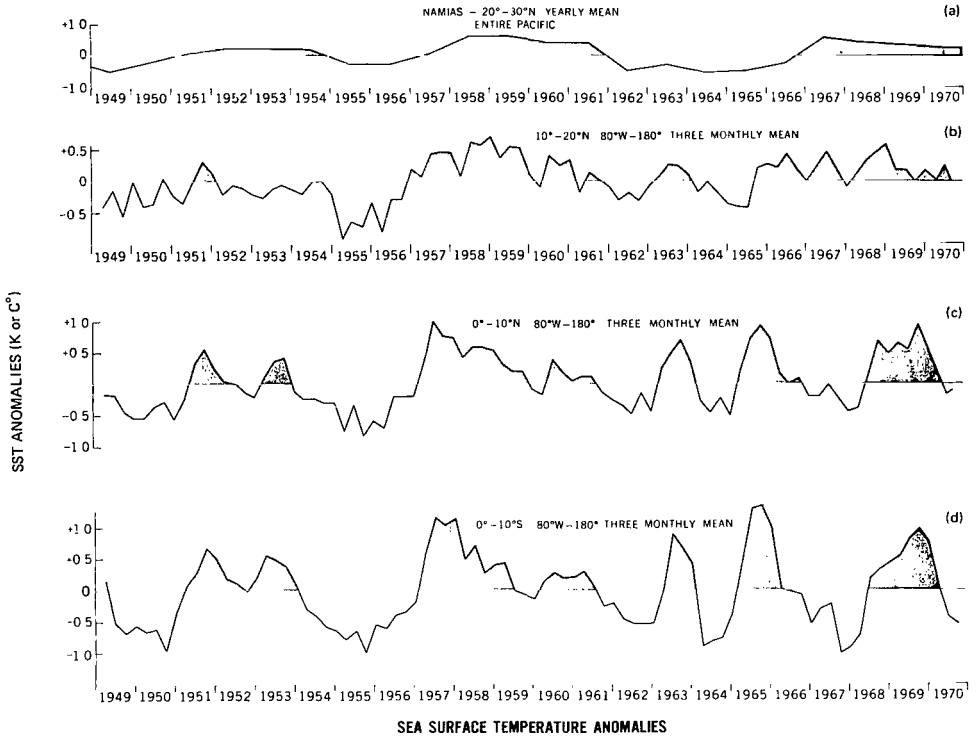

Figure 10—SST anomalies from 1949 to 1970: (a) 20°N to 30°N, entire Pacific yearly mean (Namias, 1970); (b) 10°N to 20°N, 80°W to 180°, 3-month mean; (c) 0° to 10°N, 80°W to 180°, 3-month mean; (d) 0°N to 10°S, 80°W to 180°, 3-month mean.

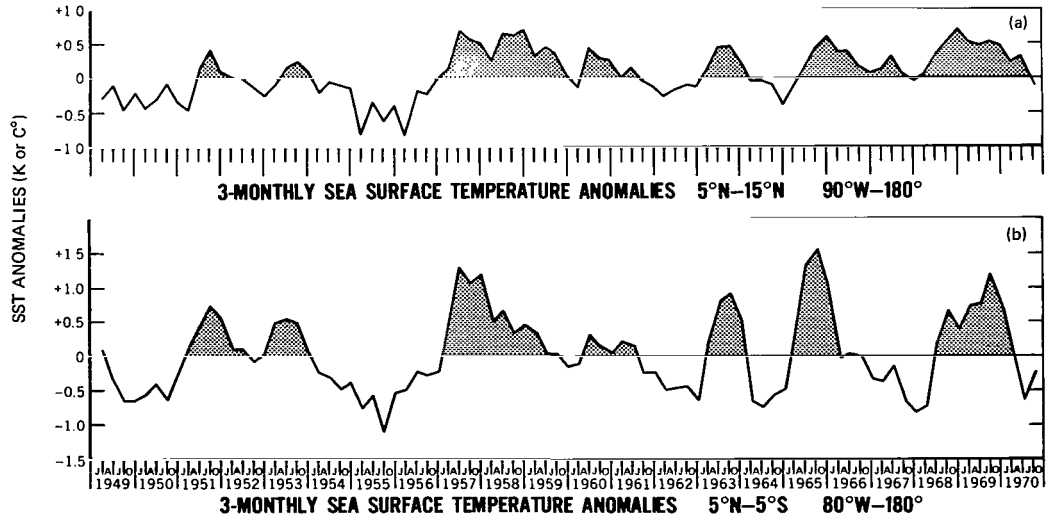

Figure 11—SST anomalies: (a) 5°N to 15°N, 90°W to 180°, and (b) 5°N to 5°S, 80°W to 180°, 3-month mean from 1949 to 1970.

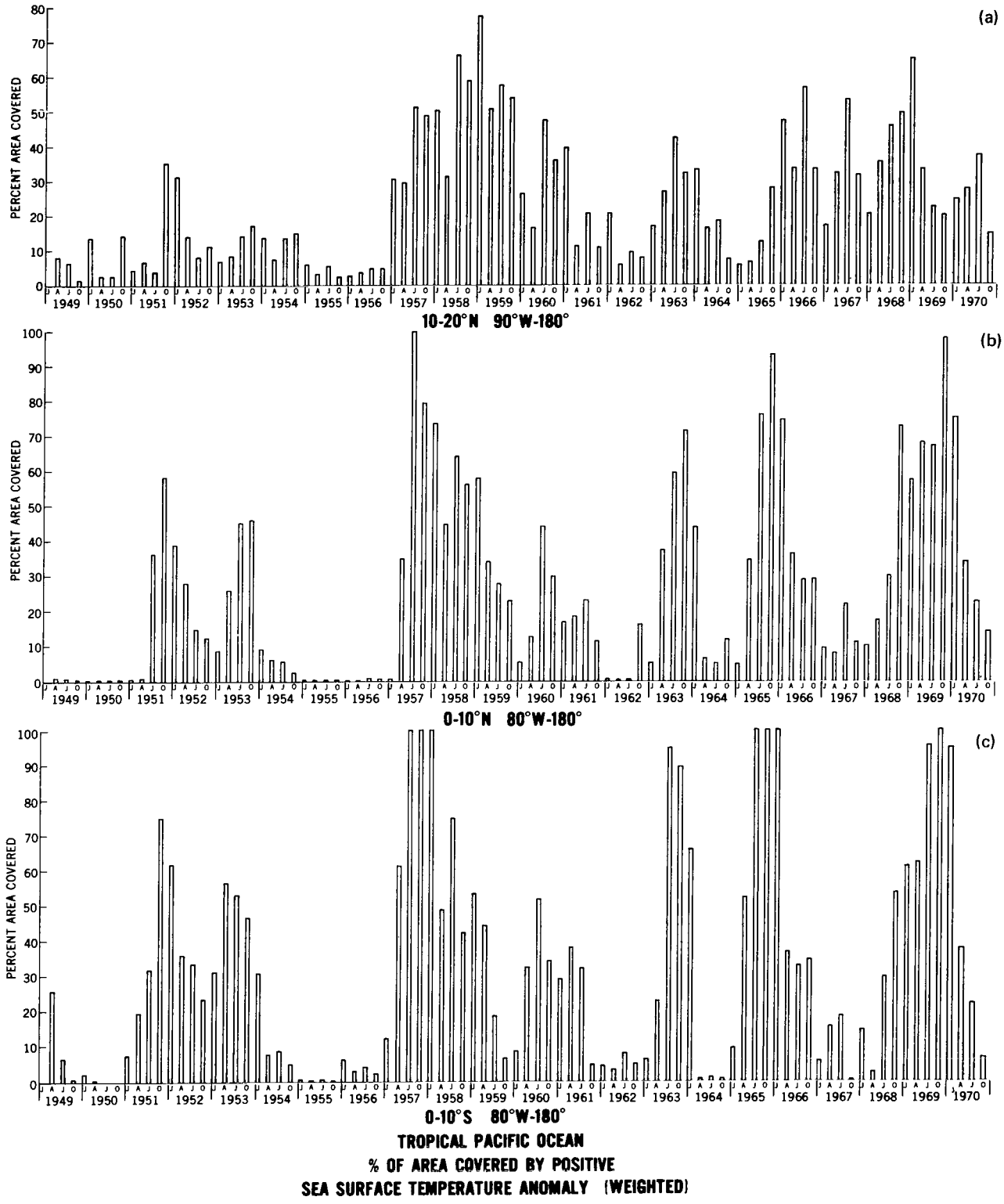

Figure 12—Tropical Pacific Ocean: percent of area covered by a positive SST anomaly (weighted) for (a) 10°N to 20°N, 90°W to 180°; (b) 0° to 10°N, 80°W to 180°; and (c) 0° to 10°S, 80°W to 180°.

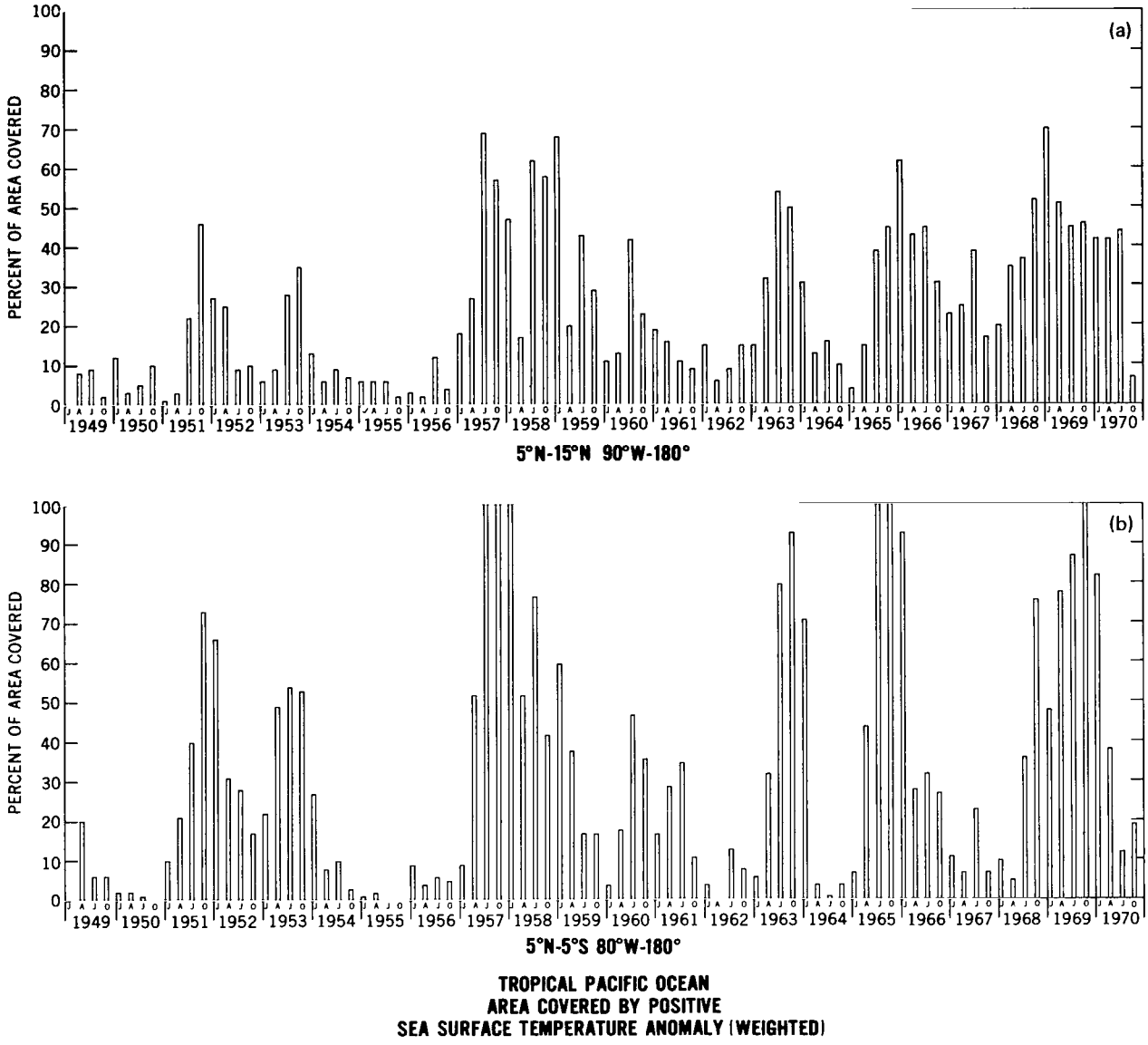

Figure 13—Tropical Pacific: percent of area covered by a positive SST anomaly (weighted) for (a) 5°N to 15°N, 90°W to 180°, and (b) 5°N to 5°S, 80°W to 180°.

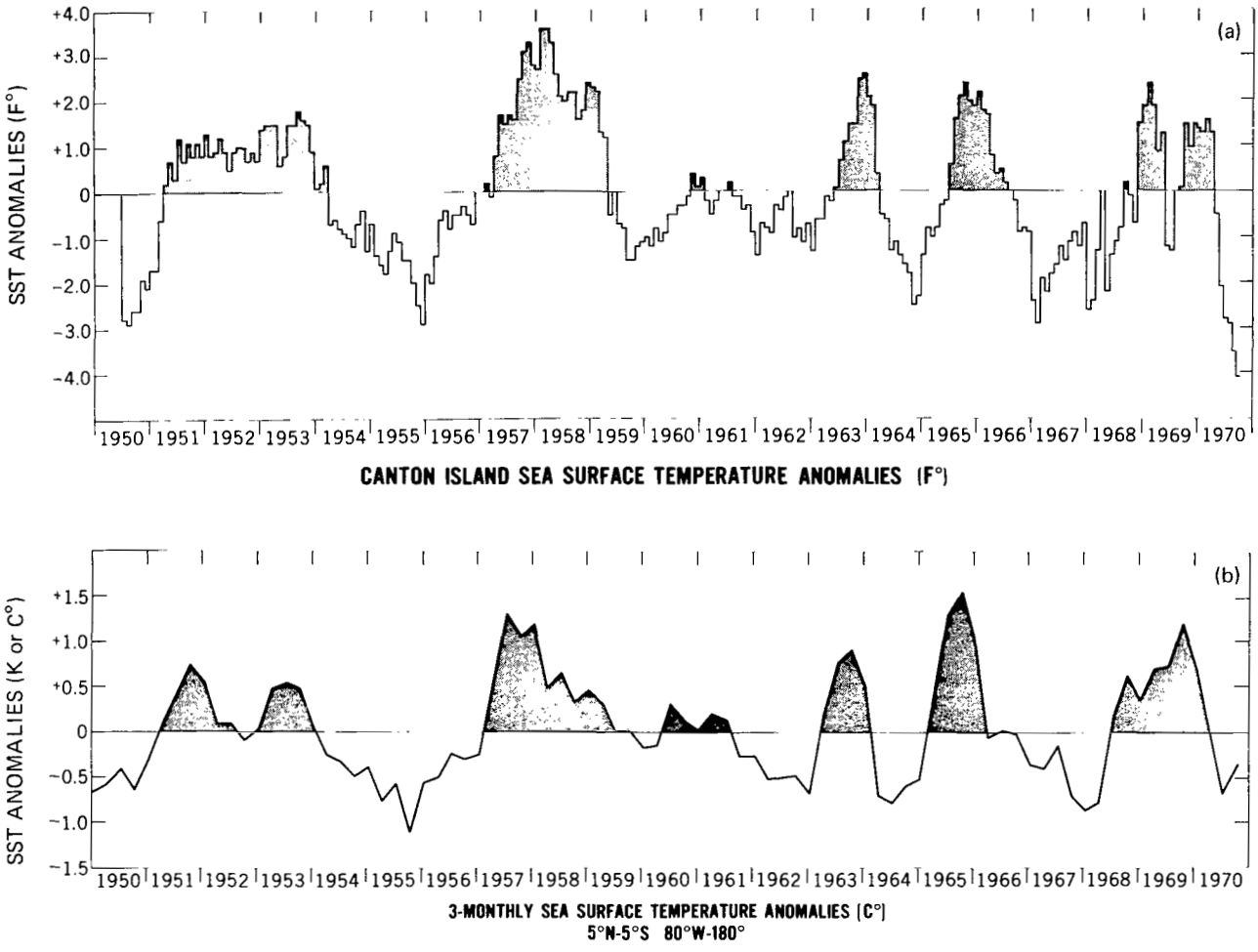

Figure 14—(a) SST anomalies for Canton Island (monthly mean) from 1950 to 1967 (Christmas Island data were inserted from 1967 to 1970); (b) SST anomalies, 5°N to 5°S, 80°W to 180°, 3-month mean from 1950 to 1970.

Table 3—Correlation coefficients r and lead/lag for SST anomalies and tropical island rainfall for six oceanographic regions.

Sea Surface Temperature Anomalies	Correlation Coefficient	Month Lead/Lag*
South American west coast stations	+0.75	-2
0°-10°S	+0.90	-1
5°N-5°S	+0.93	-1
0°-10°N	+0.92	-1
5°N-15°N	+0.78	+1
10°N-20°N	+0.62	+2

*The entry –2 means the rainfall lags the SST anomalies by 2 months, etc.

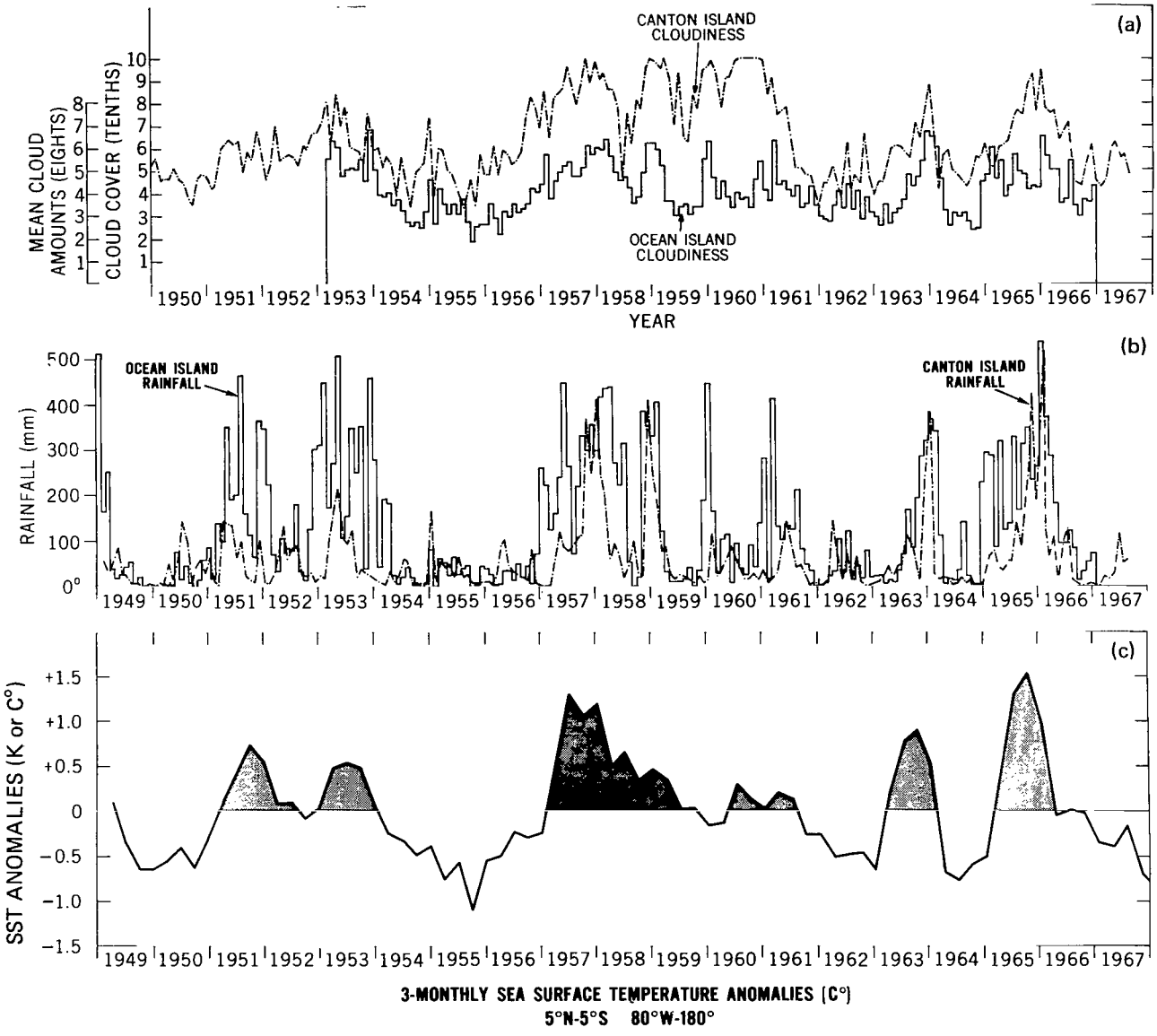

Figure 15—(a) Mean monthly cloudiness (surface observed) at Canton Island (in tenths) and Ocean Island (in eighths) from 1950 to 1967; (b) mean monthly rainfall (mm) for Canton Island and Ocean Island from 1949 to 1967; (c) SST anomalies (5°N to 5°S, 80°W to 180°), 3-month mean from 1949 to 1967.

It was then a simple step to use linear regression techniques (Panofsky and Brier, 1963) to derive SST anomalies (Figure 18b through 18d) for three latitude bands (0° to 10°S, 0° to 10°N, and 10°N to 20°N) back to 1905. The validity of this approach was checked by climatological records in two ways. Figure 18a through 18e shows that 5 out of 7 years of "El Nino" occurrences were indicated by anomalously warm periods in the derived SST data (Quinn and Burt, 1970; Bjerknes, 1966b; Berlage, 1966; Wooster, 1961a). A second check involved the favorable comparison with SST anomalies at

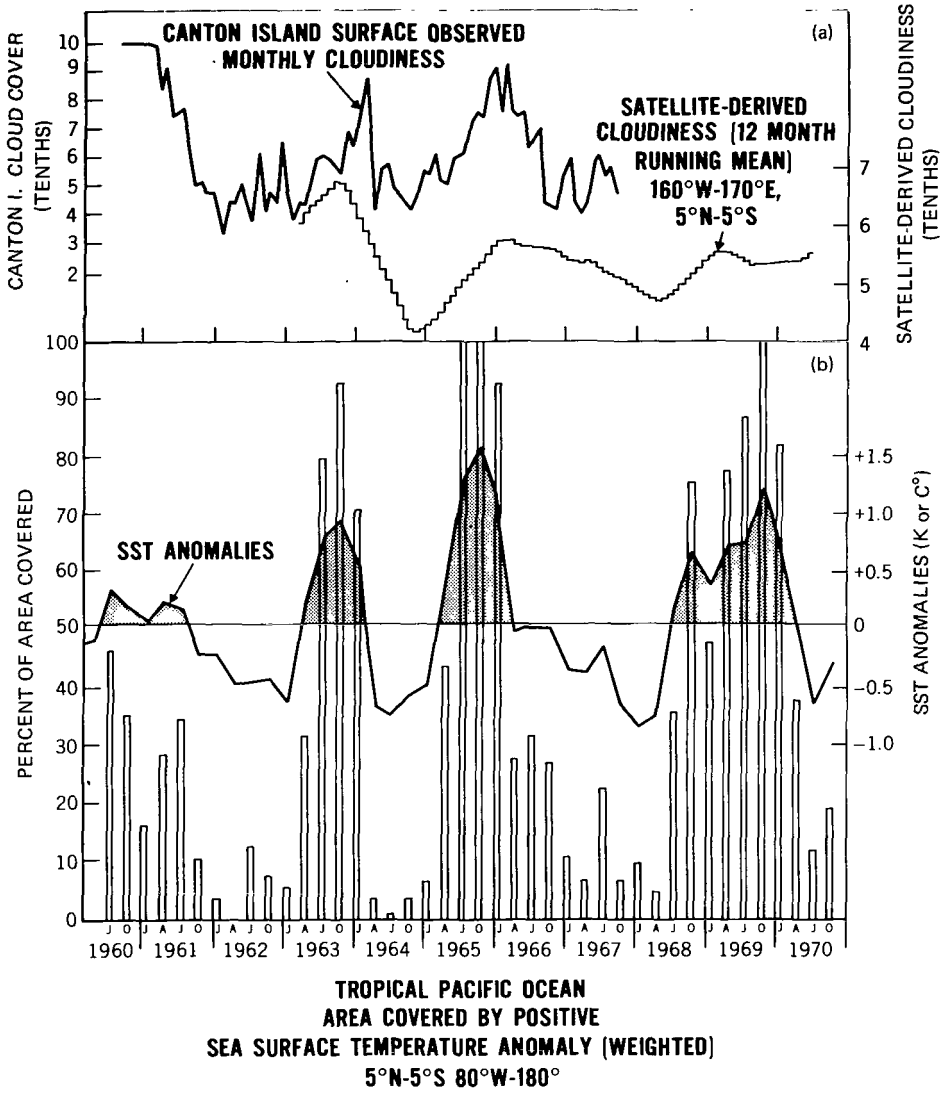

Figure 16—(a) Satellite-derived cloudiness (monthly) 160°W to 170°E, 5°N to 5°S, from 1962 to 1969, and Canton Island surface-observed cloudiness (monthly) from 1961 to 1967; (b) SST anomalies, 5°N to 5°S, 80°W to 180°, 3-month, and percent of area covered by a positive SST anomaly (weighted), from 1960 to 1970.

United States west coast stations (Roden and Reid, 1961) and Puerto Chicama, Peru, which are affected by the coastal upwelling in the California Current and Peru Current (Wooster, 1961b). By the use of the same linear regression techniques, the North Pacific 700-mb positive height anomalies (in percent of area covered), 30°N to 40°N, 180° to 130°W, were also derived back to 1905 from the long record of tropical island rainfall data. Figure 18f through 18i shows the above-mentioned parameter, the Palmer Drought Index for western Kansas (Palmer, 1965), and the derived SST anomalies (10°N to 10°S). Note the close occurrence of cold SST and 700-mb positive height anomalies and severe United States drought, in particular during 1932 to 1938, 1954 to 1956, and 1916 to 1917 (Namias, 1960).

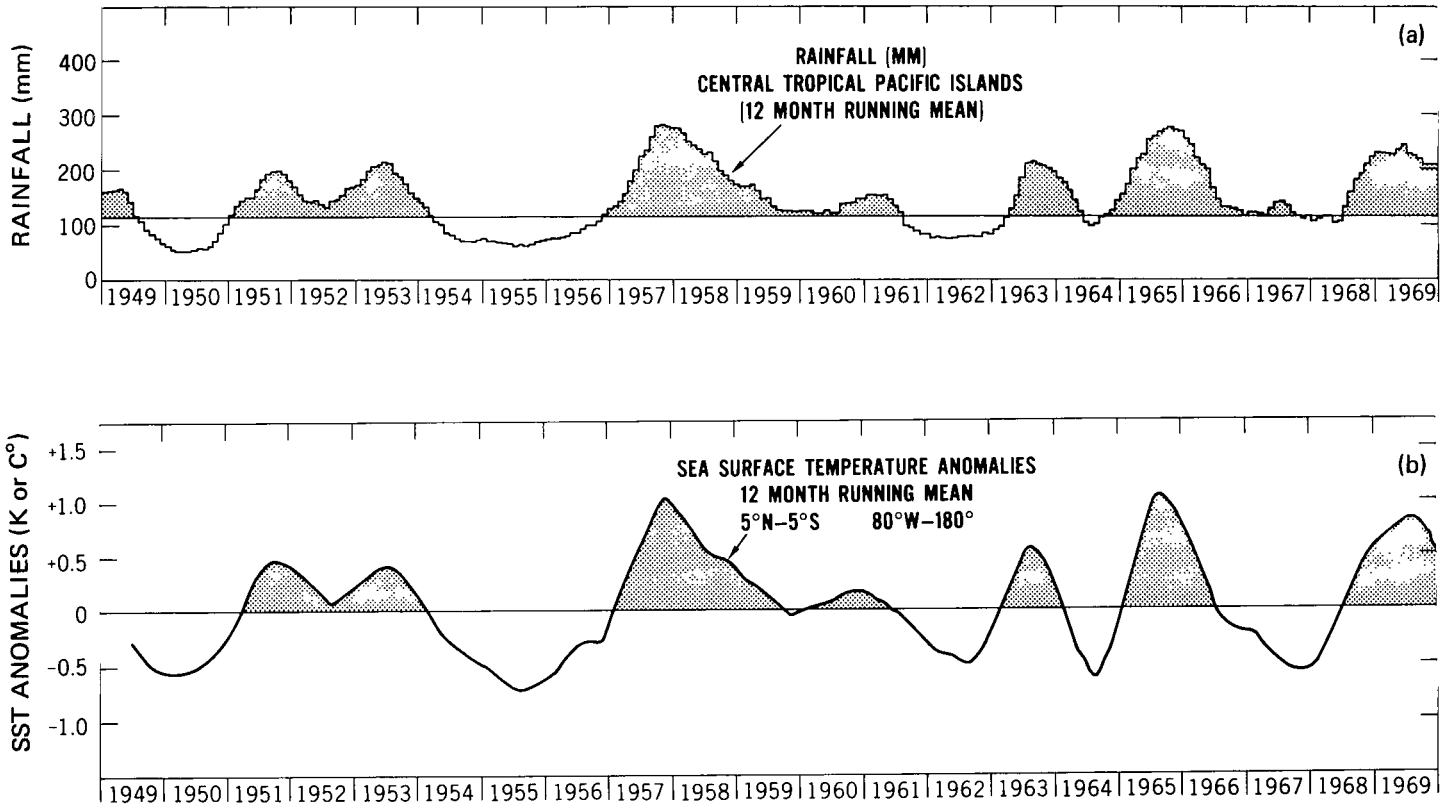

Figure 17—(a) Tropical Pacific Island rainfall (mm), 150°W to 165°E, 5°N to 5°S, 12-month running mean from 1949 to 1969; (b) SST anomalies, 5°N to 5°S, 80°W to 180°, 12-month running mean from 1949 to 1969.

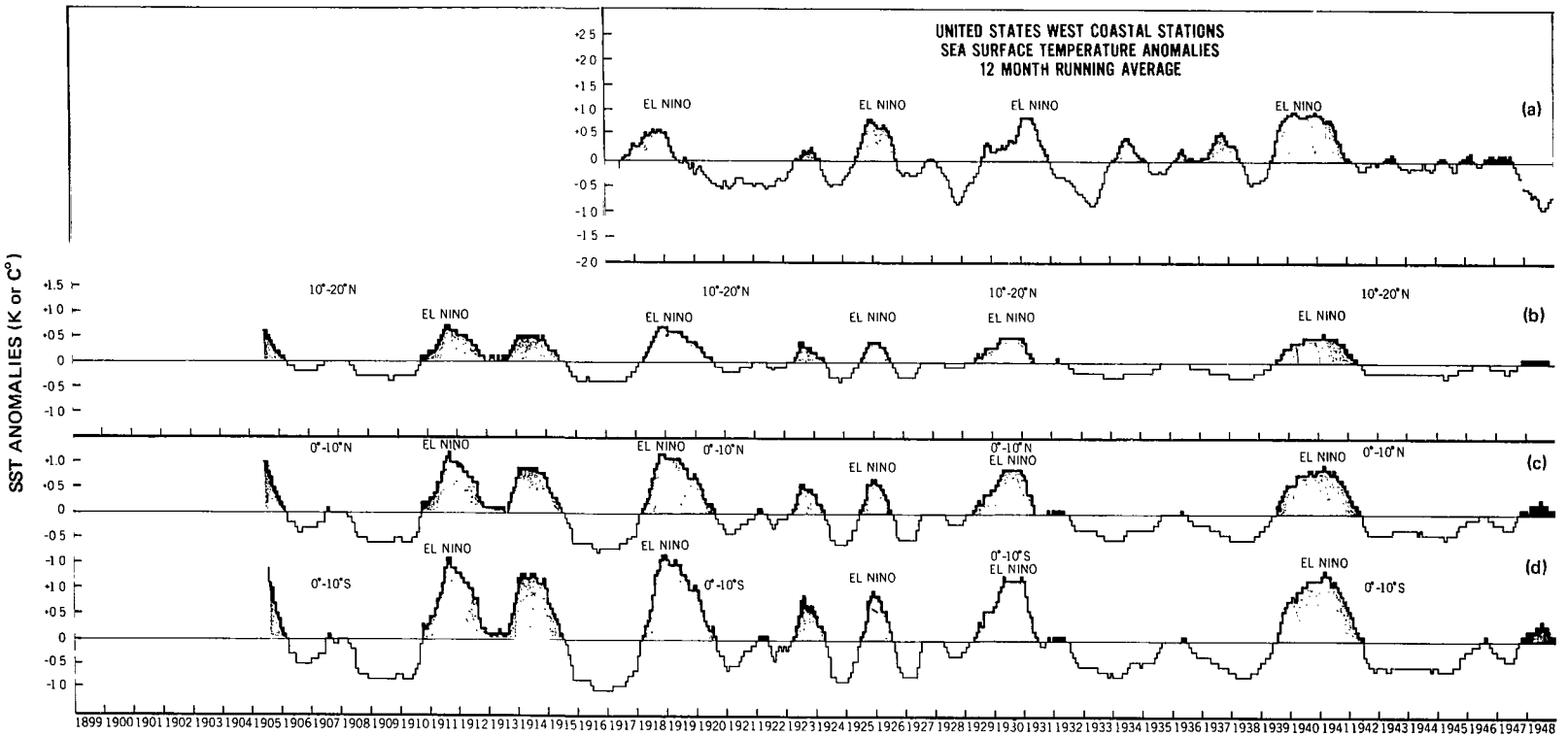

DERIVED TROPICAL PACIFIC OCEAN SEA SURFACE TEMPERATURE ANOMALIES

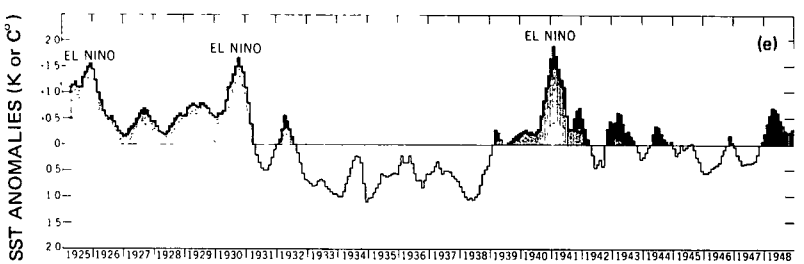

PUERTO CHICAMA, PERU
SEA-SURFACE TEMPERATURE ANOMALIES
SIX-MONTHLY RUNNING AVERAGE

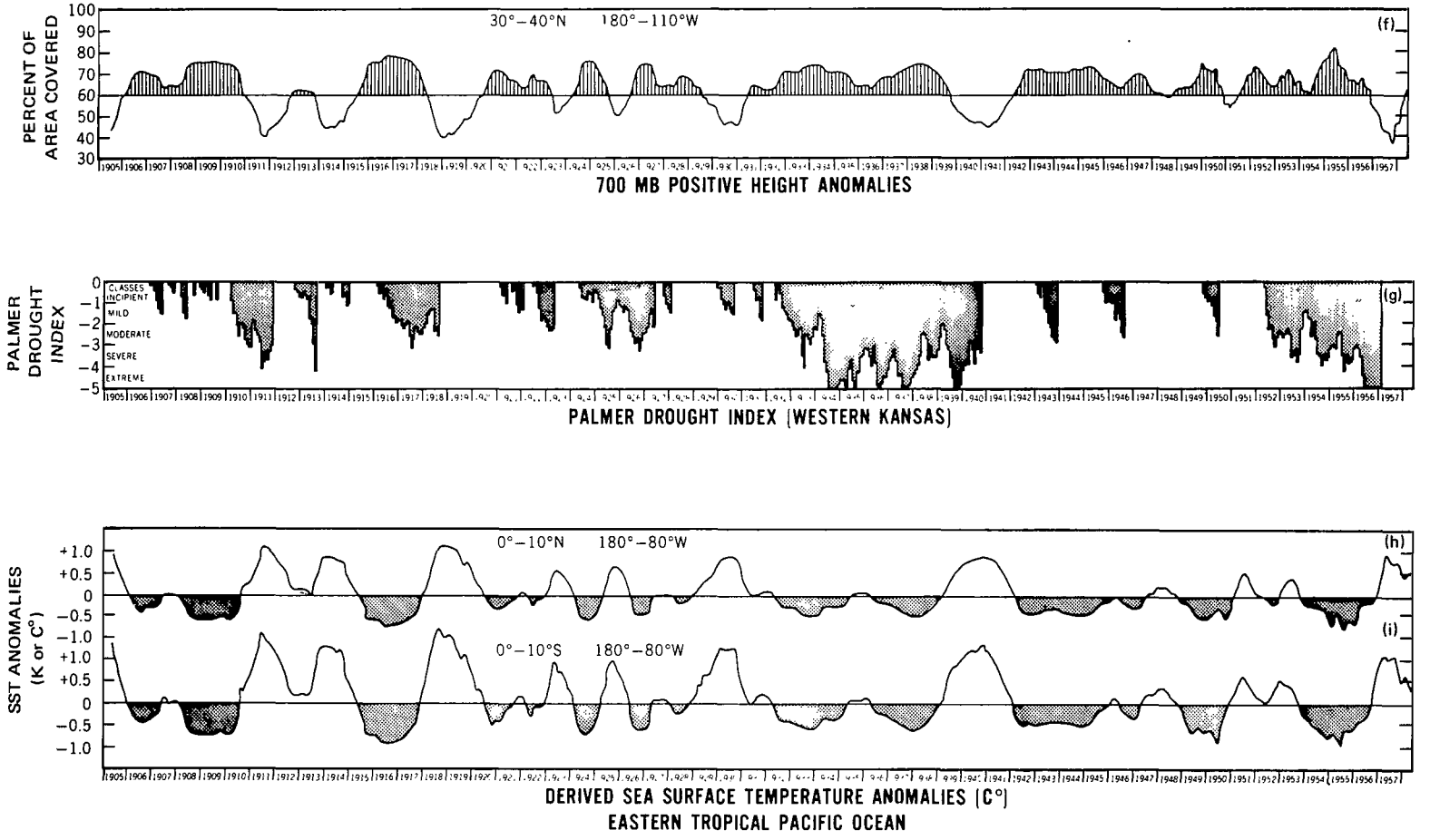

Figure 18—(a) United States west coast station (40°N to 33°N) SST anomalies, from 1917 to 1948, 12-month running mean; (b) derived SST anomalies, 10°N to 20°N, 180° to 90°W, from 1905 to 1948, 12-month running mean; (c) derived SST anomalies, 0° to 10°N, 180° to 80°W, from 1905 to 1948, 12-month running mean; (d) derived SST anomalies, 0° to 10°S, 180° to 80°W, from 1905 to 1948, 12-month running mean; (e) Puerto Chicama SST anomalies from 1925 to 1948, 6-month running mean; (f) derived North Pacific 700-mb positive height anomalies, 30°N to 40°N, 180° to 130°W, from 1905 to 1957, in percent of area covered; (g) monthly Palmer Drought Index for western Kansas (0 to −5 only) from 1905 to 1957; (h) derived SST anomalies, 0° to 10°N, 180° to 80°W, from 1905 to 1957, 12-month running mean; (i) derived SST anomalies, 0° to 10°S, 180° to 80°W, from 1905 to 1957, 12-month running mean.

RESULTS OF THE STATISTICAL ANALYSIS

Many geophysical records show a definite seasonal and/or annual variation which can be of such a large magnitude as to obscure important long-term cycles of a smaller magnitude. This creates a need for filtering out the annual cycle without losing useful information or introducing misleading statistical errors. Early in this project, the decision was made to use 12-month equally weighted running means (EWRM), a smoothing technique that is widely used in climatological research (Appendix C contains a justification of its use in this project).

The main tool used in the statistical examination of the data was the Autocovariance and Power Spectral Analysis (APSA) program, published April 20, 1966, by the Health Sciences Computing Facility at the University of California, Los Angeles (see Appendix C). Tables 4 to 6 list the total number of monthly and linearly interpolated observations of the parameters used in the statistical analysis. The first parameter to be correlated by the APSA program was satellite-derived cloudiness ($\geq 6/10$) for 30°N to 25°S from 1962 to 1970. The results are listed in Table 7. In this table, a -4 under the lag column, for example, means that the parameter at the top of the table lags the compared parameter at the side by 4 months. A +4 implies that the top parameter leads the side parameter by 4 months. The correlation coefficients that are ≥ 0.70 are underlined to indicate the more significant relationships (see Appendix C). The first impression that one gets from Table 7 is that the Northeast and Southeast Pacific cloud bands appear to be positively interrelated. Over 65 percent of the correlation coefficients are ≥ 0.65, with a very short response time of ±1 to 2 months. The cloudiness in the 20°N to 30°N and 0° to 10°N regions is more closely related to Southern Hemisphere Cloudiness than it is to any other region.

As a further check on this interesting relationship, 12-month running means of satellite-derived cloudiness for quadrants over the entire tropical Pacific Ocean (130°E to 100°W, 30°N to 25°S) were plotted (Figures 19a and 19b). The Equator and 180° meridian divided each quadrant analyzed. The high correlation coefficients (r = +0.80 to +0.93) and short (±3-month) lag which relate each quadrant's cloudiness are listed in Table 8. A single EWRM curve for the entire tropical Pacific Ocean

Table 4–Monthly and linearly interpolated observations of satellite-derived cloudiness over the eastern tropical Pacific Ocean (100°W to 180°).

Satellite-Derived Cloudiness	Monthly Observations	Linearly Interpolated Observations
20°N-30°N	34	99
10°N-20°N	34	99
5°N-15°N	34	99
0°N-10°N	34	99
5°N-5°S	34	99
0°-10°S	34	99
10°S-20°S	34	99
20°S-25°S	34	99

Table 5—Monthly and linearly interpolated observations of SST anomalies (80°W to 180°).

Sea Surface Temperature Anomalies	Monthly Observations	Linearly Interpolated Observations
U.S. West Coast Stations	624	624
20°-30°N	36 (3 mo. mean)	108
10°-20°N	60 "	240
5°N-15°N	60 "	240
0°-10°N	60 "	240
5°N-5°S	60 "	240
0°-10°S	60 "	240
South American west coast stations	240	240

Table 6—Monthly and linearly interpolated observations of various parameters.

		Monthly Observations	Linearly Interpolated Observations
NE Pacific-SLP anomalies	30°-40°N	240	240
700 mb Height anomalies	180°-100°W	240	240
SE Pacific-Area covered by ≥ 1020 mb at sea level*	30°-40°S, 180°-75°W	147	147
Juan Fernandez I sea level pressure		677	677
Darwin, Australia sea level pressure		677	677
Tropical Pacific island rainfall		677	677

* Obtained from Deutscher Wetterdienst, 1956-1970.

cloudiness is shown in Figure 19c. A possible explanation for the apparent in-phase relationship between the cloudiness variations in the four Pacific quadrants may lie in the effect of the Southern Oscillation, a large surface-pressure pulsation common to the Pacific and Indian Oceans, described by Troup (1965), Berlage (1966), Bjerknes (1969), Walker and Bliss (1932), and Kyle (1970). (A brief discussion of evidence of a satellite-derived global tropical cloudiness oscillation is found in Appendix D.)

Next, the SST anomalies were correlated from the United States west coast stations (33°N to 40°N) through the tropical ocean bands to 0° to 40°S along the South American west coast. Figure 20 shows the interesting similarity in the warm and cool patterns through each latitude band over this vast stretch of the eastern Pacific Ocean. Table 9 confirms the areal coherence and positive relationship between these sectors. Approximately 60 percent of the correlation coefficients were ≥ 0.65 with a short response time of ± 1 to 3 months. The 0° to 10°N and 5°N to 15°N SST bands are more closely related to Southern Hemisphere SST bands than they are to any other band.

Table 7—Correlation coefficients r with lag for various regions for satellite-derived cloudiness (percent of area covered by $\geq 6/10$ cloudiness) over the eastern tropical Pacific Ocean.

Satellite-Derived Cloudiness ($\geq 6/10$)	Satellite-Derived Cloudiness (Percent of Area Covered by $\geq 6/10$ Cloudiness) over the Eastern Tropical Pacific Ocean																	
	20°-30°N	lag	10°-20°N	lag	5°-15°N	lag	0°-10°N	lag	5°N-5°S	lag	0°-10°S	lag	10°-20°S	lag	20°-25°S	lag
20°-30°N			+0.82	-1	+0.71	0	+0.93	-1	+0.76	-2	+0.68	-1	+0.87	-1	+0.63	-1
10°-20°N	+0.82	+1			+0.92	0	+0.85	+2	+0.66	+2	+0.66	+4	+0.69	+2	+0.63	-1
5°-15°N	+0.71	0	+0.92	0			+0.75	+1	+0.40	+1	+0.38	+3	+0.60	+2	+0.77	-1
0°-10°N	+0.93	+1	+0.85	-2	+0.75	-1			+0.80	-1	+0.67	+1	+0.83	+1	+0.63	-1
5°N-5°S	+0.76	+2	+0.66	-2	+0.40	-1	+0.80	+1			+0.96	+1	+0.63	+2	-0.40	-9
0°-10°S	+0.68	+1	+0.66	-4	+0.38	-3	+0.67	-1	+0.96	-1			+0.60	+1	-0.30	-9
10°-20°S	+0.87	+1	+0.69	-2	+0.60	-2	+0.83	-1	+0.63	-2	+0.60	-1			+0.75	-1
20°-25°S	+0.63	+1	+0.63	+1	+0.77	+1	+0.63	+1	-0.40	+9	-0.30	+9	+0.75	+1		

Table 8—Correlation coefficients r with lag for satellite-derived cloudiness ($\geq 6/10$) for various quadrants of the tropical Pacific Ocean.

	NE Pacific 0°-30°N	lag	SE Pacific 0°-25°S	lag	NW Pacific 0°-30°N	lag	SW Pacific 0°-25°S	lag
NE Pacific 0°-30°N			+0.84	0	+0.93	+3	+0.87	0
SE Pacific 0°-25°S	+0.84	0			+0.80	+2	+0.87	-1
NW Pacific 0°-30°N	+0.93	-3	+0.92	-3			+0.92	-3
SW Pacific 0°-25°S	+0.87	0	+0.87	+1	+0.92	+3		

The SST anomalies were next correlated with the satellite-derived cloudiness from 30°N to 25°S in the eastern Pacific (Table 10). (See Appendix C for an explanation of the double correlation values present in Table 10.) Two correlations appear in this table that seem to have importance. Approximately 50 percent of the correlation coefficients are negative and ≥ 0.65. A simple description of this relationship would be that cool SST follows heavy cloudiness by a -7- to -9-month lag. This effect occurs mainly over the 5°N to 15°N, 0° to 10°N oceanic bands and along the United States west coast and is related to cloudiness on both sides of the Equator. Bjerknes' (1969) description of the localized Hadley-cell circulation in the eastern Pacific could be a possible dynamical explanation for this negative cloud-SST correlation with slow feedback loop.

A smaller group of positive correlations (approximately 20 percent of the total) varying from +0.45 to +0.87 with generally a +3- to +8-month lead, was also found in the data. This would relate increased cloudiness with warmer SST's and vice versa; however, this effect was not dominant in the region of the Pacific. Figure 20 graphically illustrates these two air-sea interaction effects. Note the

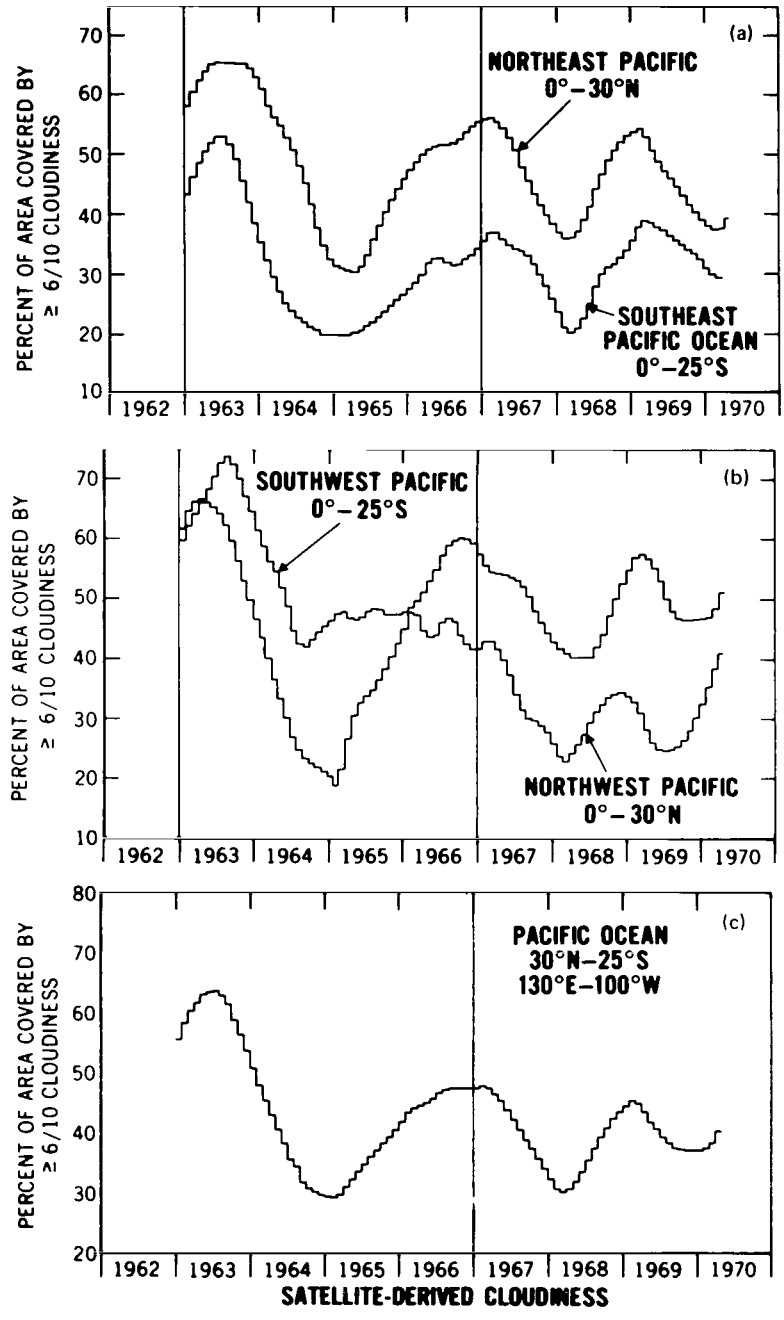

Figure 19—A comparison of satellite-derived cloudiness in percent of area covered by ⩾ 6/10 clouds over (a) the Northeast Pacific (0° to 30°N) and Southeast Pacific (0° to 25°S), (b) the Northwest Pacific (0° to 30°N) and Southwest Pacific (0° to 25°S) (the 180° meridian divided the east and west quadrants), and (c) the entire tropical Pacific Ocean (130°E to 100°W, 30°N to 25°S). Interim months were linearly interpolated and then plotted in the 12-month running means above.

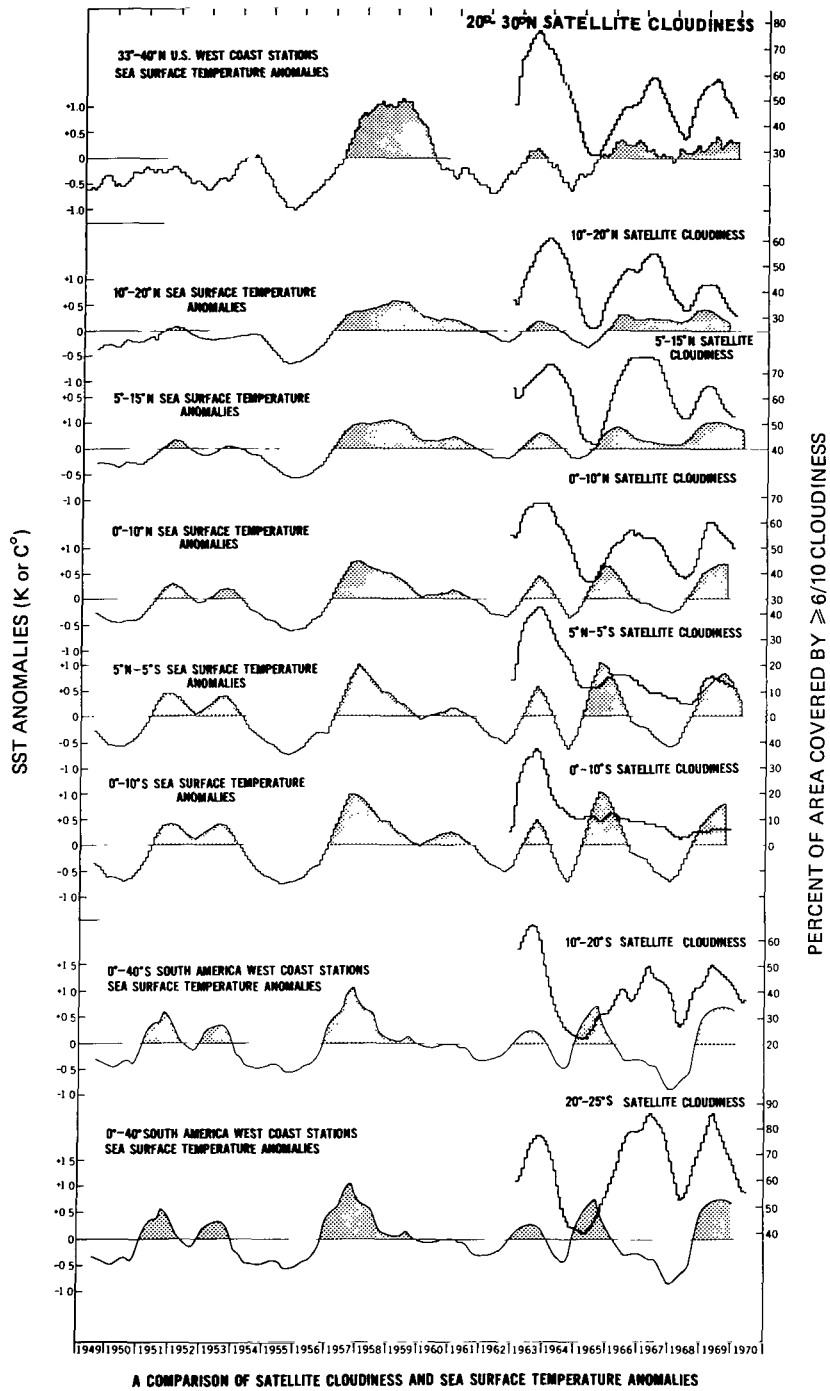

Figure 20—A comparison of 12-month running means of satellite-derived cloudiness (in percent of area covered by $\geq$ 6/10 clouds) from 1962 to 1970 and SST anomalies from 1949 to 1970.

Table 9—Correlation coefficients r with lag for SST anomalies.

Sea Surface Temp. Anomalies	33 -40°N (U.S. West Coast)	lag	20°-30°N	lag	10°-20°N	lag	5°-15°N	lag	0°-10°N	lag	5°N-5°S	lag	0°-10°S	lag	0°-40°S (S.A. West Coast)	lag
33°-40°N (U.S. West Coast)			+0.65	-8	+0.87	-1	+0.84	0	+0.76	+2	+0.62	+3	+0.61	+4	+0.53	+6
20°-30°N	+0.65	+8			+0.77	+3	+0.35	0	-0.25	+8	-0.35	+8	-0.35	-5	-0.59	+7
10°-20°N	+0.87	+1	+0.77	-3			+0.95	0	+0.66	+4	+0.63	+3	+0.53	+5	+0.46	+5
5°-15°N	+0.84	0	+0.35	0	+0.95	0			+0.92	+1	+0.79	+1	+0.79	+1	+0.62	+3
0°-10°N	+0.76	-2	-0.25	-8	+0.66	-4	+0.92	-1			+0.96	0	+0.96	0	+0.85	+1
5°N-5°S	+0.62	-3	-0.35	-8	+0.63	-3	+0.79	-1	+0.96	0			+0.98	0	+0.89	+1
0°-10°S	+0.61	-4	-0.35	+5	+0.53	-5	+0.79	-1	+0.96	0	+0.98	0			+0.90	+1
0°-40°S (S.A. West Coast)	+0.53	-6	-0.59	-7	+0.46	-5	+0.62	-3	+0.85	-1	+0.89	-1	+0.90	-1		

Table 10—Correlation coefficients r with lag for SST anomalies vs. satellite-derived cloudiness.

Satellite-Derived Cloudiness (≥ 6/10)	33°-40°N (U.S. West Coast)	lag	20°-30°N	lag	10°-20°N	lag	5°-15°N	lag	0°-10°N	lag	5°N-5°S	lag	0°-10°S	lag	0°-40°S (S.A. West Coast)	lag
20°-30°N	-0.66	-8	+0.23	0	+0.45 -0.41	+3 -8	-0.52	-8	-0.49	-8	-0.50	-8	-0.55	-8	-0.29	-8
10°-20°N	-0.76	-9	-0.31	+9	+0.47 -0.48	+2 -8	-0.84	-9	+0.42 -0.87	+8 -8	-0.82	-8	+0.47 -0.88	+8 -8	-0.60	-8
5°-15°N	+0.69	-7	+0.35	+3	+0.66	+3	-0.70	-9	-0.87	-8	-0.85	-8	-0.92	-8	-0.69	-8
0°-10°N	-0.74	-9	+0.02 -0.13	+1 -9	+0.42 -0.49	+3 -8	-0.73	-9	+0.50 -0.65	+6 -8	-0.61	-9	+0.50 -0.66	+7 -8	-0.39	-8
5°N-5°S	-0.89	-9	-0.50 -0.36	-9 +5	-0.69	-8	-0.71	-9	-0.39	-8	-0.35	-9	-0.33	-8	+0.45	+6
0°-10°S	-0.81	-9	-0.49	+6	-0.53	-8	-0.59	-9	+0.13 -0.33	0 -8	-0.37	-9	-0.30	-8	-0.41	+5
10°-20°S	+0.52	+4	+0.36	-4	-0.50	-1	+0.44	+1	-0.50	-8	-0.56	-9	-0.61	-8	-0.54	-8
20°-25°S	+0.87	+6	+0.63	-2	-0.89	+3	+0.71	+4	-0.72	-8	-0.75	-9	-0.84	-8	-0.80	-8

depressed cloudiness in the presence of warm SST anomalies from 5°N to 10°S during the winter of 1966, which was reported by Krueger and Gray (1969), and the increased cloudiness at 10°S to 25°S in the presence of cool SST anomalies of the Peru current. The presence of dense stratiform clouds in this region has been noted in daily ATS 3 and ESSA-ITOS cloud photography (U.S. Department of Commerce, 1970b; Goddard Space Flight Center, 1969a and 1969b).

Tables 11, 12, and 13 correlate the Northeast Pacific anticyclone surface pressure anomalies, 700-mb height anomalies, the percent of area covered by ≥ 1020 mb in the region 30°S to 40°S, 140°W to 100°W (South Pacific anticyclone), Juan Fernandez Island and Darwin surface pressure, and tropical Pacific island rainfall with sea surface temperature anomalies (Table 11), satellite-derived cloudiness (Table 12), and each other (Table 13).

Three interesting features shown in Table 11 are the crossequatorial relationship between the Northeast Pacific 700-mb height anomalies (see Figure 5), the Darwin and tropical island rainfall, the surface pressure, and the SST anomalies. Since these data are based upon 20 years of record, the authors feel that these positive and negative correlations are highly significant and useful for meteoro-

Table 11—Correlation coefficients (r) with lag for various parameters with SST anomalies.

Sea Surface Temp. Anomalies	30°-40°N (NE Pacific) Surface Pressure	lag	30°-40°N (NE Pacific) 700 mb HT.	lag	30°-40°S (SE Pacific) Surface Pressure	lag	Juan Fernandez Surface Pressure	lag	Darwin Surface Pressure	lag	Tropical Pacific I. Rainfall	lag
33°-40°N (U.S. West Coast)	-0.68	+6	-0.68	+8	-0.41	+5	-0.43	+3	+0.59	0	+0.53	0
20°-30°N	-0.69	+8	-0.41	+8	-0.55	-8	+0.64	-5	-0.60	+8	-0.40	-8
10°-20°N	-0.72	+7	-0.73	+9	-0.34 -0.69	+10 +30	-0.61	+5	+0.56	+2	+0.62	+2
5°-15°N	-0.74	+7	-0.74	+8	-0.56	+5	-0.66	+3	+0.73	0	+0.78	+1
0°-10°N	-0.67	+6	-0.74	+6	-0.67	+4	-0.69	+2	+0.80	-1	+0.92	-1
5°N - 5°S	-0.56	+6	-0.72	+6	-0.71	+3	-0.64	+2	+0.83	-1	+0.93	-1
0°-10°S	-0.51	+5	-0.70	+5	-0.66	+3	-0.63	+2	+0.82	-2	+0.90	-1
0°-40°S (S.A. West Coast)	-0.36	+4	-0.56	+4	-0.51	+1	-0.52	0	+0.71	-3	+0.75	-2

Table 12—Correlation coefficients (r) with lag for various parameters with satellite-derived cloudiness ($\geq$ 6/10).

Satellite-Derived Cloudiness ($\geq$ 6/10)	30°-40°N (NE Pacific) Surface Pressure	lag	30°-40°N (NE Pacific) 700 mb HT.	lag	30°-40°S (SE Pacific) Surface Pressure	lag	Juan Fernandez Surface Pressure	lag	Darwin Surface Pressure	lag	Tropical Pacific I. Rainfall	lag
20°-30°N	+0.39	-8	+0.76	-4	+0.65	-8	+0.54	+3	-0.55	-8	-0.41	-8
10°-20°N	+0.53	-1	+0.78	-2	+0.67	-4	+0.37	-4	-0.84	-8	-0.73	-9
5°-15°N	+0.36	0	+0.62	-2	+0.79	-5	+0.48	-4	-0.78	-9	-0.79	-9
0°-10°N	+0.48	-5	+0.82	-5	+0.60	-4	+0.33	+3	-0.59	-8	-0.55	-9
5°N-5°S	+0.86	-7	+0.89	-6	+0.26	+3	+0.27	+8	-0.33	-9	-0.25	-9
0°-10°S	+0.88	-7	+0.89	-7	+0.27	+4	+0.29	+8	+0.22	-1	-0.20	-9
10°-20°S	-0.52	+9	+0.73	-7	+0.65	-6	+0.51	-7	-0.67	-9	-0.44	-8
20°-25°S	-0.55	+9	-0.60	+9	-0.80	-5	+0.68	-7	-0.83	-9	-0.74	-8

logical and oceanographic prediction. It was noted also that the Northeast Pacific surface pressure leads the 5°N to 20°N SST's by 7 months, whereas the Southeast Pacific surface pressure had a shorter (3-month) lead time in its effective region. The faster wind-stress coupling time could be explained by the greater seasonal stability and size of the South Pacific anticyclone as compared with those of the North Pacific anticyclone.

Table 12 indicates the good correlations shown by the Northeast Pacific 700-mb height anomalies and crossequatorial satellite-derived cloudiness, but since the period of record is only 9 years, the confidence level is lower than shown for Table 11. Note the consistent negative correlations (-0.73 to -0.84) between Darwin surface pressure, tropical rainfall, and 5°N to 20°N cloudiness.

Table 13—Correlation coefficients (r) with lag among various parameters.

	30°-40°N (NE Pacific) Surface Pressure	lag	30°-40°N (NE Pacific) 700 mb HT.	lag	30°-40°S (SE Pacific) Surface Pressure	lag	Juan Fernandez Surface Pressure	lag	Darwin Surface Pressure	lag	Tropical Pacific I Rainfall	lag
30°-40°N (NE Pacific) Surface Pressure			+0.80	0	+0.30	-5	+0.39	-4	-0.52	-6	-0.55	-7
30°-40°N (NE Pacific) 700 mb HT	+0.80	0			+0.53	0	+0.46	-4	-0.54	-6	-0.65	-6
30°-40°S (SE Pacific) Surface Pressure	+0.30	+5	+0.53	0			+0.76	-1	-0.67	-3	-0.81	-4
Juan Fernandez Surface Pressure	+0.39	+4	+0.46	+4	+0.76	+1			-0.50	-3	-0.58	0
Darwin Surface Pressure	-0.52	+6	-0.54	+6	-0.67	+3	-0.50	+3			+0.80	0
Tropical Pacific I. Rainfall	-0.55	+7	-0.65	+6	-0.81	+4	-0.58	0	+0.80	0		

Table 13 indicates the good positive correlation (+0.80) between the Northeast Pacific surface pressure and 700-mb height anomalies (see Figure 2). This maritime relationship had been noted previously by Klein (1967). In addition, tropical Pacific island rainfall related positively (r = +0.80) with Darwin surface pressure (Figures 21 and 22). This useful meteorological relationship implies a cross-equatorial coupling that has not been completely described dynamically in the literature (Quinn and Burt, 1970).

CONCLUSIONS

SST variations in the California and Peru Currents from 1949 to 1970 have been traced from the west coasts of North and South America, respectively, to the central tropical Pacific Ocean by means of a newly produced atlas of SST anomalies (Appendix A). These SST anomalies did indeed show a strong relation to Canton Island SST data, as was hypothesized by Bjerknes in 1966 (Bjerknes, 1966b).

Tropical Pacific rainfall was found to be strongly correlated with tropical SST anomalies (r = +0.93), and by use of this direct relationship, it was possible to derive tropical SST anomalies back to 1905, a period of sparse oceanographic data. The relationship between cold tropical SST and North Pacific 700-mb positive height anomalies and central United States drought was noted.

The Northeast Pacific 700-mb height field (30°N to 40°N) was found to be positively correlated (r = +0.73 to +0.89) with satellite-derived cloudiness from 30°N to 20°S and negatively correlated (r = -0.70 to -0.74) with SST anomalies from 20°N to 10°S.

The tropical SST's were negatively correlated with and lagged the satellite-derived cloudiness from 20°N to 10°S, implying the presence of a localized Hadley circulation, previously suggested by Bjerknes (1969). The Eastern Pacific SST bands and coastal waters showed a close areal coherence in

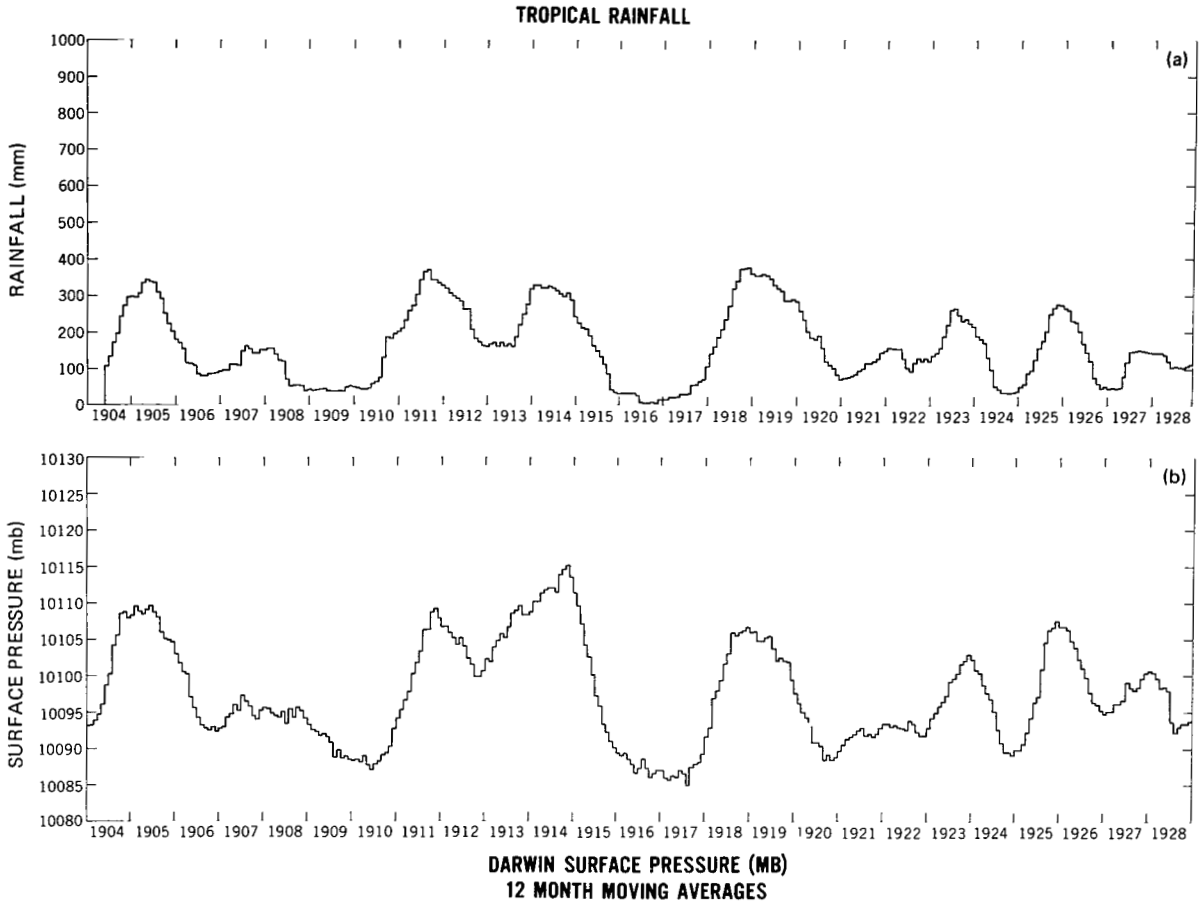

Figure 21—A comparison of 12-month running means of (a) tropical Pacific island rainfall (see Figure 6) and (b) Darwin, Australia, surface pressure from 1904 to 1928.

temperature pattern from 40°N to 40°S, and the satellite-derived cloudiness over the entire Pacific appeared to be pulsating in resonance. A similar global tropical cloudiness pulsation was noted over the Pacific, Atlantic, and Indian Oceans from J. C. Sadler's monthly satellite nephanalyses.*

The South Pacific anticyclone appeared to couple faster (3-month lead) through wind stress to the sea surface than the North Pacific anticyclone (7-month lead).

Tropical Pacific island rainfall was well correlated with Darwin surface pressure ($r = +0.80$) and implied a local atmospheric coupling, which has not been completely documented in the literature.

This study has shown the various time frames of direct local and crossequatorial air-sea relationships which exist over the tropical Pacific Ocean. With further analytical refinement, several of these geophysical parameters could become useful for seasonal meteorological and oceanographic prediction.

*J. C. Sadler, University of Hawaii, Honolulu, unpublished data.

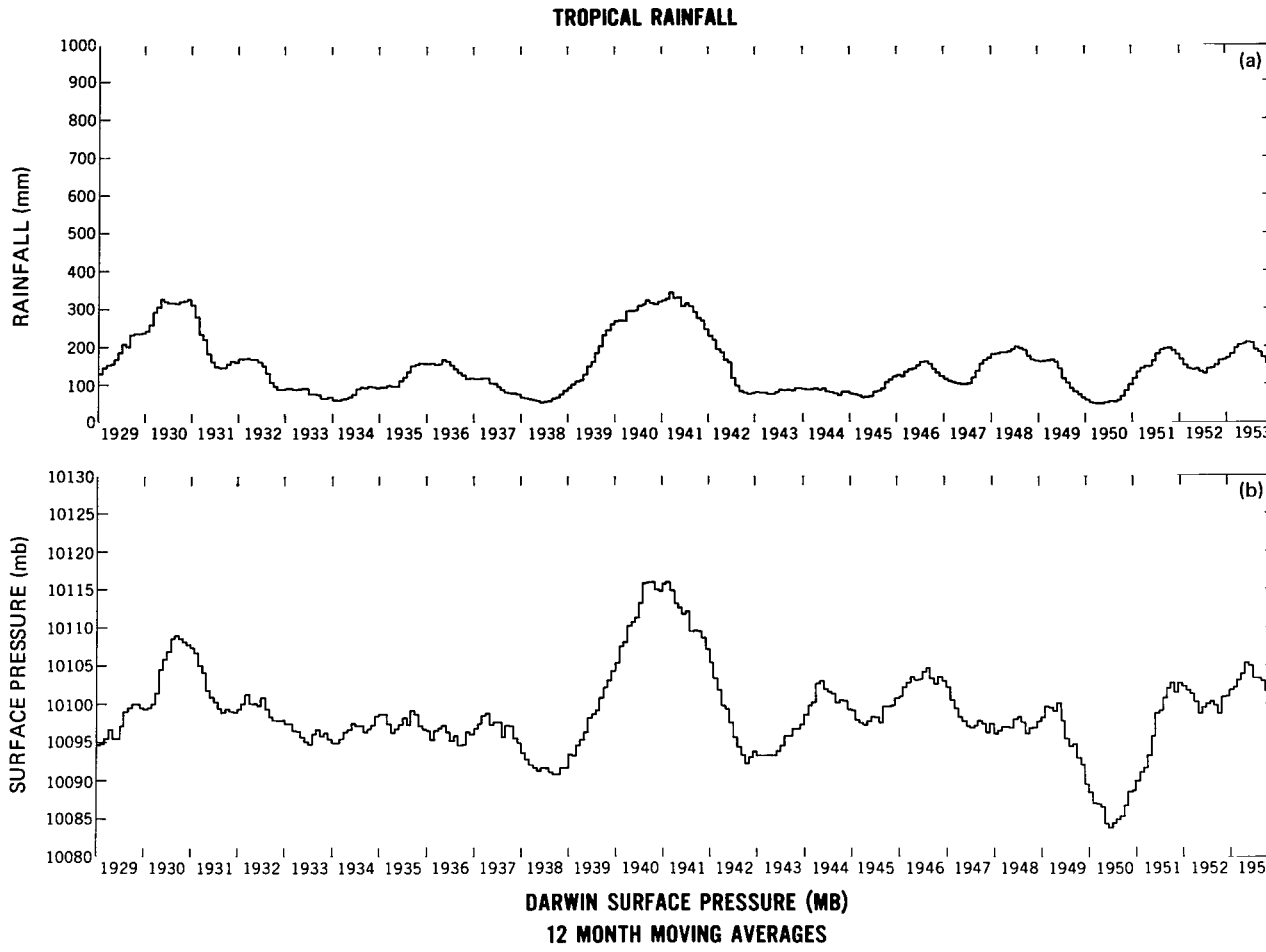

Figure 22—A comparison of 12-month running means of (a) tropical Pacific island rainfall (see Figure 6) and (b) Darwin, Australia, surface pressure from 1929 to 1953.

ACKNOWLEDGMENTS

The authors wish to thank Dr. Jacob Bjerknes, Professor Emeritus, University of California, Los Angeles, Dr. Alan Longhurst, Scripps Institution of Oceanography, Dr. Thomas Austin, NOAA, and Dr. William Quinn, Oregon State University, for their continued interest and encouragement during the course of this study, and Dr. Raymond Wexler, GSFC, for his suggestions and helpful editorial comments on the manuscript.

Goddard Space Flight Center
National Aeronautics and Space Administration
Greenbelt, Maryland, July 28, 1971
160-44-55-01-51

REFERENCES

Allison, L. J., Kreins, E. R., Godshall, F., and Warnecke, G., "Examples of the Usefulness of Satellite Data in General Circulation Research: Part I—Monthly Global Circulation Characteristics as Reflected in TIROS 7 Radiometric Measurements", NASA Technical Note D-5630, December 1969.

Allison, L. J., "The Applications of the Nimbus Meteorological-Satellite Data", U.S. Air Force Air Weather Service Technical Report 242, Scott Air Force Base, Illinois, April 1971, pp. 261-290.

Anderson, R. K., Ashman, J. P., Bittner, F., Farr, G. R., Ferguson, E. W., Oliver, V., and Smith, A. H., "Application of Meteorological Satellite Data in Analysis and Forecasting", U.S. Air Force Air Weather Service (MAC) Technical Report 212, Scott Air Force Base, Illinois, 1969.

Atkinson, G. D., and Sadler, J. C., "Mean Cloudiness and Gradient-Level-Wind Charts Over the Tropics", Vol. 1 and 2, U.S. Air Force Air Weather Service Technical Report 215, Scott Air Force Base, 1970.

Berlage, H. P., "The Southern Oscillation and World Weather", Mededeel. Verhandel, Kon. Ned. Meteor. Inst., No. 88, 152 pp., 1966.

Bjerknes, J., "El Nino Study Based on Analyses of Ocean Surface Temperatures, 1935-1957", *Bulletin of the Inter-American Tropical Tuna Commission* 5(3):217-303, 1961.

Bjerknes, J., "Survey of El Nino (1957-58) in its Relation to Tropical Pacific Meteorology", Vol. 12, No. 2, Inter-American Tropical Tuna Commission, La Jolla, California, 1966a, p. 45.

Bjerknes, J., "A Possible Response of the Hadley Circulation to Variations of the Heat Supply from the Equatorial Pacific", *Tellus* XVIII:820-829, 1966b.

Bjerknes, J., "Atmospheric Teleconnections from the Equatorial Pacific, *Monthly Weather Review* 97(3):163-172, 1969.

Bjerknes, J., Allison, L. J., Kreins, E. R., Godshall, F. A., and Warnecke, G., "Satellite Mapping of the Tropical Pacific Cloudiness", *Bulletin of the American Meteorological Society* 50(5):313-322, 1969.

Bjerknes, J., "Studies in Climate Dynamics for Environmental Security: Large-Scale Ocean/Atmosphere Interaction Resulting From Variable Heat Transfer at the Equator", RM-6353-ARPA, Rand, Santa Monica, California, August 1970.

Crutcher, H. L., and Meserve, J. M., "Selected Level Heights, Temperatures and Dew Points for the Northern Hemisphere", NAVAIR 50-1C-52, U.S. Naval Weather Service Command, Washington, D.C., 1970.

Deutscher Wetterdienst, "Seewetteramt, Die Witterung in Ubersee", Hamburg, Germany, 1956 to 1970.

Doberitz, R., "Koharenzanalyse von Niederschlag und Wassertemperatur im tropischen Pazifischen Ozean", Berichte Deutscher Wetterdienstes, NR 112 (Band 15), Selbstverlag des Deutscher Wetterdienstes, 1968a.

Doberitz, R., "Cross Spectrum Analysis of Rainfall and Sea Temperature at the Equatorial Pacific Ocean", Meteorologisches Institut der Universität Bonn, Bonner Meteorologische Abhandlungen, Heft 8, p. 61, 1968b.

Eber, L. E., Saur, J. F. T., and Sette, O. E., "Monthly Mean Charts, Sea Surface Temperature, North Pacific Ocean", Bureau of Commercial Fisheries Circular 258, U.S. Department of the Interior, Washington, D.C., June 1968.

Goddard Space Flight Center, "Meteorological Data Catalog for the Applications Technology Satellites", Vol. III NASA Technical Memorandum X-66468, 1969a.

Goddard Space Flight Center, "Meteorological Data Catalogue for the Applications Technology Satellites", Vol. IV, NASA Technical Memorandum X-66469, 1969b.

Godshall, F., "Intertropical Convergence Zone and Mean Cloud Amount in the Tropical Pacific Ocean", *Monthly Weather Review* 96(3):172-175, 1968.

Godshall, F., Allison, L. J., Kreins, E. R., and Warnecke, G., "Examples of the Usefulness of Satellite Data in General Atmospheric Circulation Research: Part II—An Atlas of Average Cloud Cover over the Tropical Pacific Ocean", NASA Technical Note D-5631, 1969, p. 41.

Klein, W. H., "Specification of Sea Level Pressure From 700-mb Heights", *Quarterly Journal of the Royal Meteorological Society* 93(396):214-226, 1967.

Krueger, A. F., and Gray, T. I., Jr., "Long-Term Variations in Equatorial Circulation and Rainfall", *Monthly Weather Review* 97(10):700-711, 1969.

Kyle, A. C., "Longitudinal Variation of Large Scale Vertical Motion in the Tropics", M.S. Thesis, Massachusetts Institute of Technology, Cambridge, January 15, 1970.

Leese, J. A., Booth, A. L., and Godshall, F. A., "Archiving and Climatological Applications of Meteorological Satellite Data", Environment Science Services Administration Technical Report NESC 53, U.S. Department of Commerce, Washington, D.C., 1970.

Malkus, J. S., "Large-Scale Interactions", *The Sea*, M. H. Hull, editor, Interscience Publishers, New York, 1962, Vol. 1, pp. 88-294.

Miller, D. B., "Automated Production of Global Cloud Climatology Based on Satellite Data", in Proceedings of 1970 Meteorological Technical Exchange Conference, Annapolis, Maryland, September 1970, U.S. Air Force Air Weather Service Technical Report 242, Scott Air Force Base, Illinois, 1971.

Namias, J., "Factors in the Initiation, Perpetuation, and Termination of Drought", International Union of Geodesy and Geophysics, Association of Scientific Hydrology Publication 51, 1960, pp. 81-94.

Namias, J., "Macroscale Variations in Sea-Surface Temperatures in the North Pacific", *Journal of Geophysical Research* 75(3):565-582, 1970.

Palmer, W. C., "Meteorological Drought", U.S. Weather Bureau Research Paper 45, U.S. Department of Commerce, Washington, D.C., 1965, 58 pp.

Panofsky, H. A., and Brier, G. W., *Some Applications of Statistics to Meteorology*, Pennsylvania State University, State College, Pennsylvania, 1963, p. 226.

Quinn, W., and Burt, W. V., "Prediction of Abnormally Heavy Precipitation over the Equatorial Pacific Dry Zone", *Journal of Applied Meteorology* 9(1):20-28, 1970.

Rasool, S. I., and Hogan, J. S., "Ocean Circulation and Climatic Changes", *Bulletin of the American Meteorological Society* 50(3):130-134, 1969.

Reid, J. L., Roden, G. I., and Wyllie, J. G., "Studies of the California Current System", State of California Marine Research Committee, California Cooperative Ocean–Fisheries Investigative Progress Report; 1 July 1956-1 Jan 1958, Sacramento State Printer, 1958, pp. 27-56.

Renner, J. A., "Sea Surface Temperature Charts, Eastern Pacific Ocean", California Fishery Market News Monthly Summary, Part II, Fishing Information, U.S. Dept. of Interior, Bureau of Commercial Fisheries, Biological Laboratory, San Diego, California, 1962 to 1970.

Roden, G. I., and Reid, J. L., Jr., "Sea Surface Temperature Radiation and Wind Anomalies in the North Pacific Ocean", *Records of Oceanographic Works in Japan* 6(1):36-52, 1961.

Roden, G. I., "Oceanographical Aspects of the Eastern Equatorial Pacific", Contribution 1527, *Geophysica International* 2(4):601-615, 1962.

Roden, G. I., "On Atmospheric Pressure Oscillations Along the Pacific Coast of North America, 1873-1963", *Journal of Atmospheric Sciences* 22(3):280-295, 1965.

Sadler, J. C., "Average Cloudiness in the Tropics from Satellite Observations", *International Indian Ocean Expedition Meteorological Monograph No. 2*, East-West Press, Honolulu, Hawaii, 1968.

Seckel, G. R., "Trade Wind Zone Oceanography Pilot Study", Part VIII, Special Science Report–Fisheries No. 612, U.S. Fish and Wildlife Service, Washington, D.C., 1970, 129 pp.

Shell, I. I., "The Origin and Possible Prediction of the Fluctuations in the Peru Current and Upwelling", *Journal of Geophysical Research* 70(22):5529-5540, 1965.

Sherr, P. E., Glaser, A. H., Barnes, J. C., and Willand, J. H., "World-Wide Cloud Cover Distributions for Use in Computer Simulations", NASA Contract Report 61226 (Contract No. NAS8-21040, Allied Research Associates, Inc., Concord, Massachusetts), 1968, 140 pp.

Stewart, R. W., "The Atmosphere and the Ocean", *Scientific American* 221(3):76-106, 1969.

Suomi, V. E., and VonderHaar, T. H., "Geosynchronous Meteorological Satellites", *Measurements from Satellite Platforms*, University of Wisconsin, Madison, Wisconsin, 1970, pp. 1-7.

Svedrup, H. U., *Proceedings of the National Academy of Sciences of the United States of America* 33:318-326, 1947.

Taljaard, J. J., van Loon, H., Crutcher, H. L., and Jenne, R. L., "Climate of the Upper Air: Part I—Southern Hemisphere", Vol. 1, NAVAIR 50-1C-55, U.S. Naval Weather Service Command, Washington, D.C., 1969.

Taylor, V. R., and Winston, J. S., "Monthly and Seasonal Mean Global Charts of Brightness From ESSA 3 and ESSA 5 Digitized Pictures, February 1967-February 1968", Environmental Science Services Administration Technical Report NESC 46, National Environmental Satellite Center, ESSA, Washington, D.C., 1968, 18 pp.

Troup, A. J., "The Southern Oscillation", *Quarterly Journal of the Royal Meteorological Society* 91(390):490-506, 1965.

U.S. Committee for the GARP, "Plan for U.S. Participation in the Global Atmospheric Research Program", National Academy of Sciences, Washington, D.C., 1969, p. 79.

U.S. Department of Commerce, "EASTROPAC Atlas", C. M. Love, editor, Circular 330, Vol. 4, National Oceanic and Atmospheric Administration, Washington, D.C.

U.S. Department of Commerce, "Catalog of Meteorological Satellite Data", No. 5.320-5.321, Environmental Science Services Administration, Silver Spring, Maryland, 1970b.

U.S. Navy, "Oceanography", Hydrographic Office Publication No. 9, Part 6, Washington, D.C., 1962, pp. 691-762.

U.S. Navy, "Handbook of Oceanographic Tables", Oceanographic Office SP-68, Washington, D.C., 1966, 425 pp.

U.S. Naval Oceanographic Office, 1969: "Monthly Charts of Mean, Minimum and Maximum Sea Surface Temperature of the North Pacific Ocean", Special Publication 123, 56 pp.

U.S. Weather Bureau, "Weather and Circulation", *Monthly Weather Review* January 1949 to January 1971.

Walker, G. T., and Bliss, E. W., "World Weather V", *Memoirs of the Royal Meteorological Society* 4:53, 1932.

Wallace, J. M., "Time-Longitude Sections of Tropical Cloudiness", Environmental Science Services Administration Technical Report NESC 56, U.S. Department of Commerce, Washington, D.C., 1970, p. 37.

Wooster, W. S., "Yearly Changes in the Peru Current", *Limnology and Oceanography* 6(2):222-226, 1961a.

Wooster, W. S., *Data Report, STEP-I Expedition, 15 Sept.-14 Dec. 1960, Preliminary Report Ref. 61-9: Part I—Physical and Chemical Data*, Scripps Institution of Oceanography, University of California, La Jolla, California, 1961b.

Wyrtki, K., "Surface Currents of the Eastern Tropical Pacific Ocean", Vol. IX, No. 5, Inter-American Tropical Tuna Commission, La Jolla, California, 1965, p. 304.

Wyrtki, K., "Oceanography of the Eastern Equatorial Pacific Ocean", in *Oceanography and Marine Biology Annual Review No. 4,* Harold Barnes, editor, G. Allen and Unwin Ltd., London, 1966, pp. 33-68.

Zipser, E. J., "Survey of Progress and Plans in Tropical Meteorology Experiments", U.S. Air Force Air Weather Service (MAC) Technical Report 217, Scott Air Force Base, Illinois, 1969, pp. 178-188.

Appendix A

Sea Surface Temperature Anomalies Over the Eastern Tropical Pacific Ocean (1949 to 1970)

Charts of 3-month SST anomalies over the eastern tropical Pacific Ocean for March 1949 to November 1970, in chronological order. Shaded areas indicate positive anomalies. Long-term mean SST's for December to February, March to May, June to August, and September to November are presented at the end of this appendix. The first three numbers in each column represent the respective values at that location for the three months at the bottom of each figure. The fourth number is the seasonal mean.

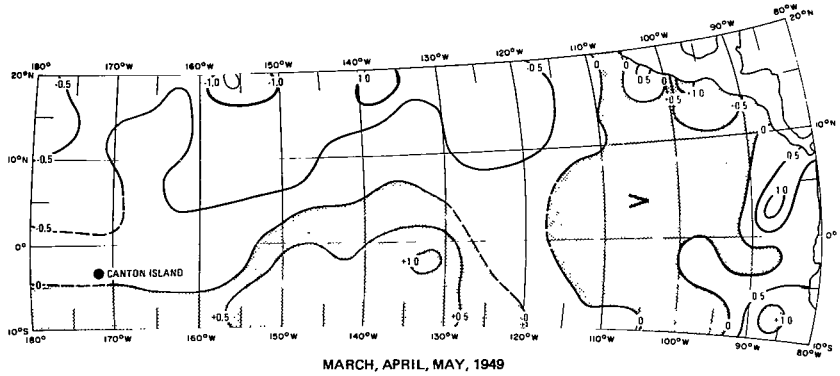

MARCH, APRIL, MAY, 1949

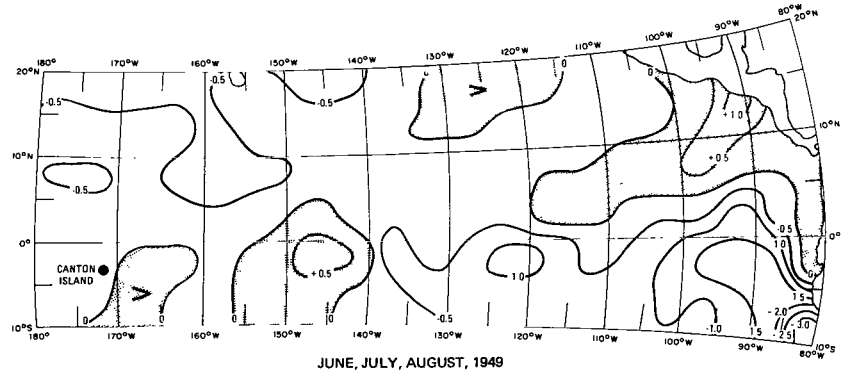

JUNE, JULY, AUGUST, 1949

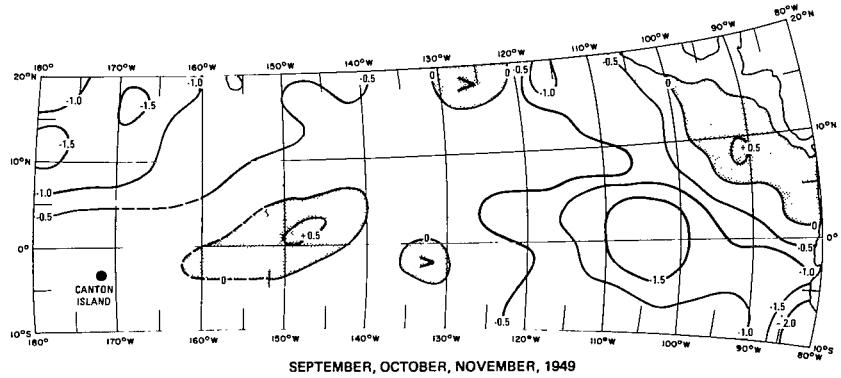

SEPTEMBER, OCTOBER, NOVEMBER, 1949

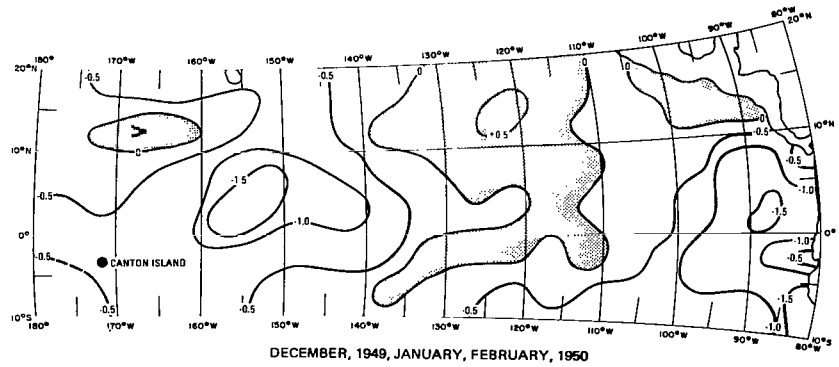

DECEMBER, 1949, JANUARY, FEBRUARY, 1950

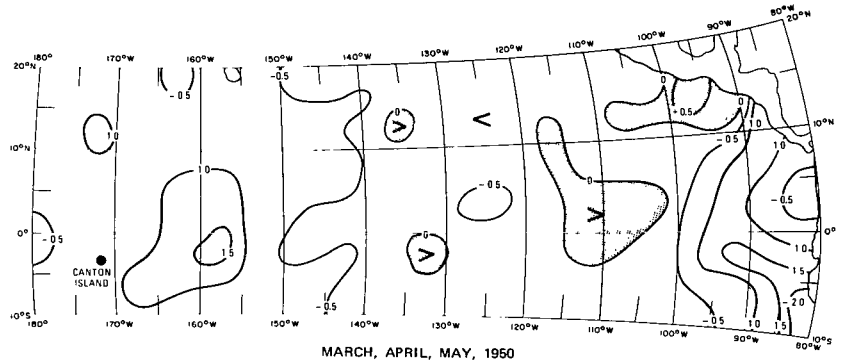

MARCH, APRIL, MAY, 1950

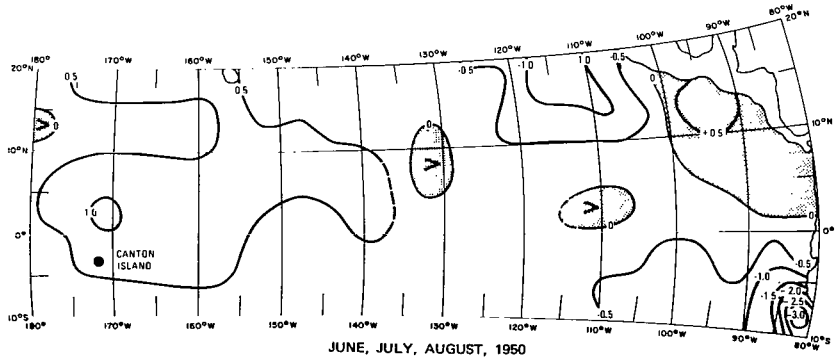

JUNE, JULY, AUGUST, 1950

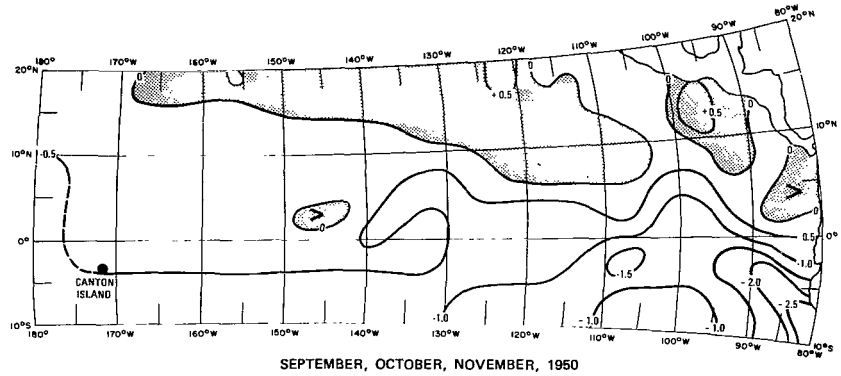

SEPTEMBER, OCTOBER, NOVEMBER, 1950

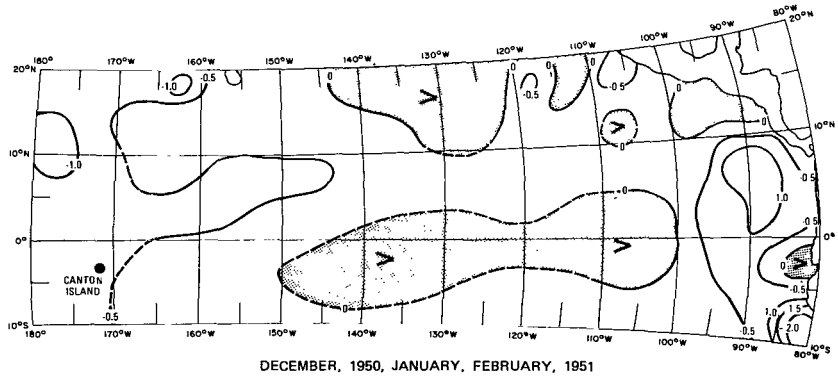

DECEMBER, 1950, JANUARY, FEBRUARY, 1951

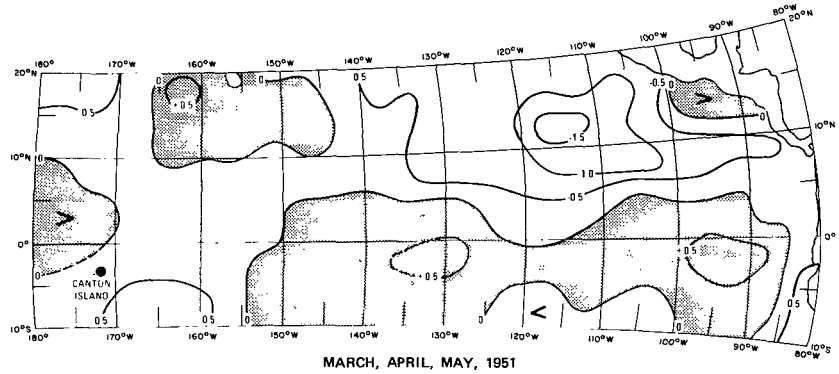

MARCH, APRIL, MAY, 1951

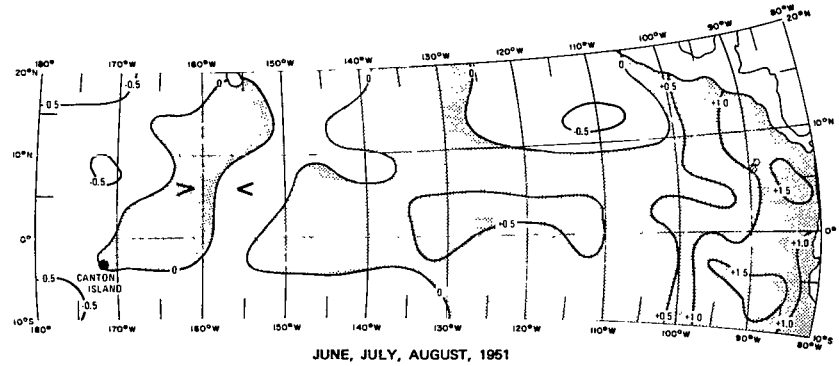

JUNE, JULY, AUGUST, 1951

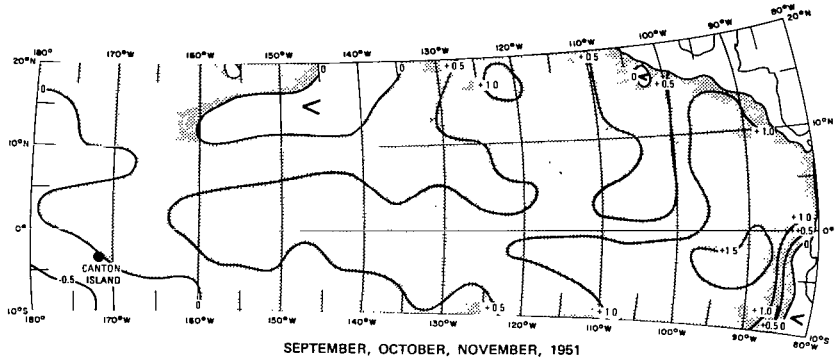

SEPTEMBER, OCTOBER, NOVEMBER, 1951

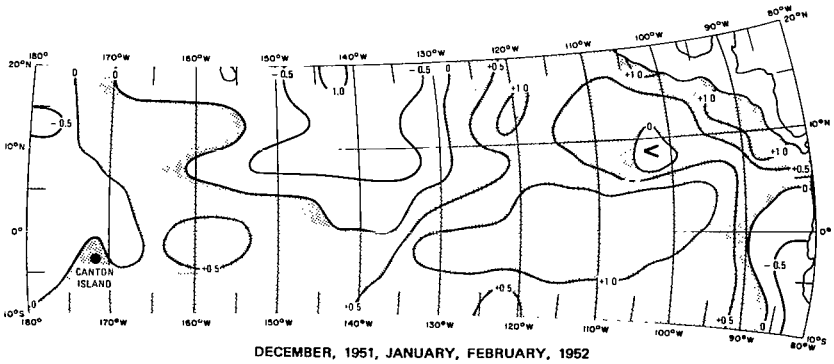

DECEMBER, 1951, JANUARY, FEBRUARY, 1952

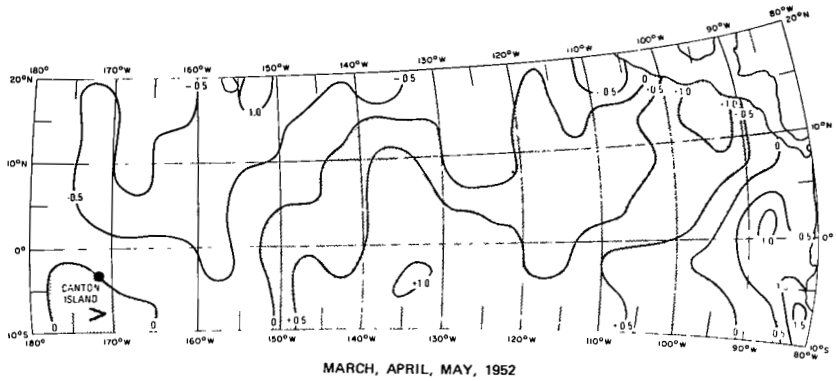

MARCH, APRIL, MAY, 1952

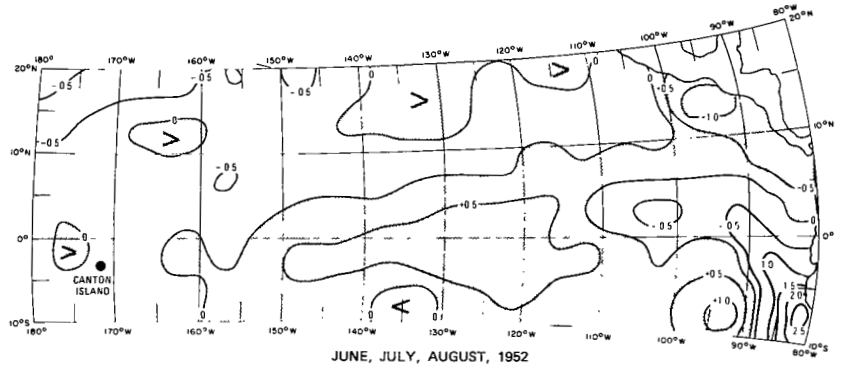

JUNE, JULY, AUGUST, 1952

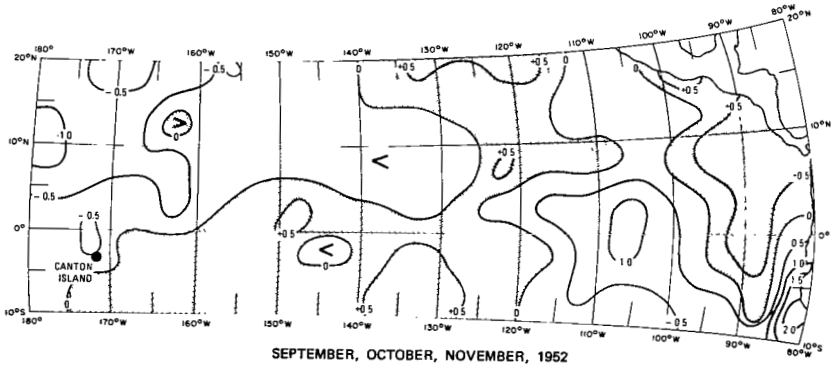

SEPTEMBER, OCTOBER, NOVEMBER, 1952

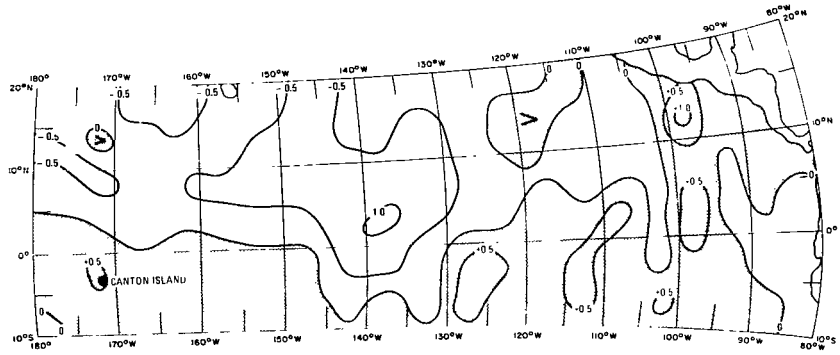

DECEMBER, 1952, JANUARY, FEBRUARY, 1953

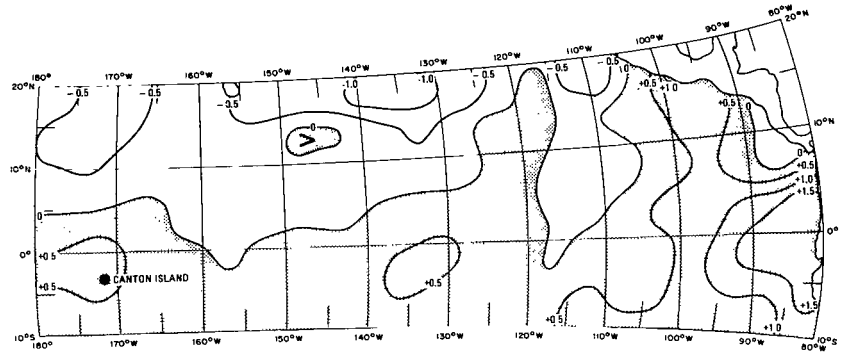

MARCH, APRIL, MAY, 1953

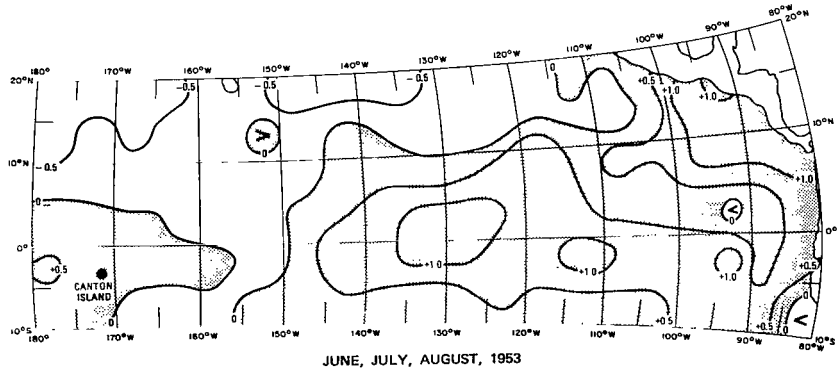

JUNE, JULY, AUGUST, 1953

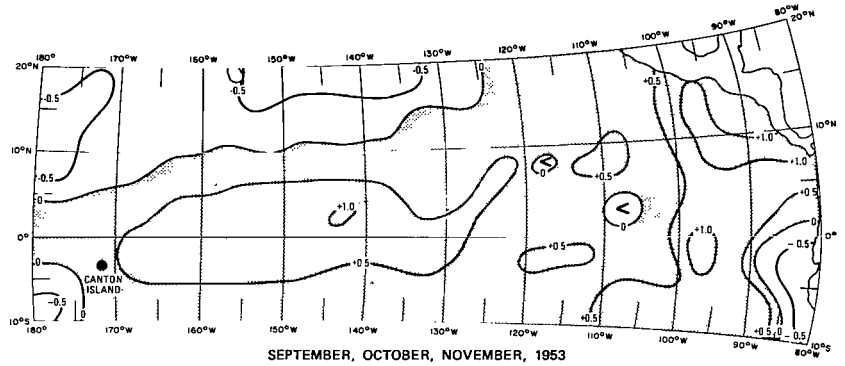

SEPTEMBER, OCTOBER, NOVEMBER, 1953

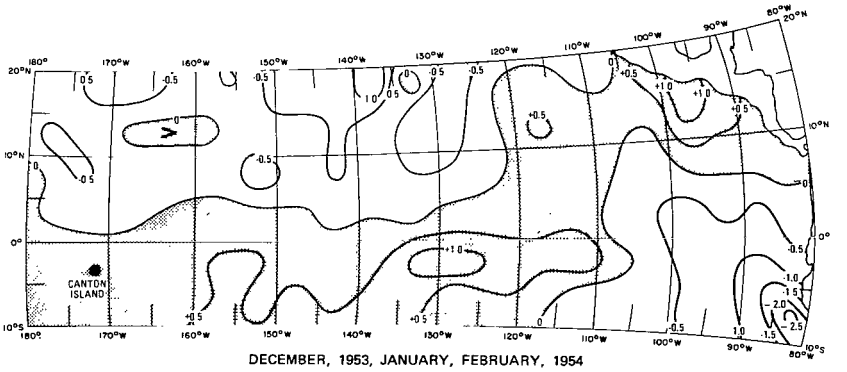

DECEMBER, 1953, JANUARY, FEBRUARY, 1954

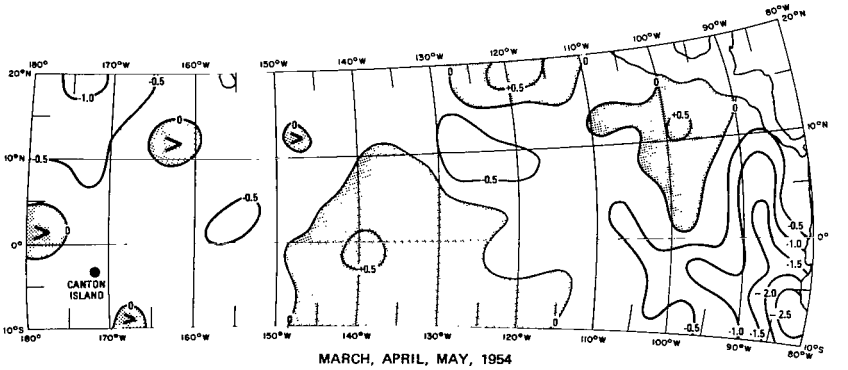

MARCH, APRIL, MAY, 1954

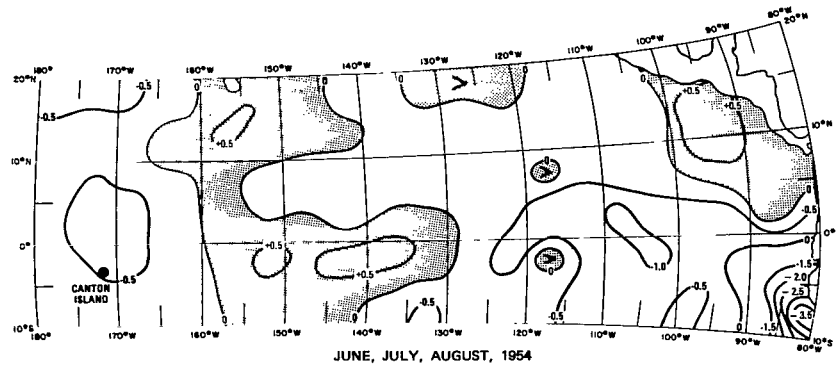

JUNE, JULY, AUGUST, 1954

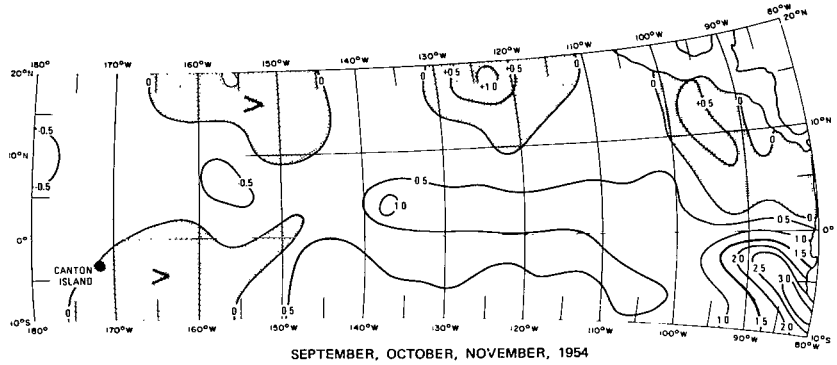

SEPTEMBER, OCTOBER, NOVEMBER, 1954

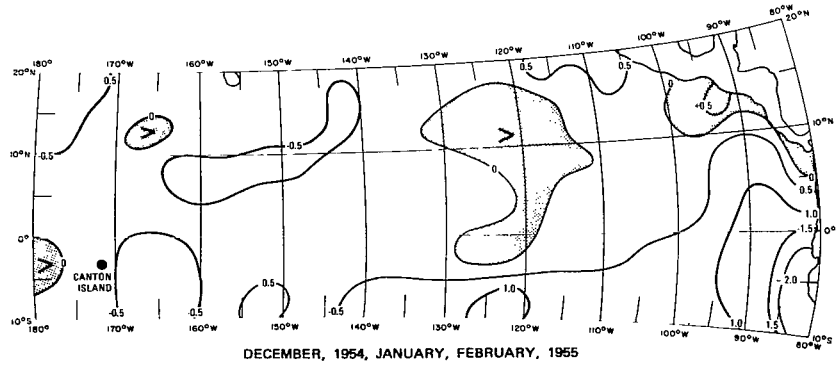

DECEMBER, 1954, JANUARY, FEBRUARY, 1955

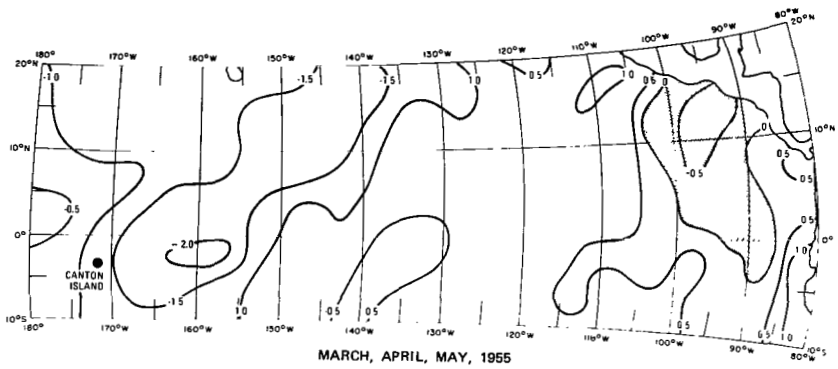

MARCH, APRIL, MAY, 1955

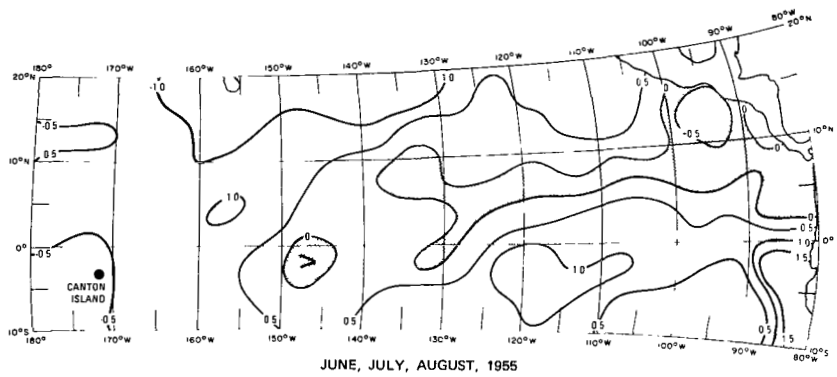

JUNE, JULY, AUGUST, 1955

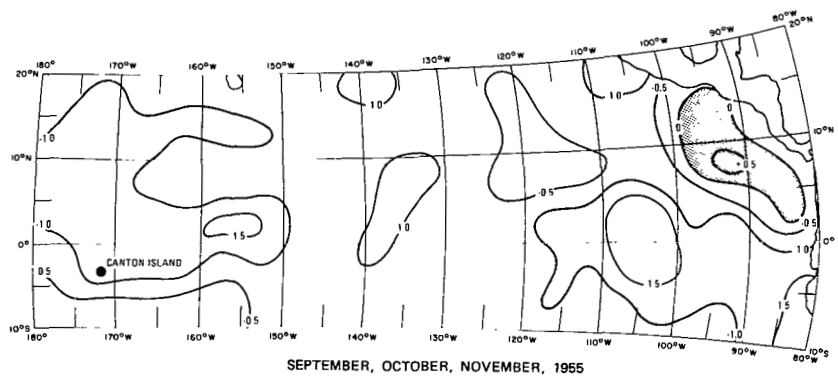

SEPTEMBER, OCTOBER, NOVEMBER, 1955

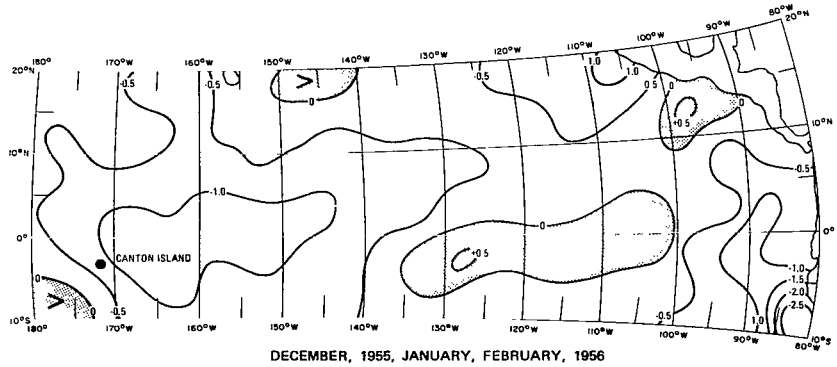

DECEMBER, 1955, JANUARY, FEBRUARY, 1956

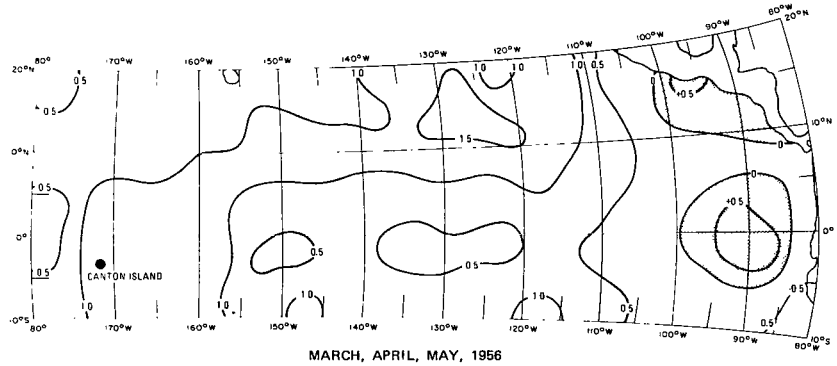

MARCH, APRIL, MAY, 1956

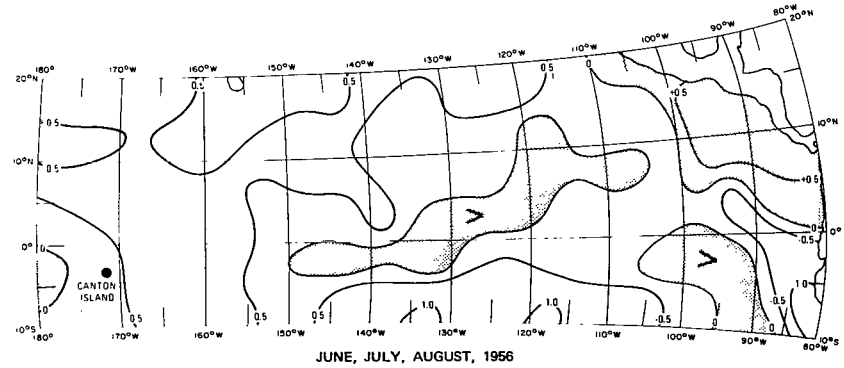

JUNE, JULY, AUGUST, 1956

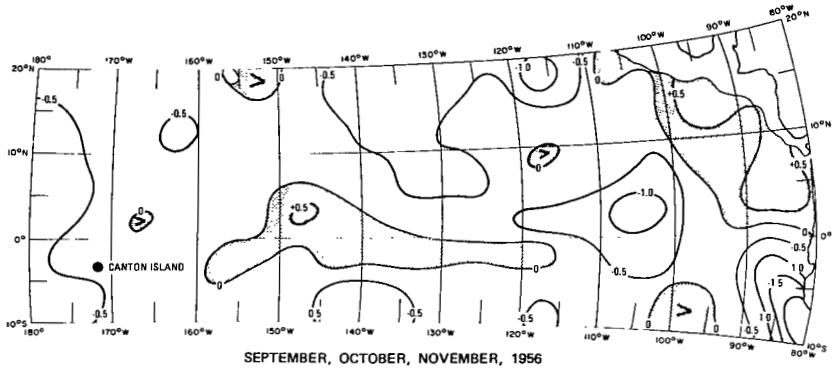

SEPTEMBER, OCTOBER, NOVEMBER, 1956

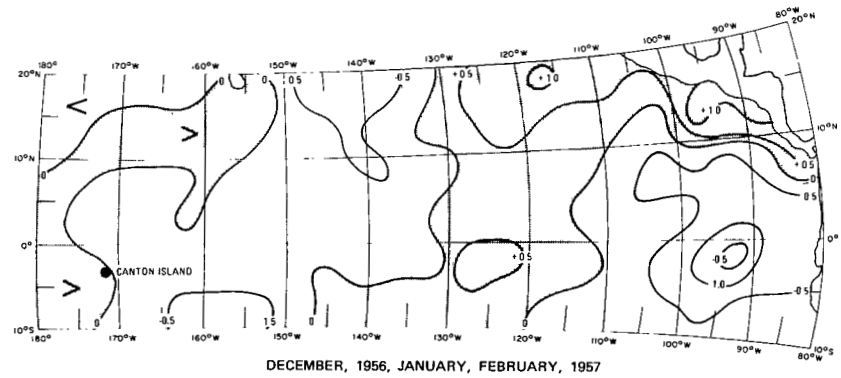

DECEMBER, 1956, JANUARY, FEBRUARY, 1957

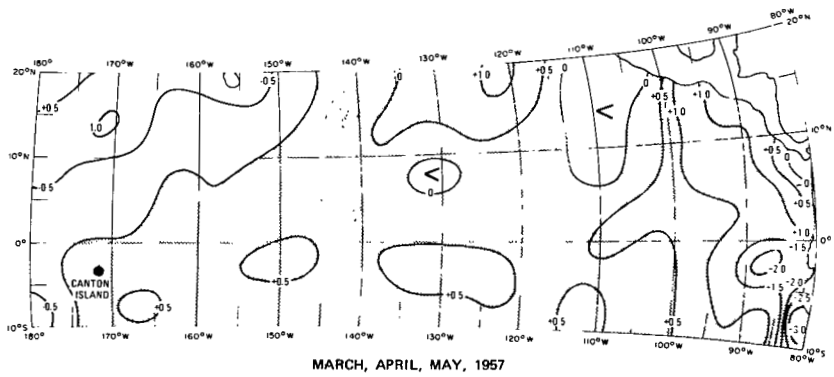

MARCH, APRIL, MAY, 1957

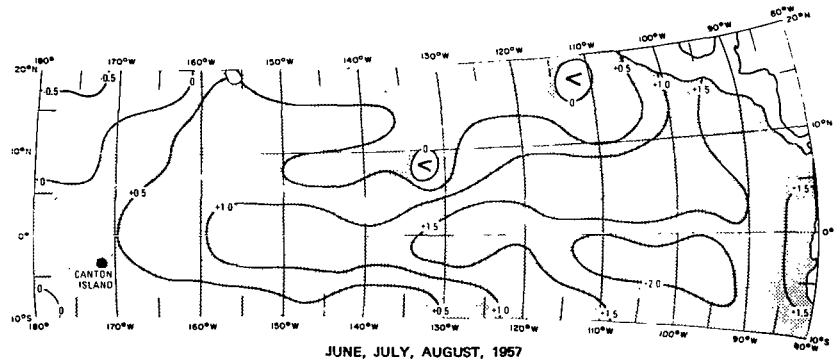

JUNE, JULY, AUGUST, 1957

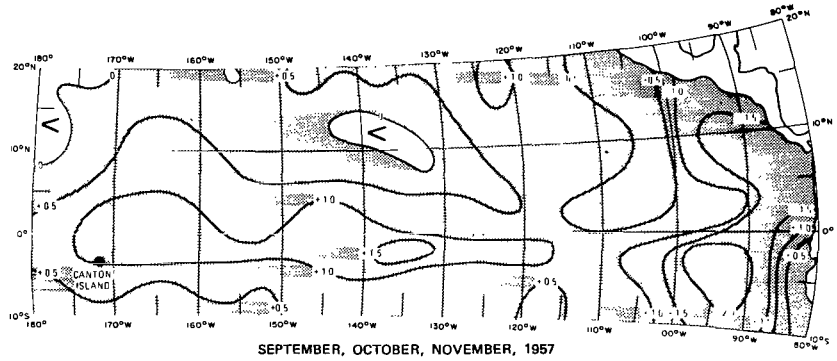

SEPTEMBER, OCTOBER, NOVEMBER, 1957

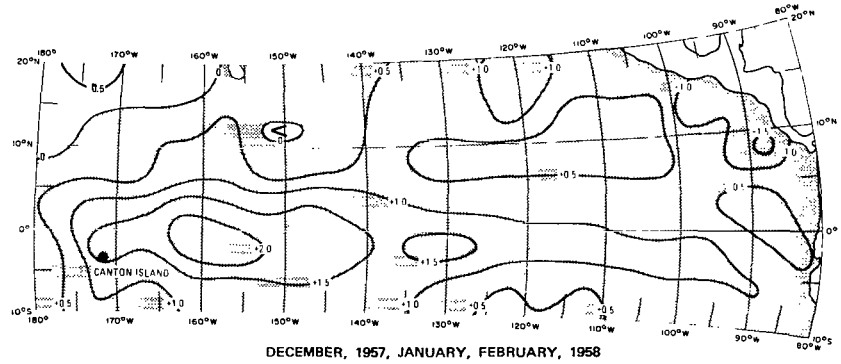

DECEMBER, 1957, JANUARY, FEBRUARY, 1958

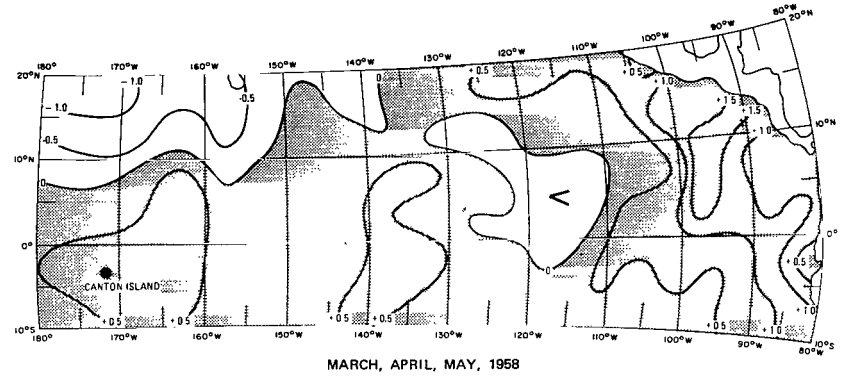

MARCH, APRIL, MAY, 1958

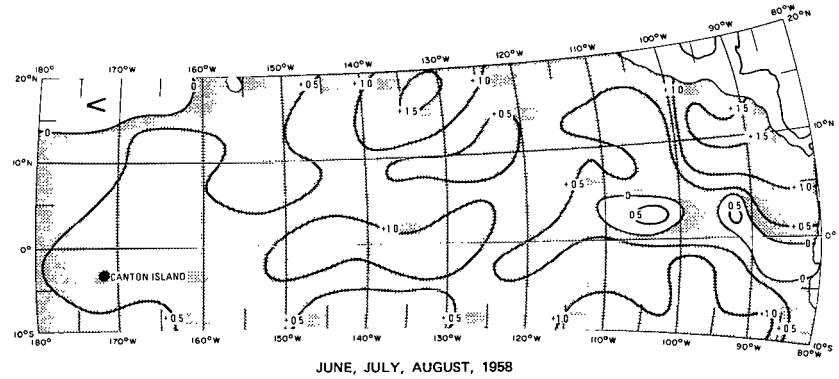

JUNE, JULY, AUGUST, 1958

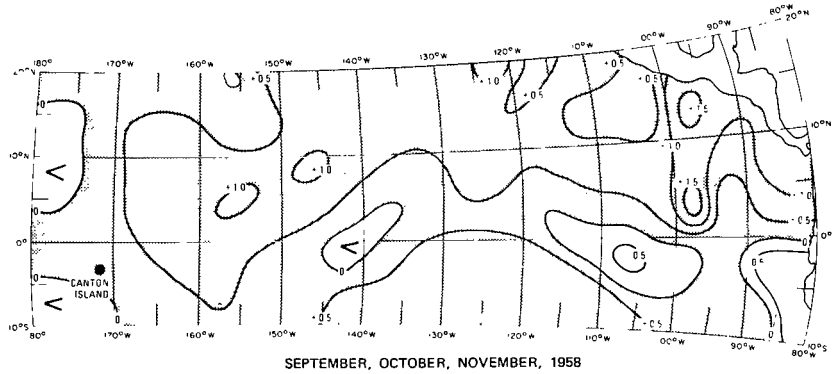

SEPTEMBER, OCTOBER, NOVEMBER, 1958

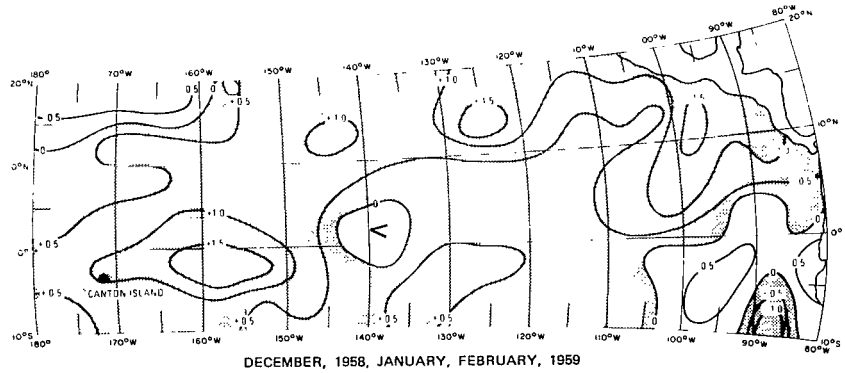

DECEMBER, 1958, JANUARY, FEBRUARY, 1959

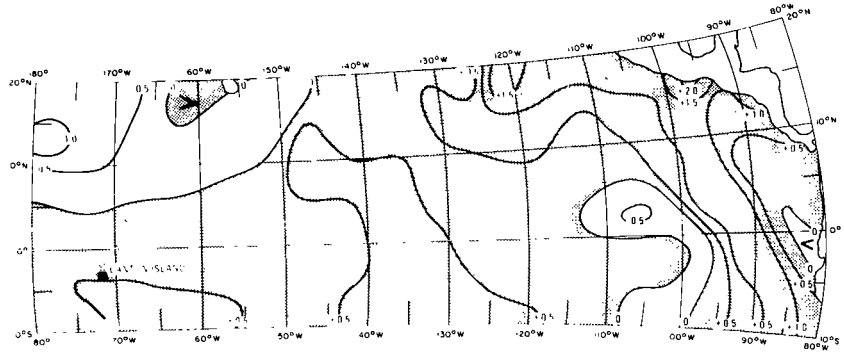

MARCH, APRIL, MAY, 1959

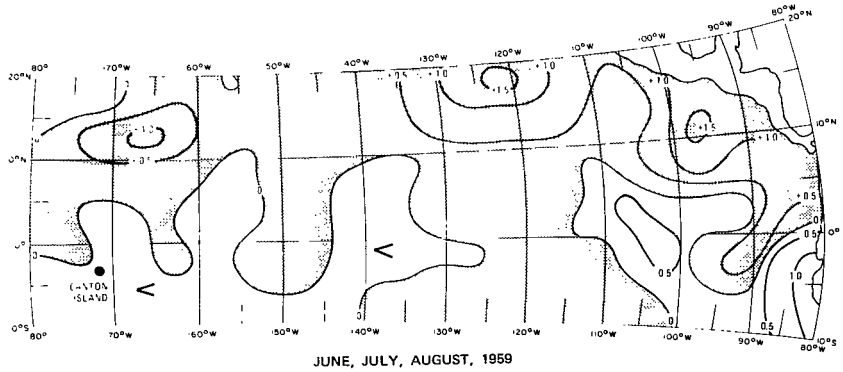

JUNE, JULY, AUGUST, 1959

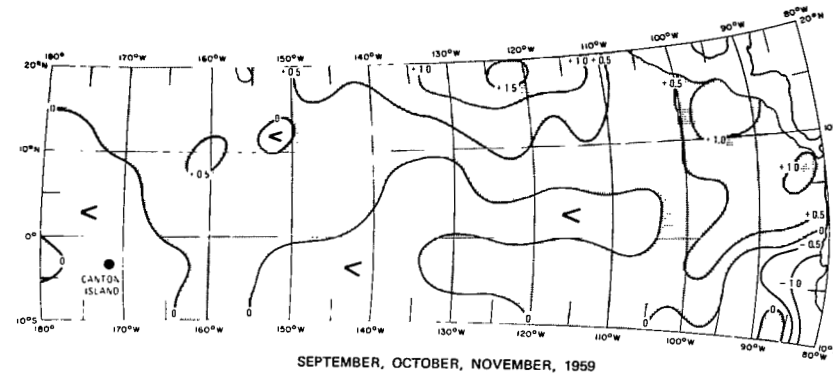

SEPTEMBER, OCTOBER, NOVEMBER, 1959

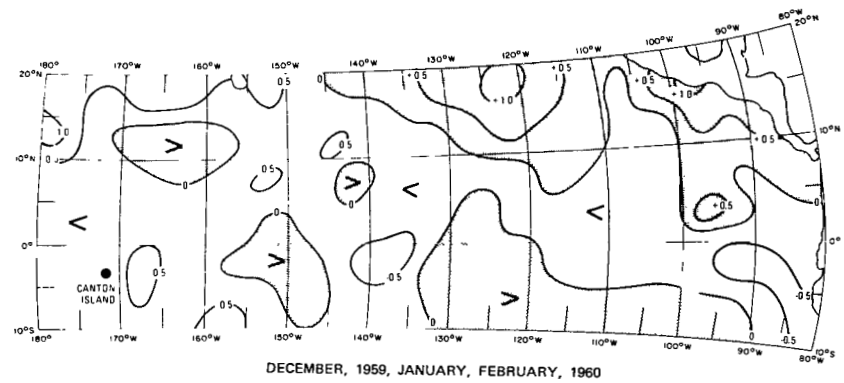

DECEMBER, 1959, JANUARY, FEBRUARY, 1960

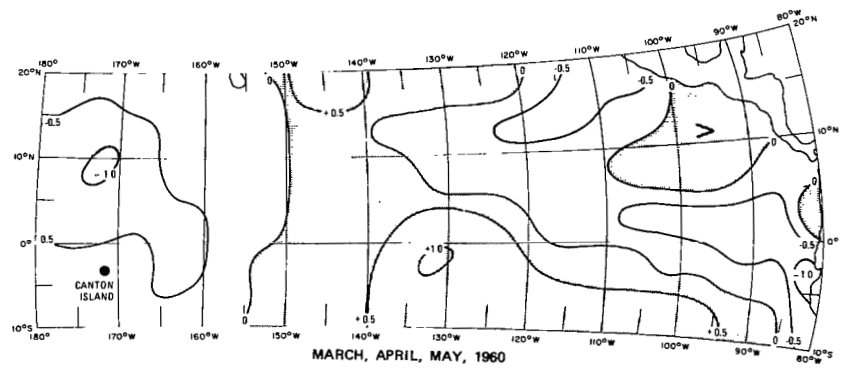

MARCH, APRIL, MAY, 1960

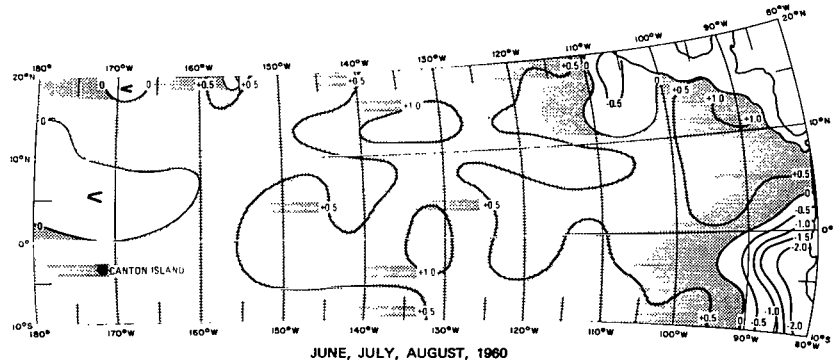

JUNE, JULY, AUGUST, 1960

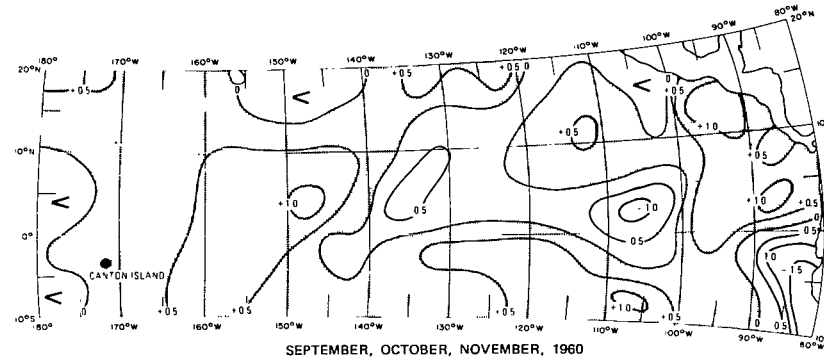

SEPTEMBER, OCTOBER, NOVEMBER, 1960

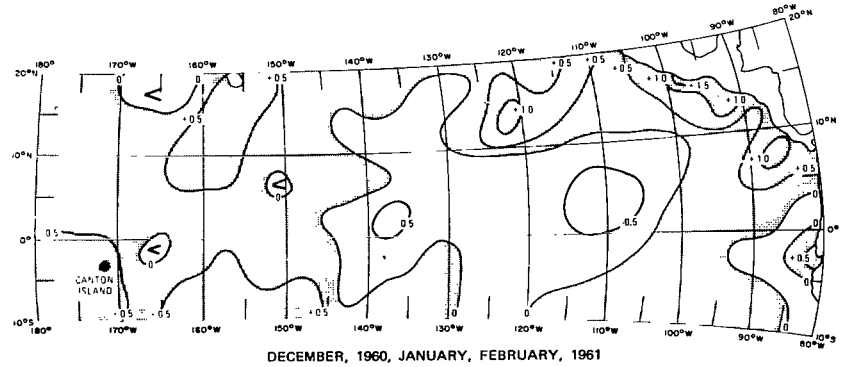

DECEMBER, 1960, JANUARY, FEBRUARY, 1961

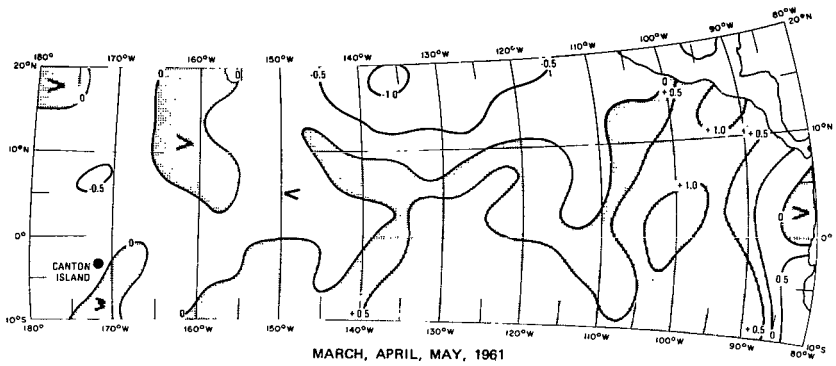

MARCH, APRIL, MAY, 1961

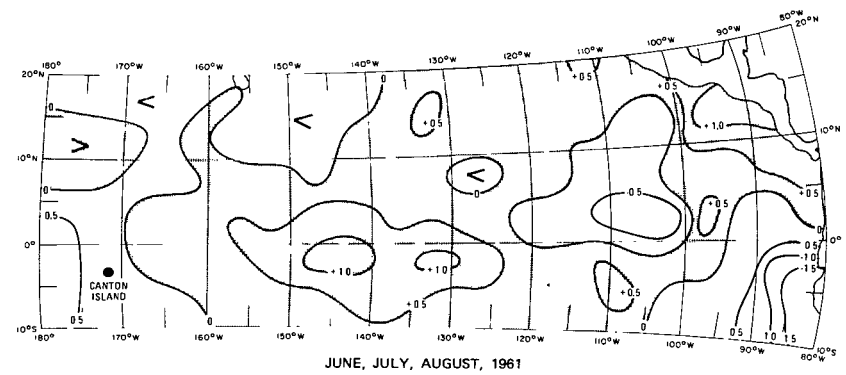

JUNE, JULY, AUGUST, 1961

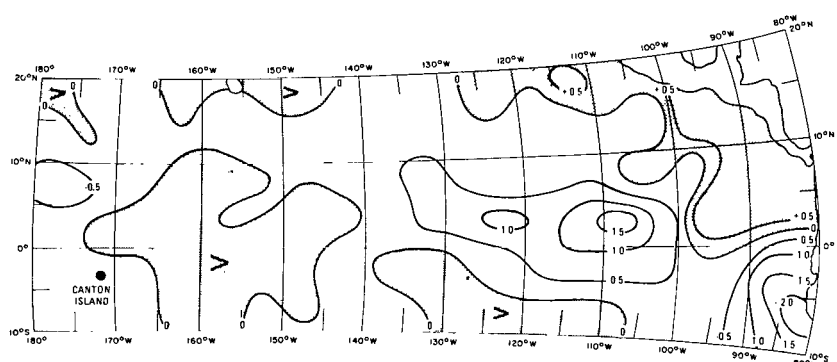

SEPTEMBER, OCTOBER, NOVEMBER, 1961

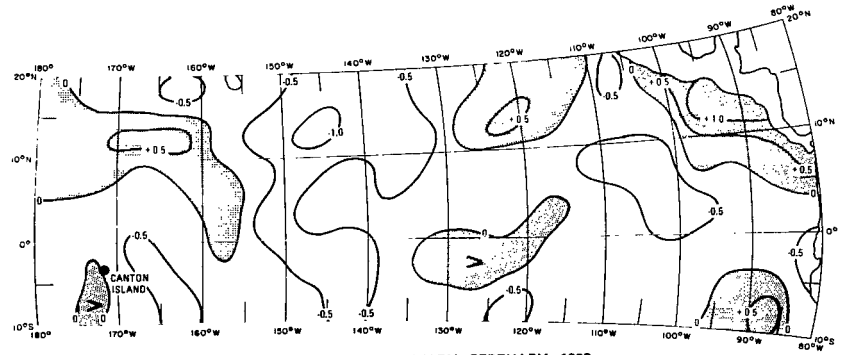

DECEMBER, 1961, JANUARY, FEBRUARY, 1962

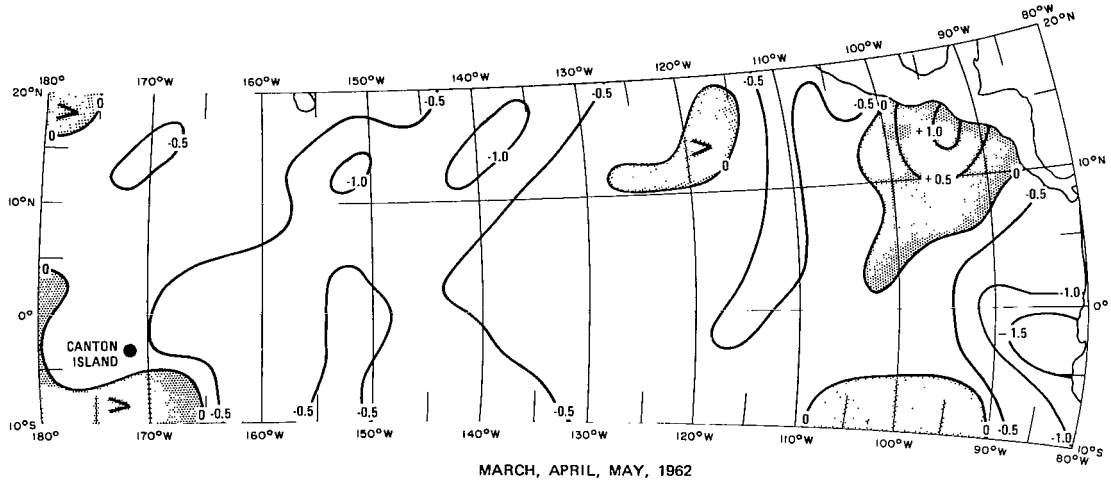

MARCH, APRIL, MAY, 1962

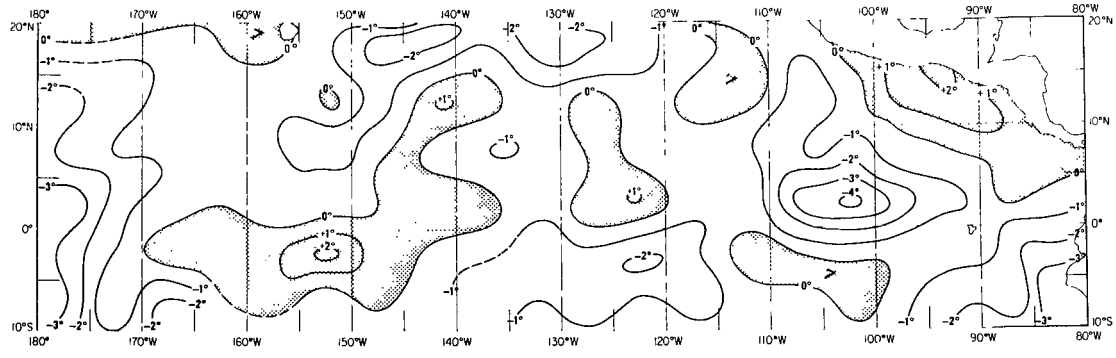

JUNE, JULY, AUGUST, 1962

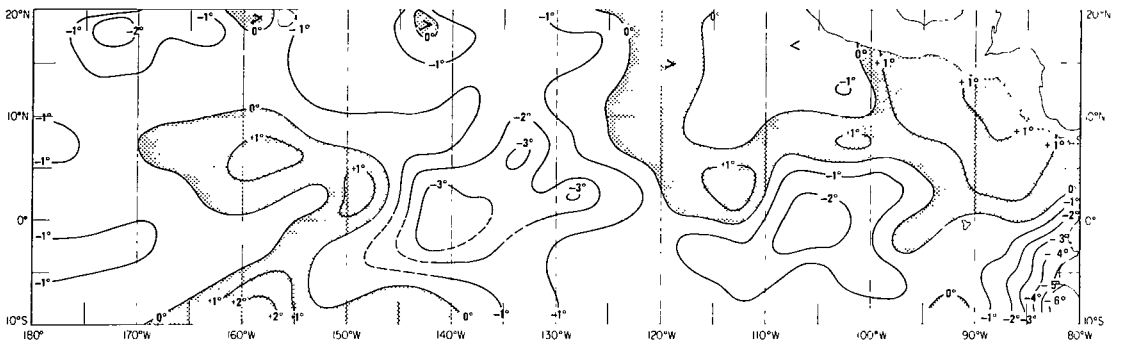

SEPTEMBER, OCTOBER, NOVEMBER, 1962

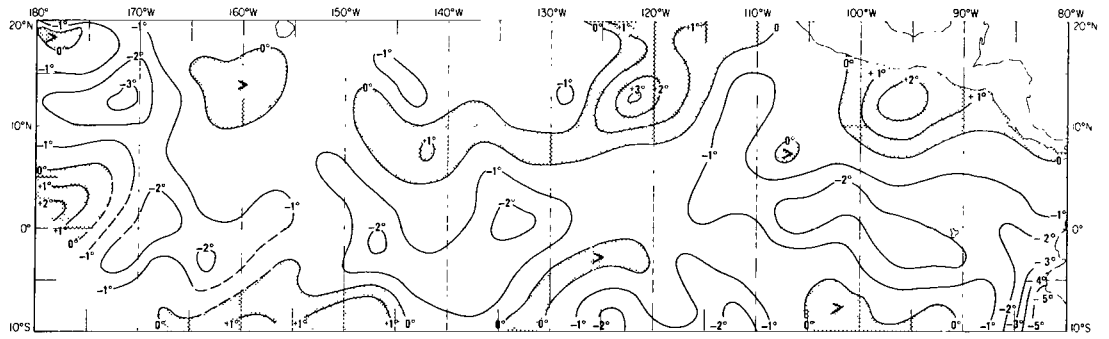

DECEMBER, 1962, JANUARY, FEBRUARY, 1963

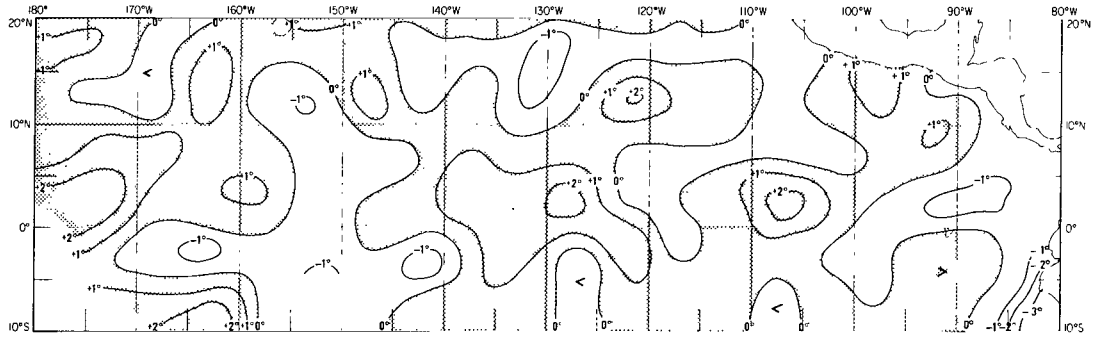

MARCH, APRIL, MAY, 1963

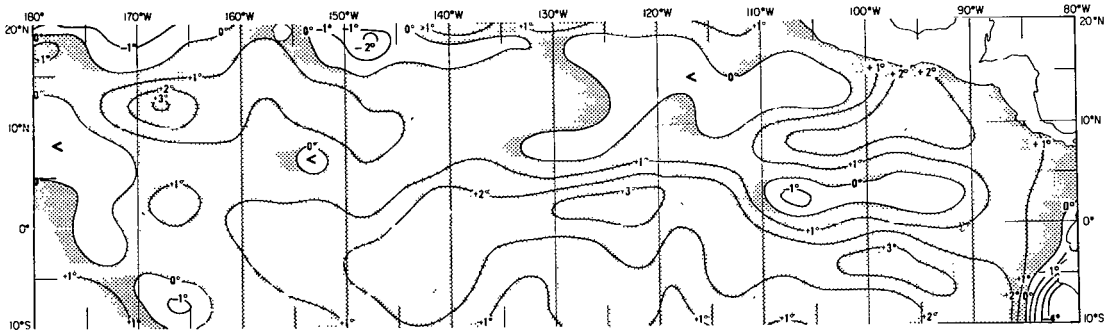

JUNE, JULY, AUGUST, 1963

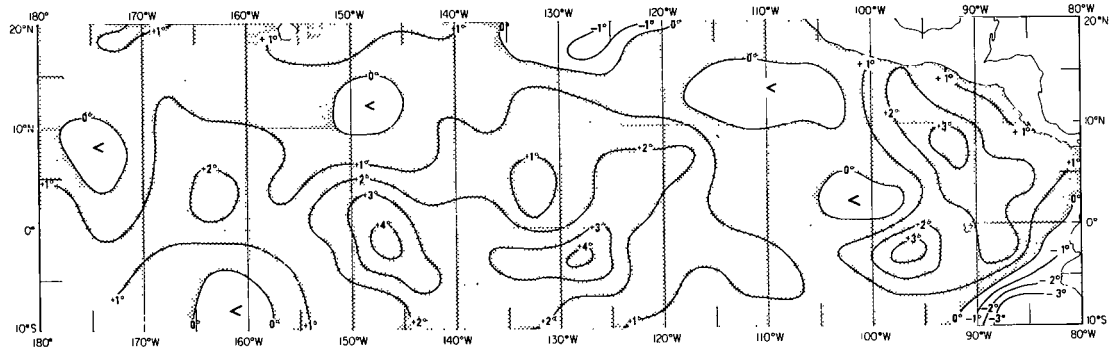

SEPTEMBER, OCTOBER, NOVEMBER, 1963

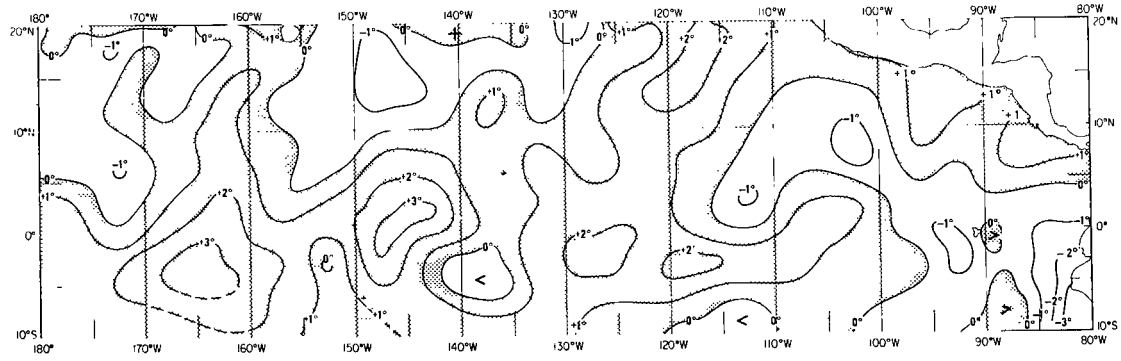

DECEMBER, 1963, JANUARY, FEBRUARY, 1964

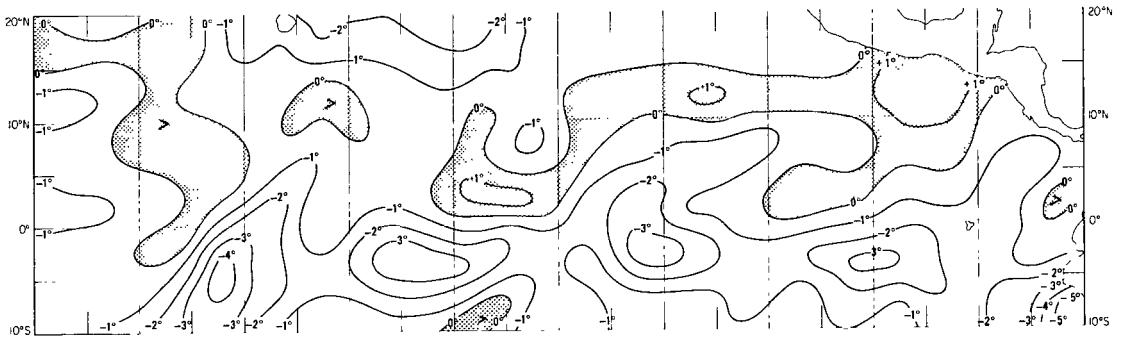

MARCH, APRIL, MAY, 1964

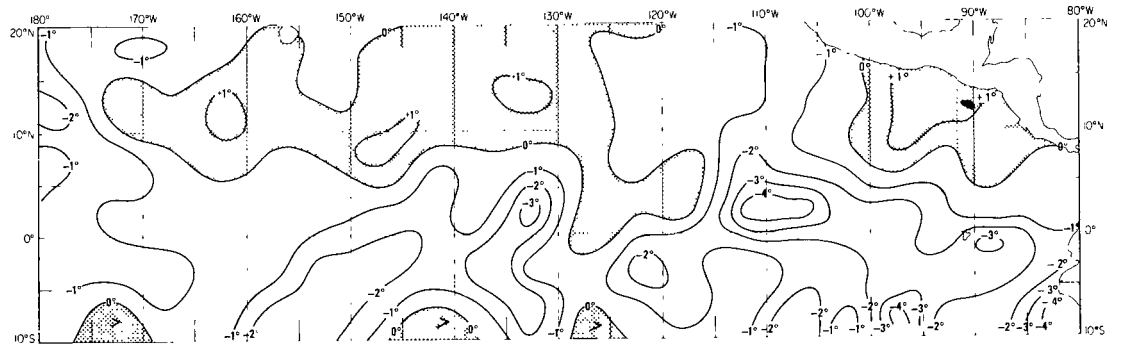

JUNE, JULY, AUGUST, 1964

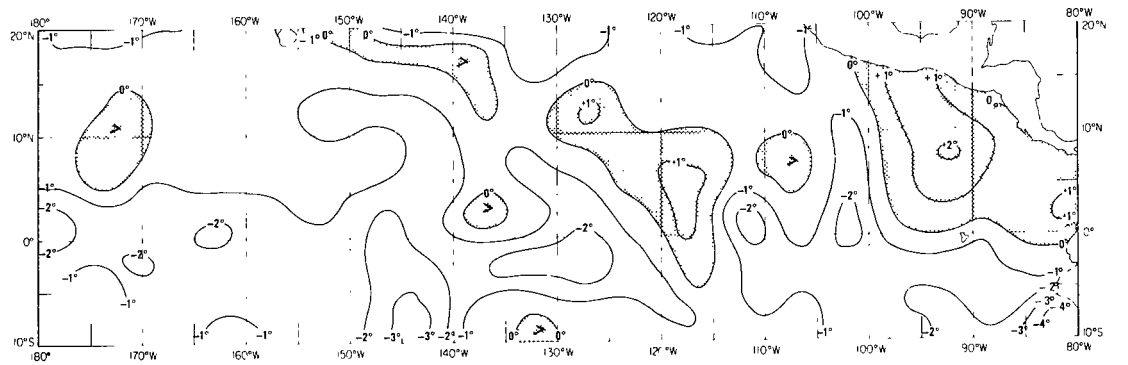

SEPTEMBER, OCTOBER, NOVEMBER, 1964

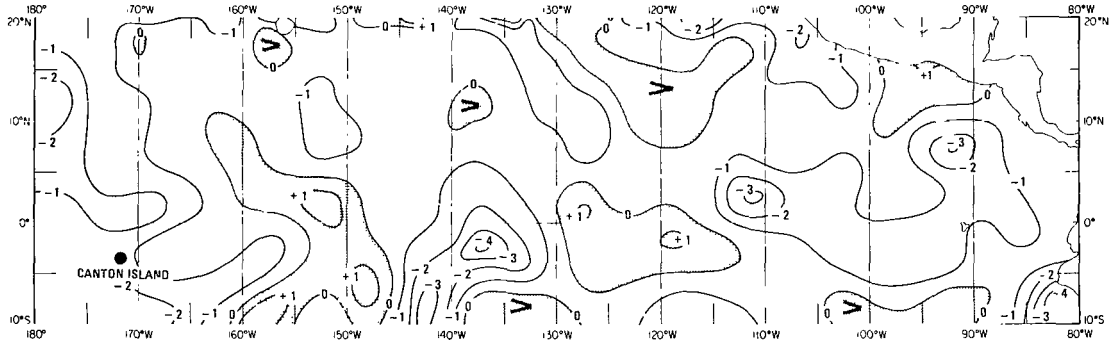

DECEMBER, 1964, JANUARY, FEBRUARY, 1965

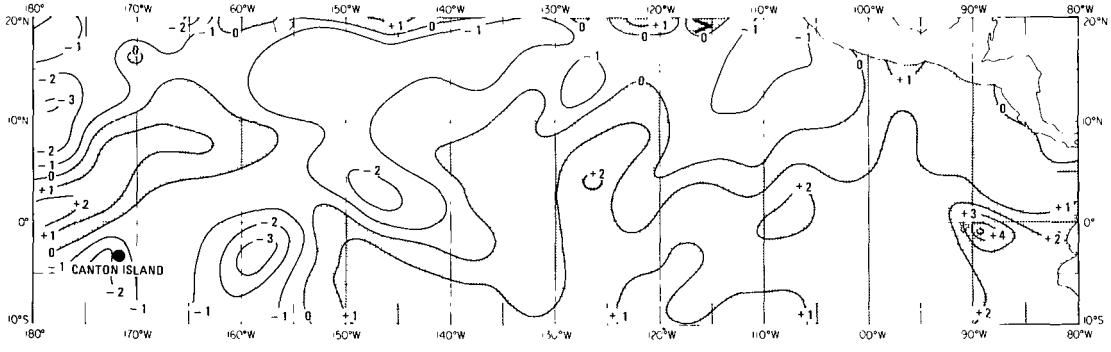

MARCH, APRIL, MAY, 1965

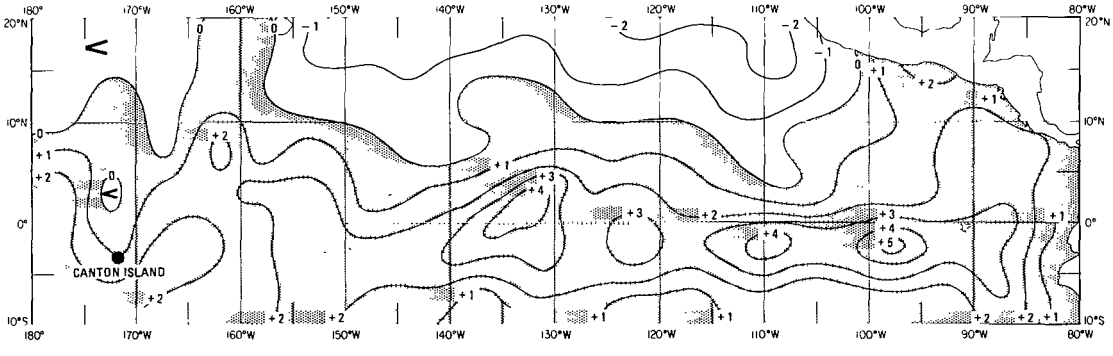

JUNE, JULY, AUGUST, 1965

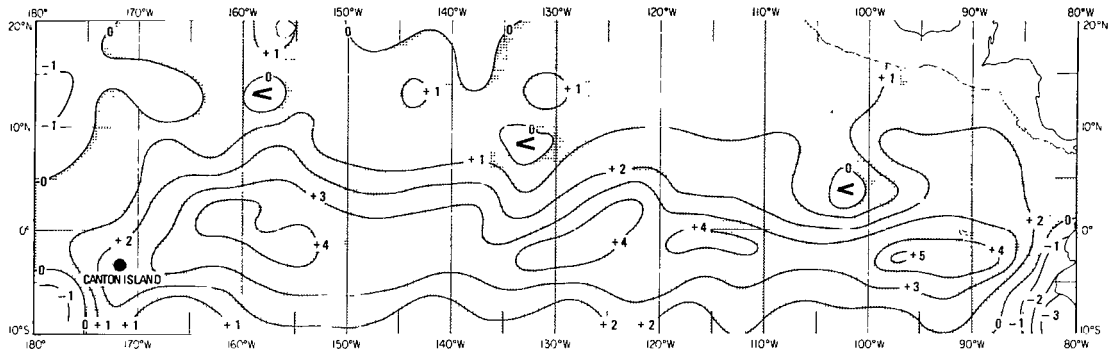

SEPTEMBER, OCTOBER, NOVEMBER, 1965

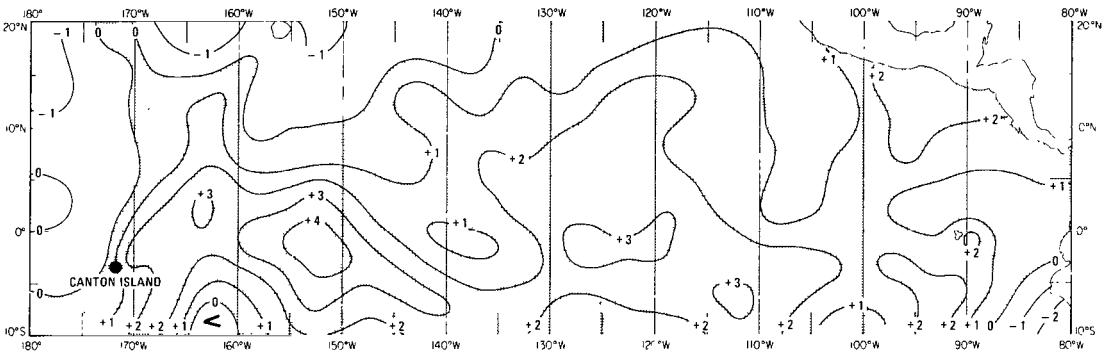

DECEMBER, 1965, JANUARY, FEBRUARY, 1966

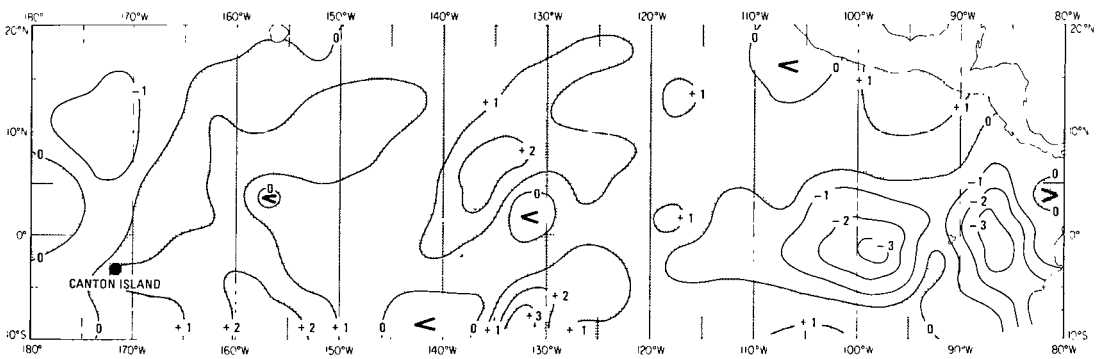

MARCH, APRIL, MAY, 1966

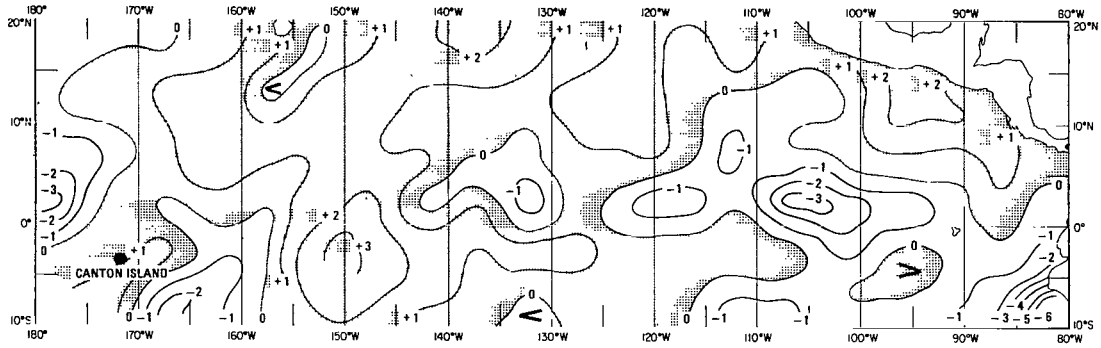

JUNE, JULY, AUGUST, 1966

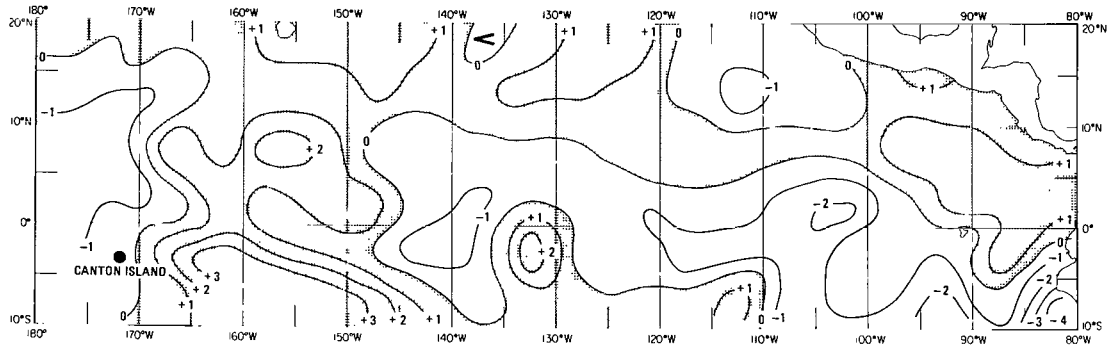

SEPTEMBER, OCTOBER, NOVEMBER, 1966

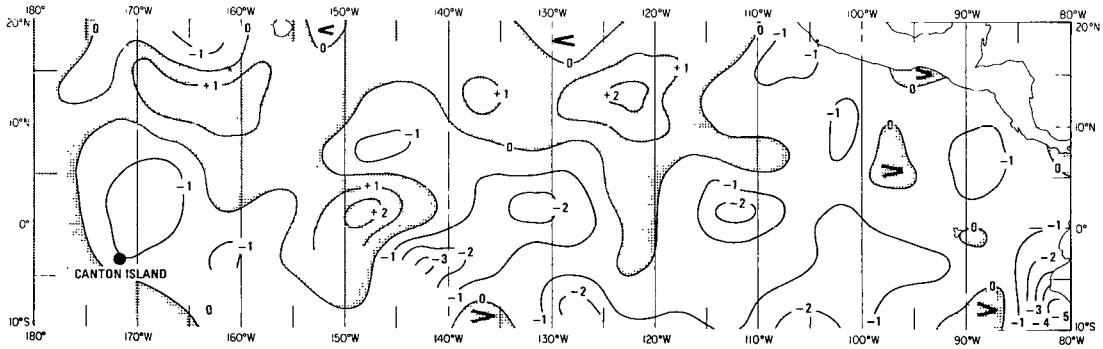

DECEMBER, 1966, JANUARY, FEBRUARY, 1967

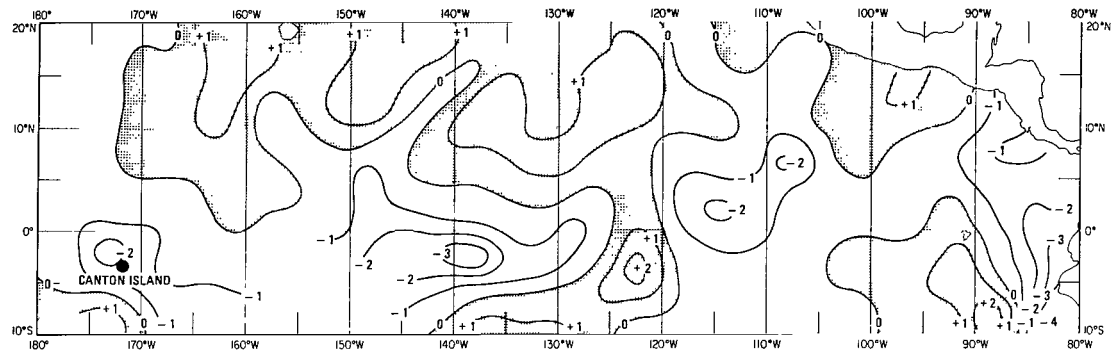

MARCH, APRIL, MAY, 1967

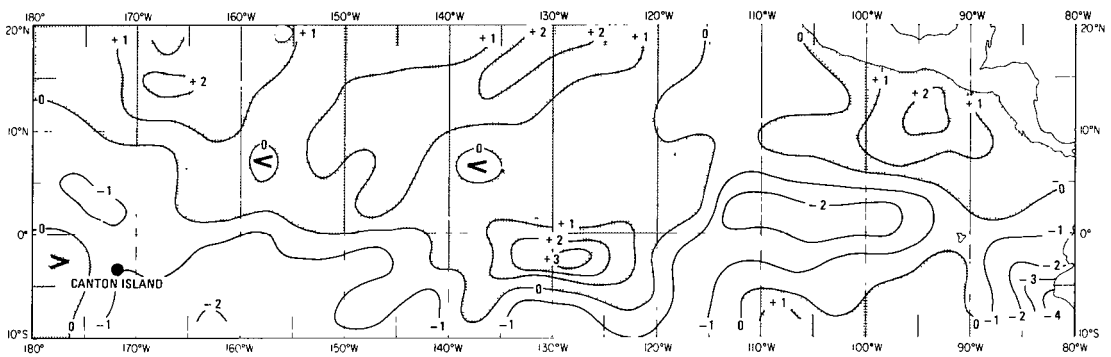

JUNE, JULY, AUGUST, 1967

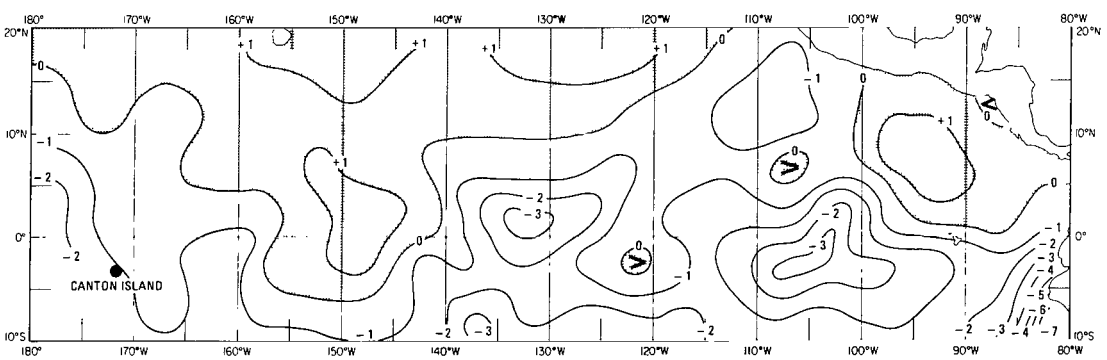

SEPTEMBER, OCTOBER, NOVEMBER, 1967

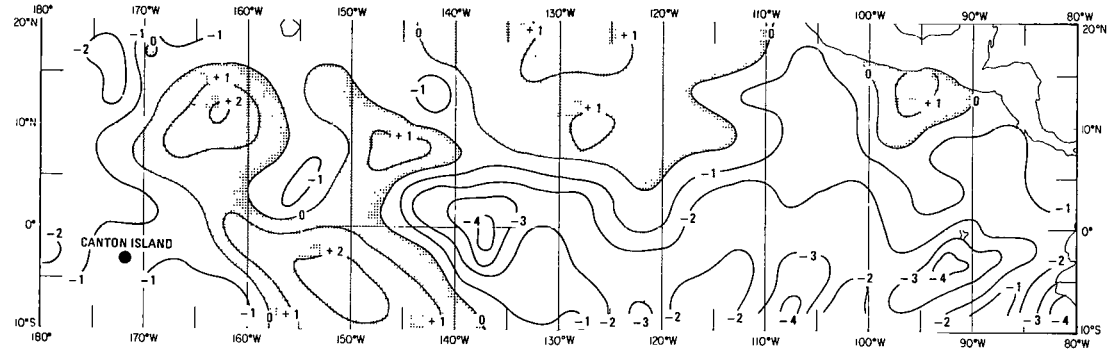

DECEMBER, 1967, JANUARY, FEBRUARY, 1968

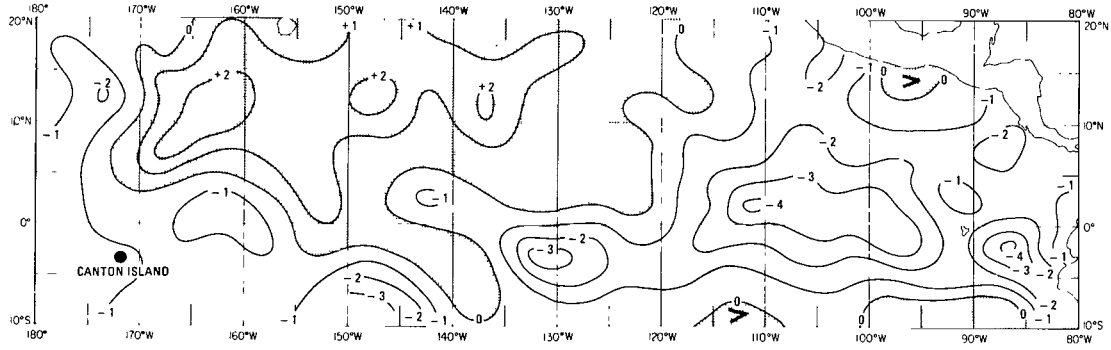

MARCH, APRIL, MAY, 1968

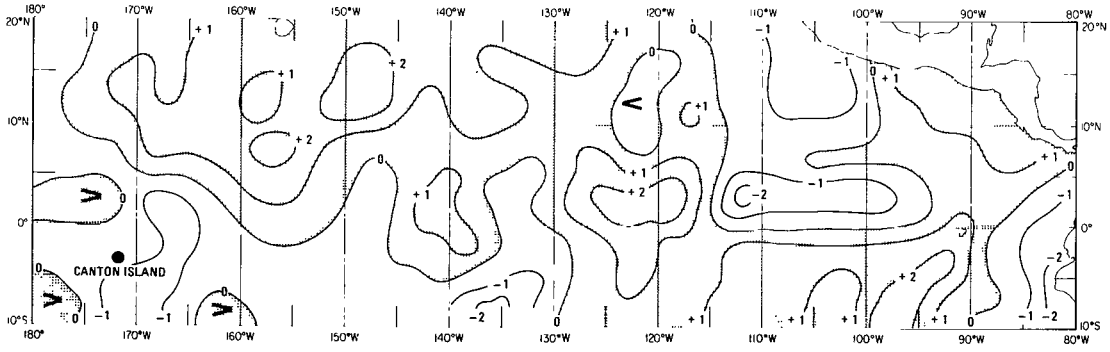

JUNE, JULY, AUGUST, 1968

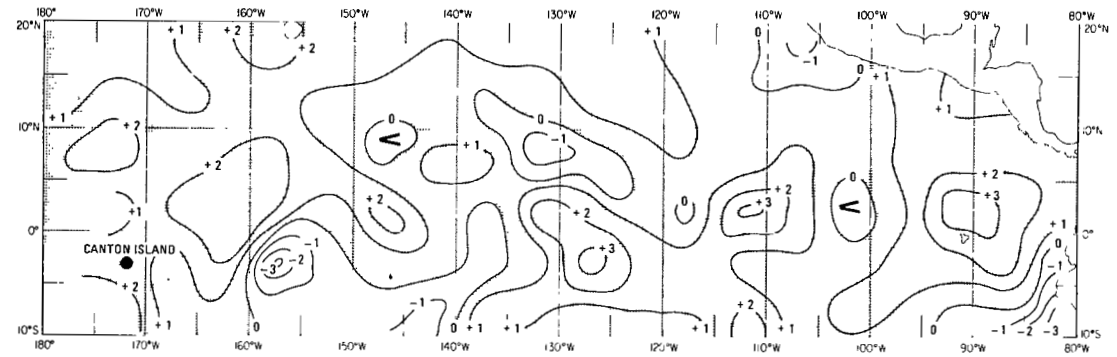

SEPTEMBER, OCTOBER, NOVEMBER, 1968

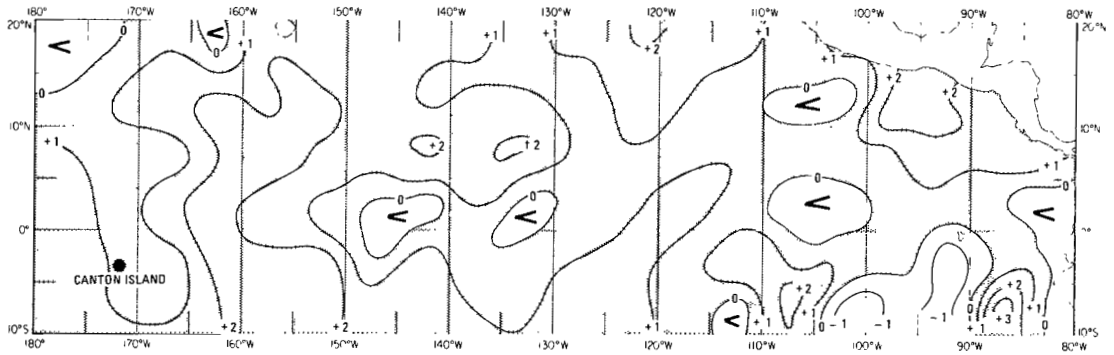

DECEMBER, 1968, JANUARY, FEBRUARY, 1969

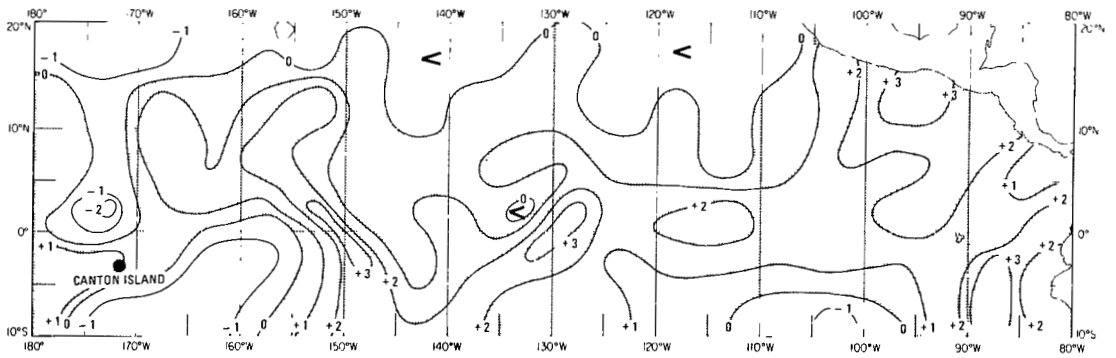

MARCH, APRIL, MAY, 1969

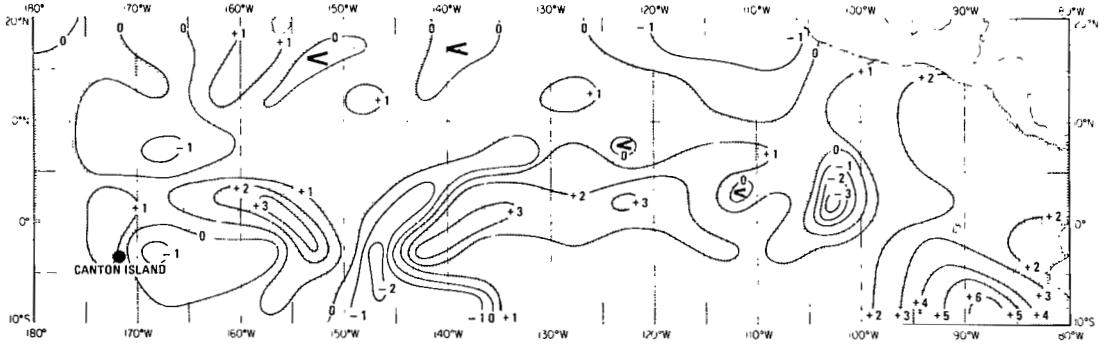

JUNE, JULY, AUGUST, 1969

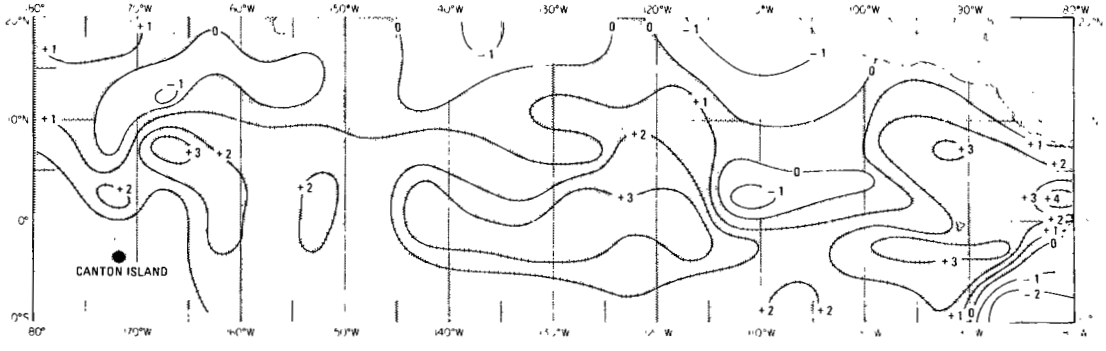

SEPTEMBER, OCTOBER, NOVEMBER, 1969

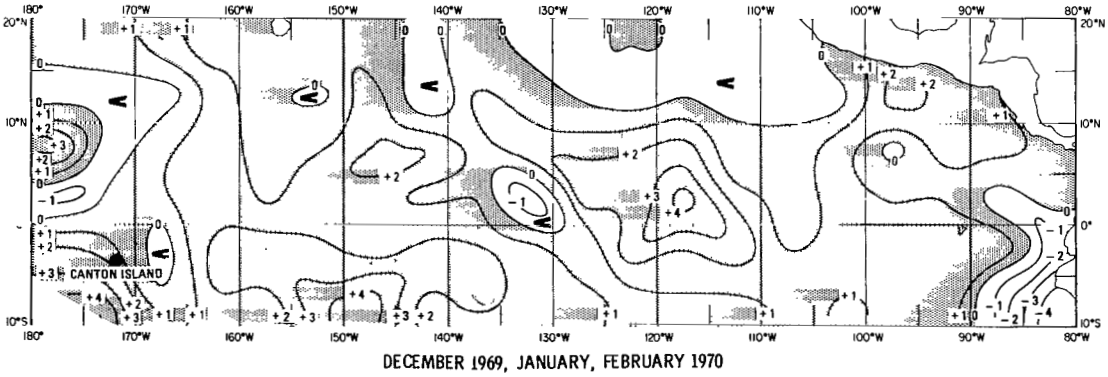

DECEMBER 1969, JANUARY, FEBRUARY 1970

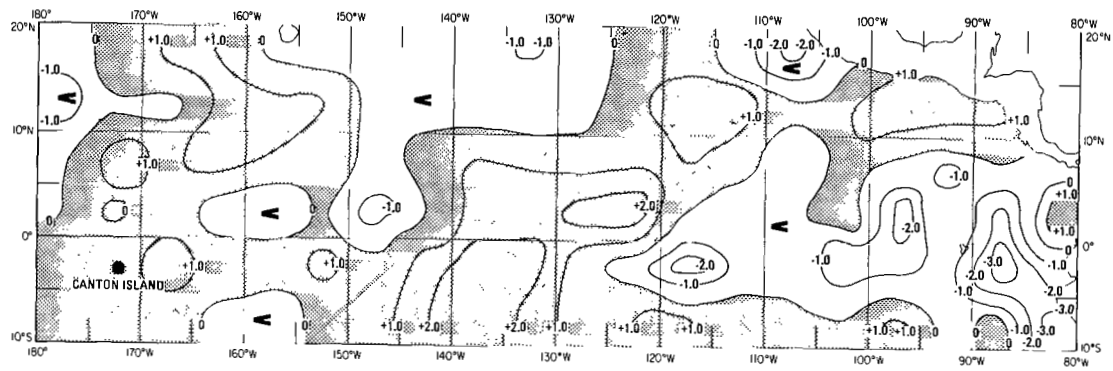

MARCH, APRIL, MAY 1970

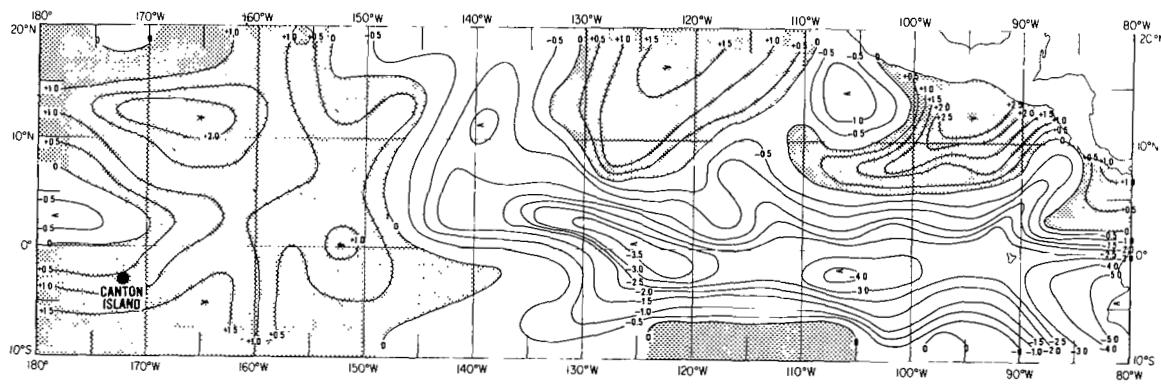

JUNE, JULY, AUGUST, 1970

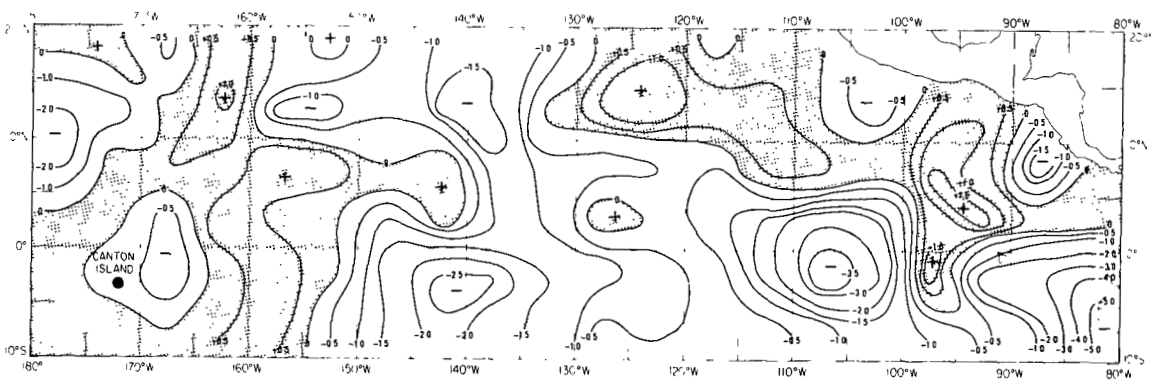

SEPTEMBER, OCTOBER, NOVEMBER, 1970

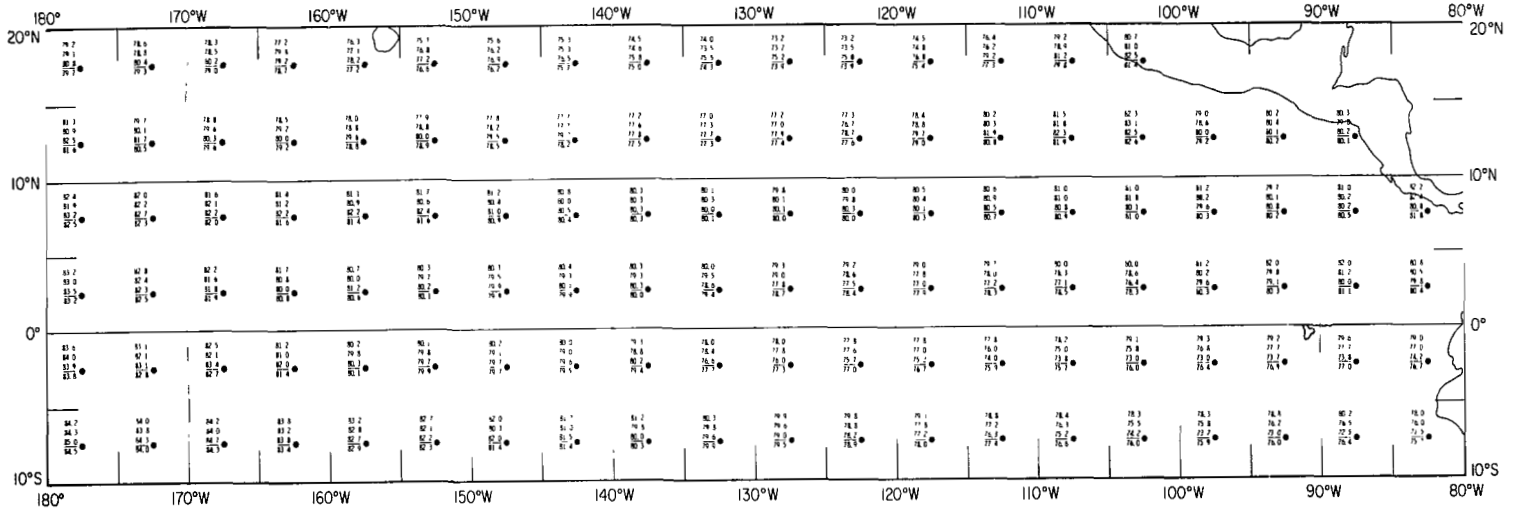

DECEMBER, JANUARY, FEBRUARY

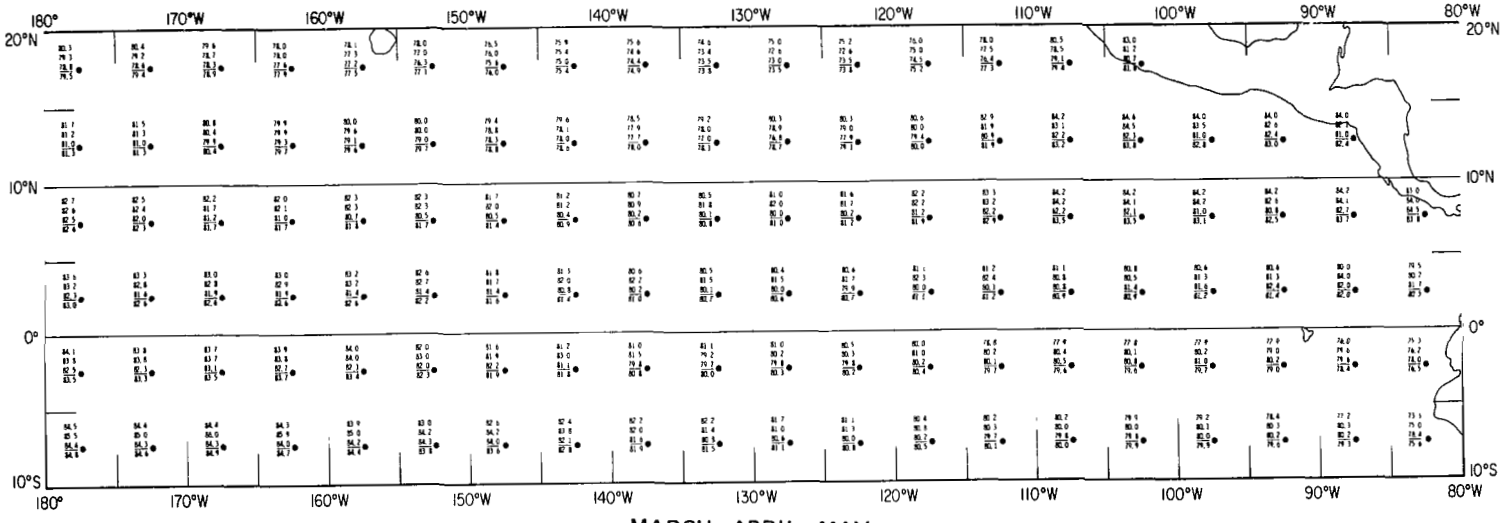

MARCH, APRIL, MAY

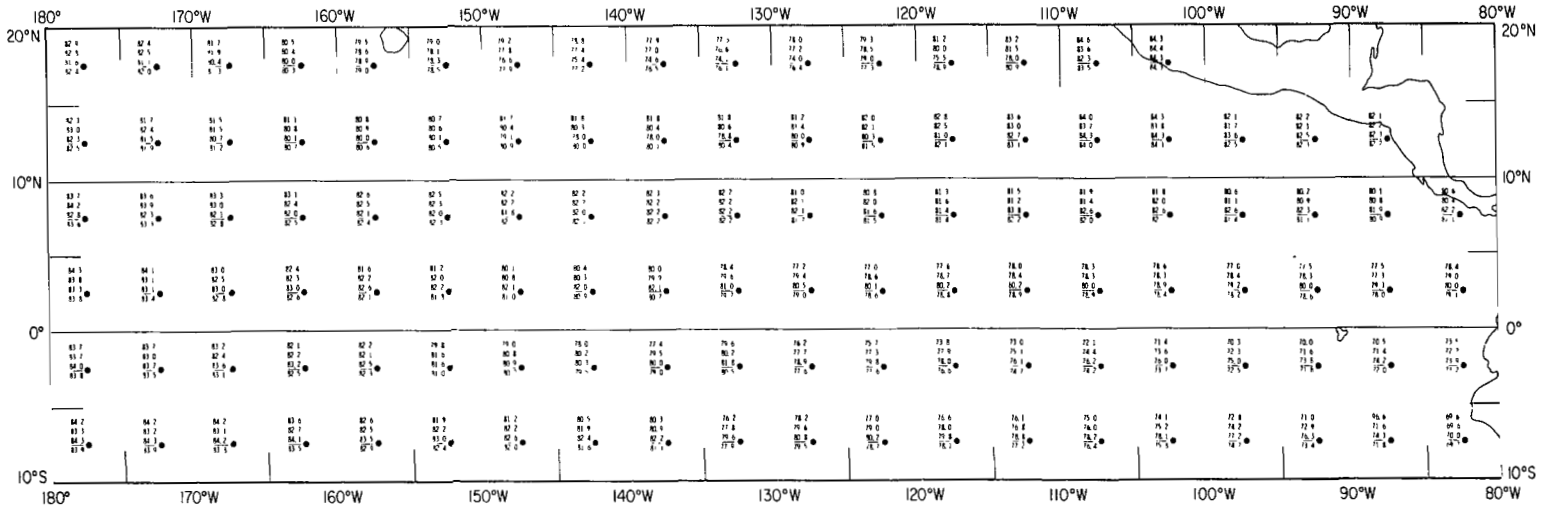

JUNE, JULY, AUGUST

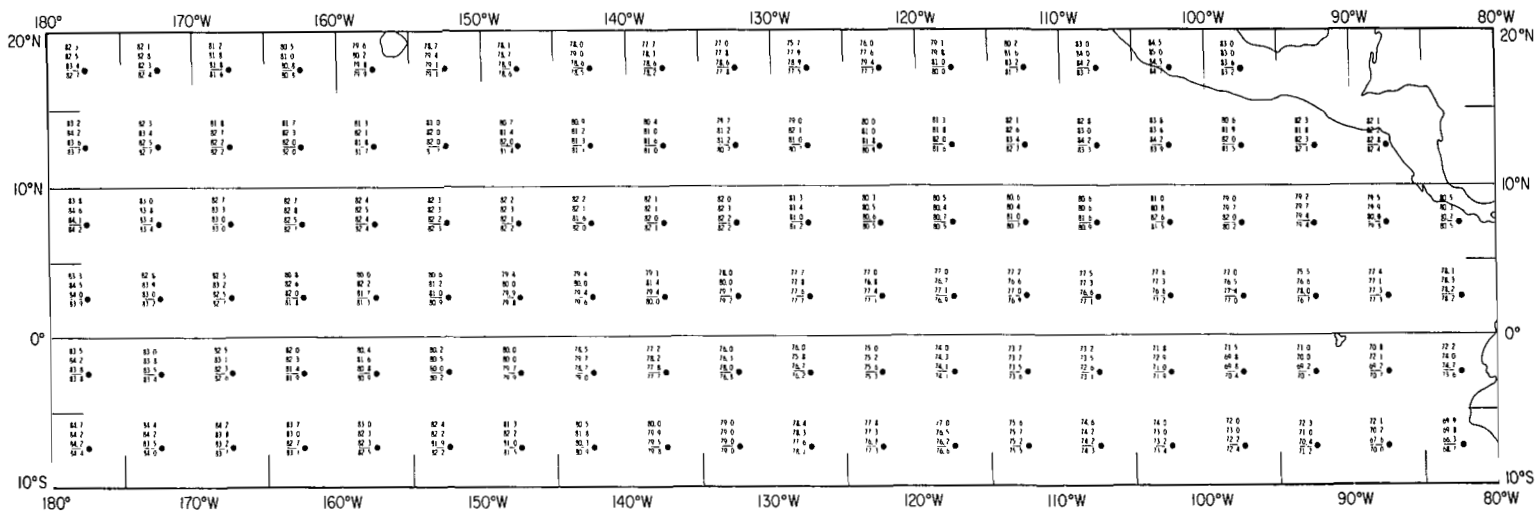

SEPTEMBER, OCTOBER, NOVEMBER

Appendix B

Satellite-Derived Cloudiness and Sea Surface Temperature Anomalies Over the Tropical Pacific Ocean (1962 to 1970)

A comparison of satellite-derived monthly cloudiness (in percent of area covered by $\geq 6/10$ clouds) and 3-month SST anomalies (weighted) from 1962 to 1970 for the regions indicated in each figure.

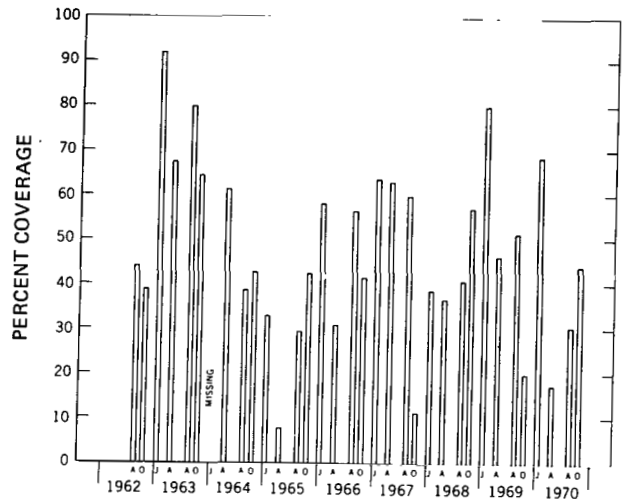

EASTERN PACIFIC
% OF AREA COVERED BY ≥ 6/10 CLOUD COVER
20°–30°N 100°W–180°

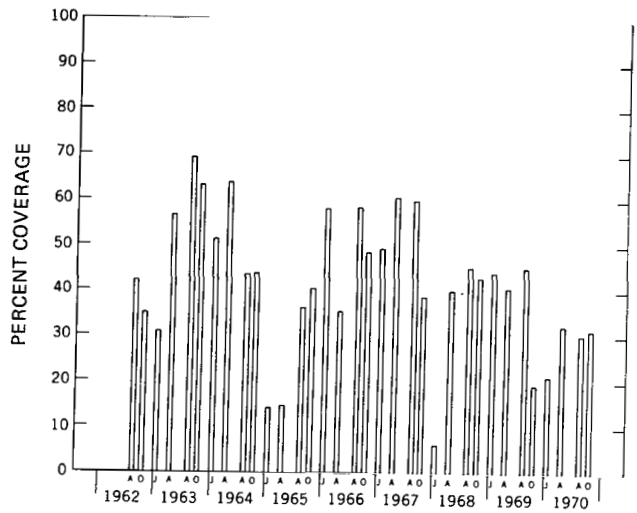

EASTERN PACIFIC
% OF AREA COVERED BY ≥ 6/10 CLOUD COVER
10°–20°N 100°W–180°

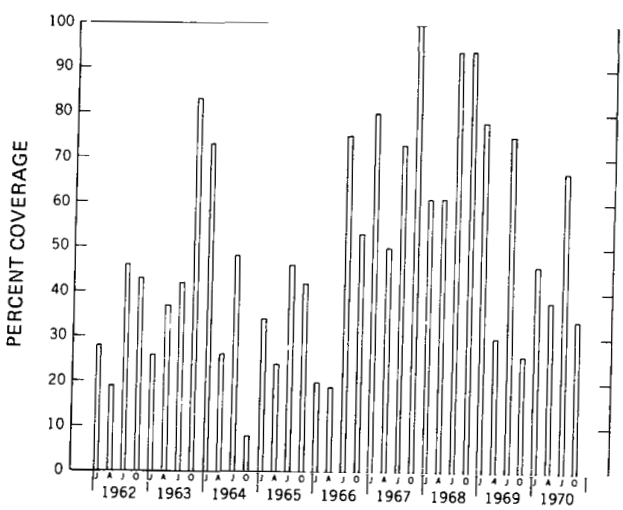

EASTERN PACIFIC
% OF AREA COVERED BY A POSITIVE
SEA SURFACE TEMPERATURE ANOMALY (WEIGHTED)
20°–30°N 100°W–180°

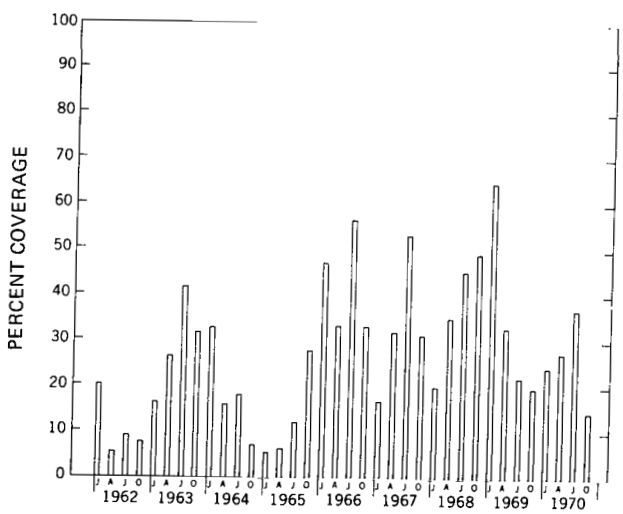

EASTERN PACIFIC
% OF AREA COVERED BY A POSITIVE
SEA SURFACE TEMPERATURE ANOMALY (WEIGHTED)
10–20°N 90°W–180°

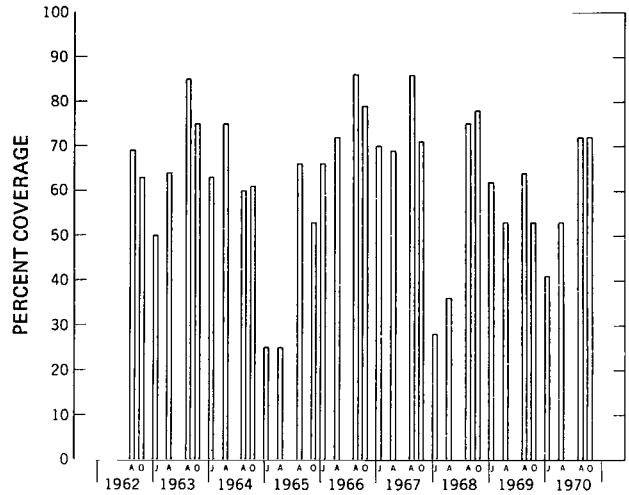

EASTERN PACIFIC
% OF AREA COVERED BY ≥ 6/10 CLOUD COVER
5°N–15°N 100°W–180°

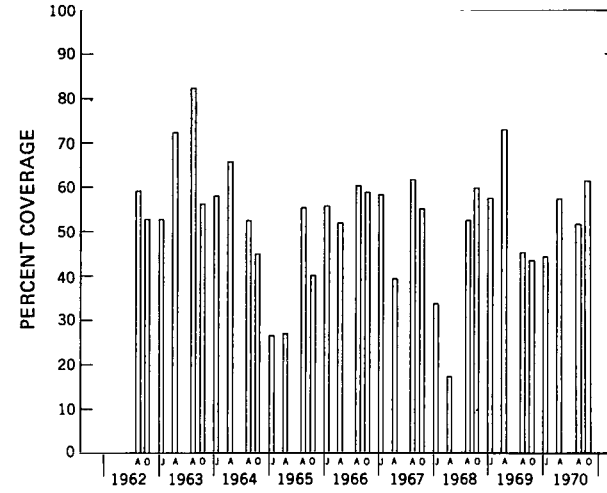

EASTERN PACIFIC
% OF AREA COVERED BY ≥ 6/10 CLOUD COVER
0°–10°N 100°W–180°

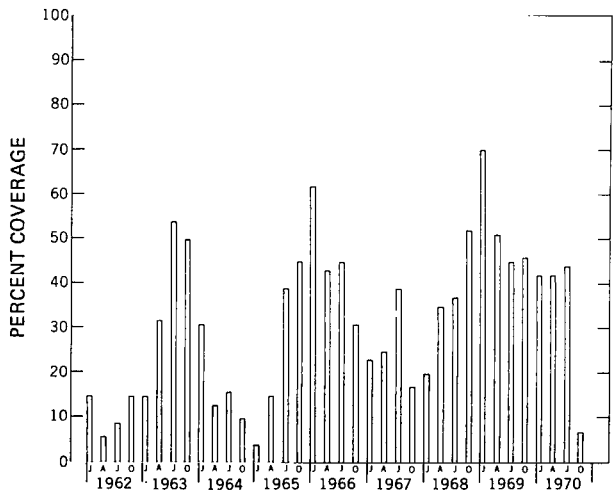

EASTERN PACIFIC
% OF AREA COVERED BY A POSITIVE
SEA SURFACE TEMPERATURE ANOMALY (WEIGHTED)
5°N–15°N 90°W–180°

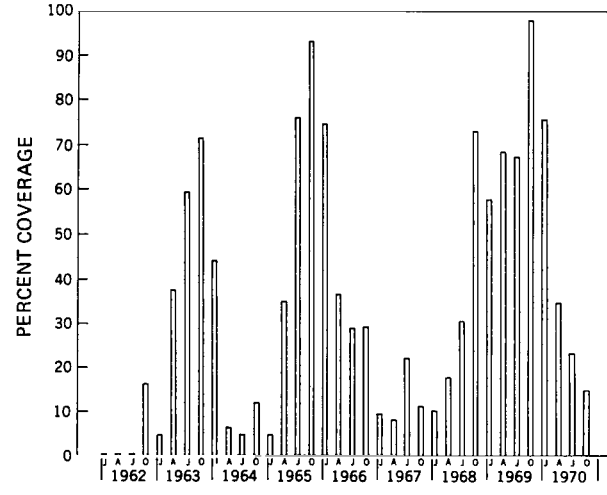

EASTERN PACIFIC
% OF AREA COVERED BY A POSITIVE
SEA SURFACE TEMPERATURE ANOMALY (WEIGHTED)
0–10°N 80°W–180°

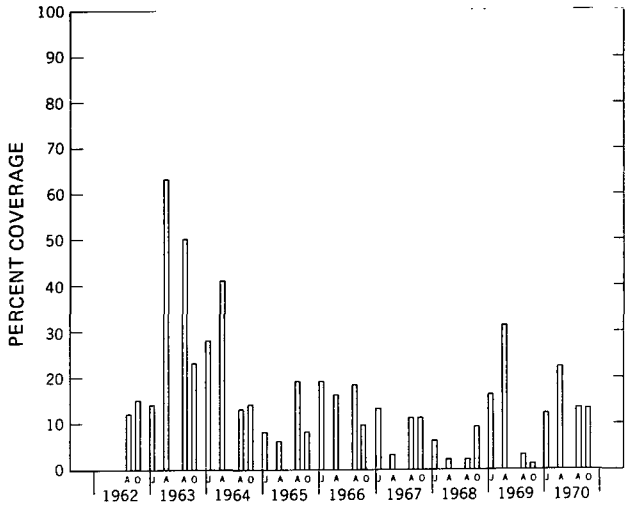

EASTERN PACIFIC
% OF AREA COVERED BY ≥ 6/10 CLOUD COVER
5°N–5°S 100°W–180°

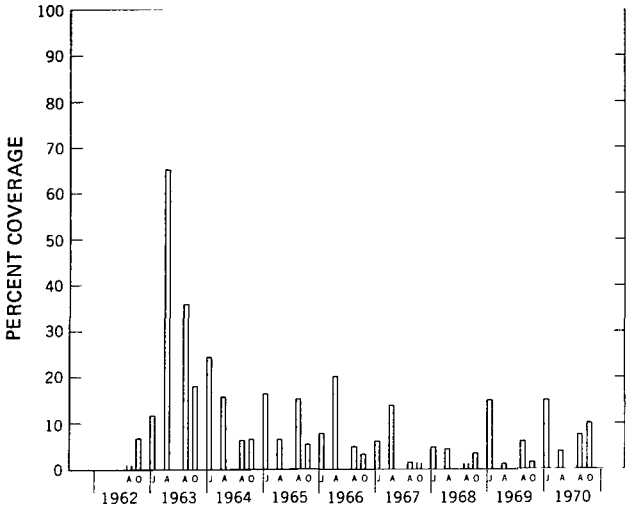

EASTERN PACIFIC
% OF AREA COVERED BY ≥ 6/10 CLOUD COVER
0°–10°S 100°W–180°

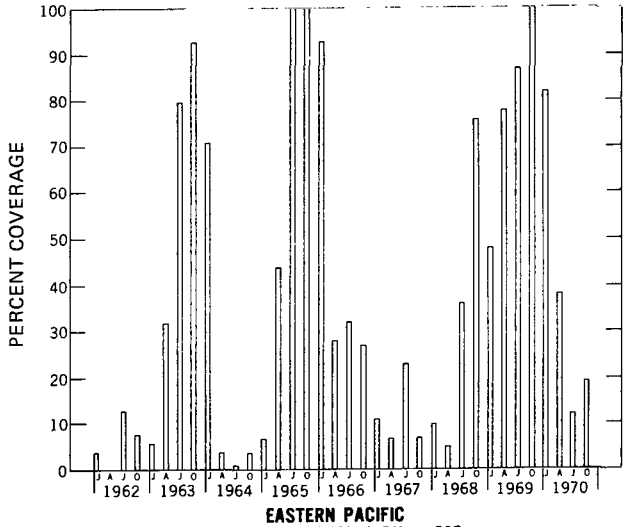

EASTERN PACIFIC
% OF AREA COVERED BY ≥ 0°C
SEA SURFACE TEMPERATURE ANOMALY (WEIGHTED)
5°N–5°S 80°W–180°

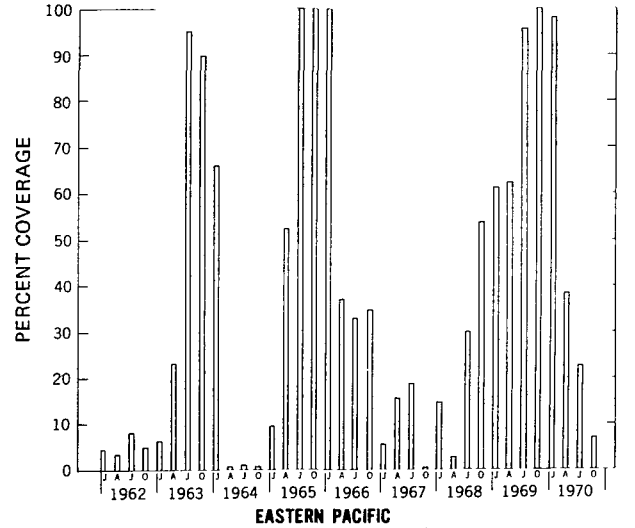

EASTERN PACIFIC
% OF AREA COVERED BY A POSITIVE
SEA SURFACE TEMPERATURE ANOMALY (WEIGHTED)
0–10°S 80°W–180°

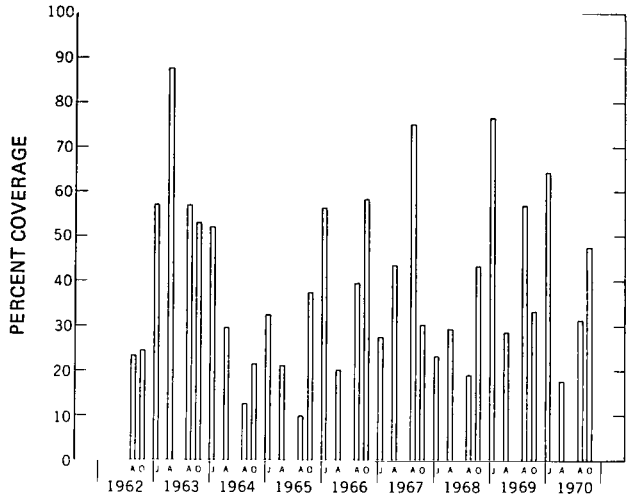

EASTERN PACIFIC
% OF AREA COVERED BY ≥ 6/10 CLOUD COVER
10°–20° S 100°W–180°

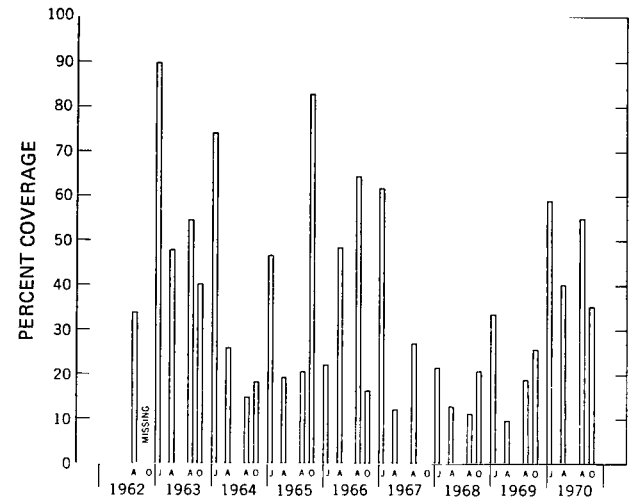

WESTERN PACIFIC
% OF AREA COVERED BY ≥ 6/10 CLOUD COVER
20°–30°N 180°–130°E

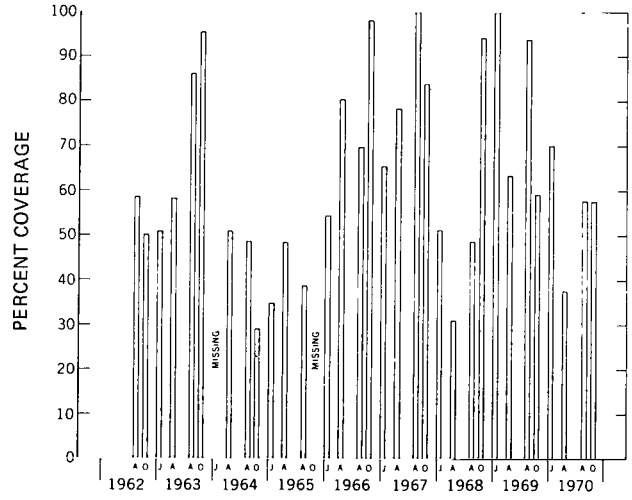

EASTERN PACIFIC
% OF AREA COVERED BY ≥ 6/10 CLOUD COVER
20°–25°S 100°W–180°

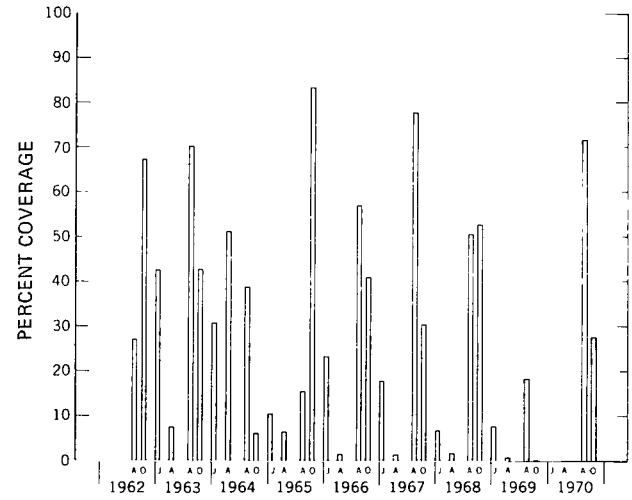

WESTERN PACIFIC
% OF AREA COVERED BY ≥ 6/10 CLOUD COVER
10°–20°N 180°–130°E

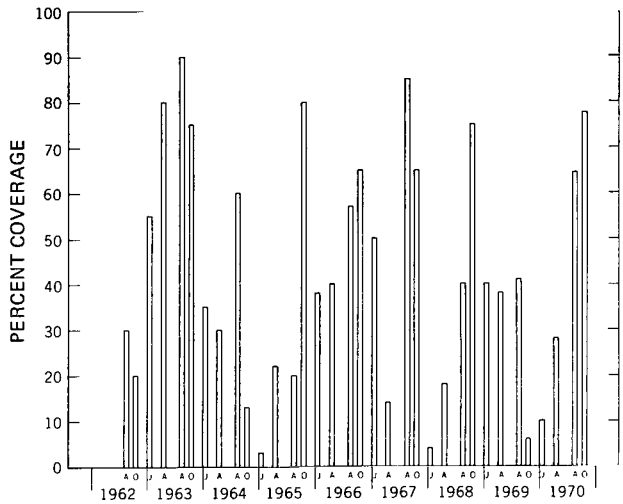

WESTERN PACIFIC
% OF AREA COVERED BY ≥ 6/10 CLOUD COVER
5°–15°N 180°–130°E

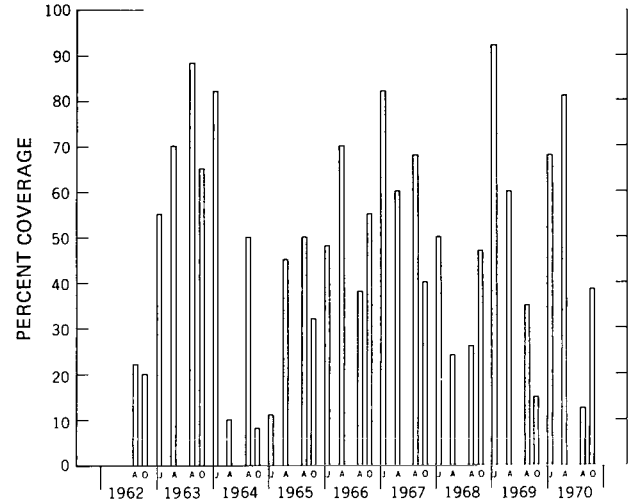

WESTERN PACIFIC
% OF AREA COVERED BY ≥ 6/10 CLOUD COVER
5°N–5°S 180°–130°E

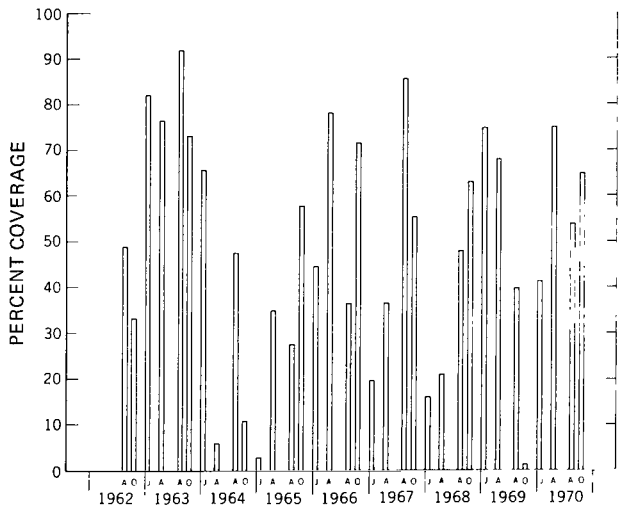

WESTERN PACIFIC
% OF AREA COVERED BY ≥ 6/10 CLOUD COVER
0°–10°N 180°–130°E

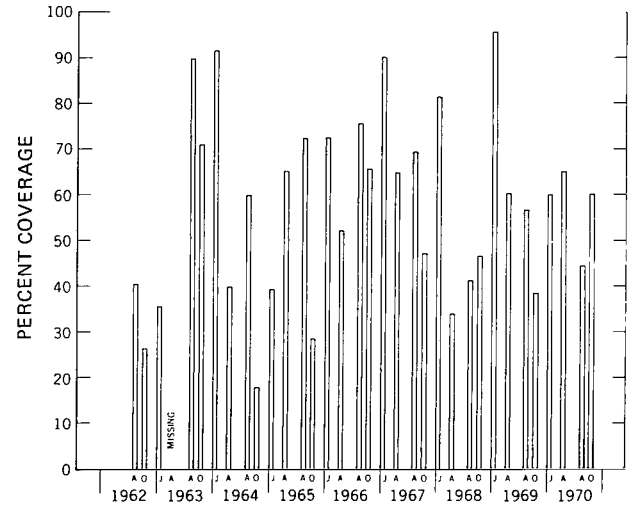

WESTERN PACIFIC
% OF AREA COVERED BY ≥ 6/10 CLOUD COVER
0°–10°S 180°–130°E

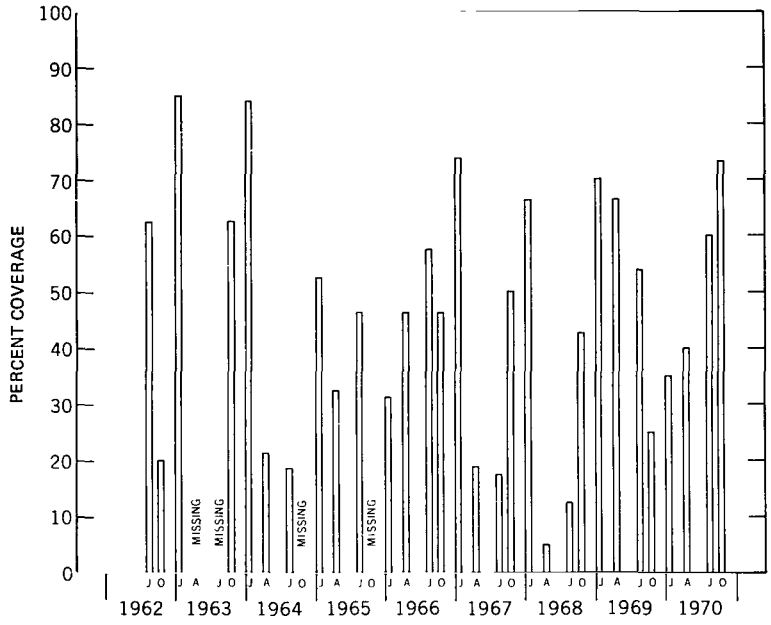

WESTERN PACIFIC
% OF AREA COVERED BY ≥ 6/10 CLOUD COVER
10°–20°S 180°–130°E

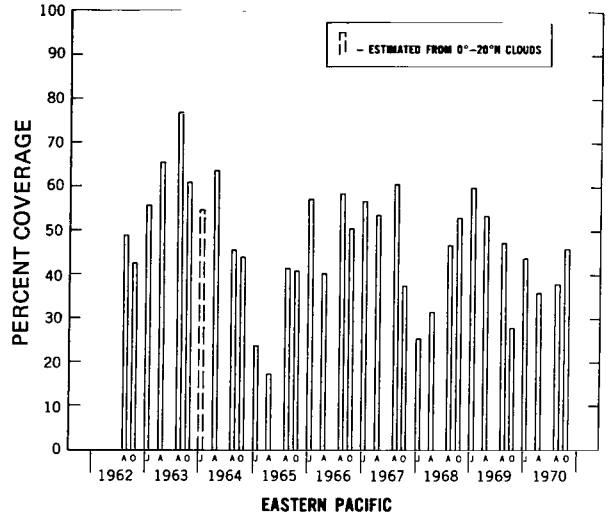

EASTERN PACIFIC
% OF AREA COVERED BY ≥ 6/10 CLOUD COVER
0°–30°N 100°W–180°

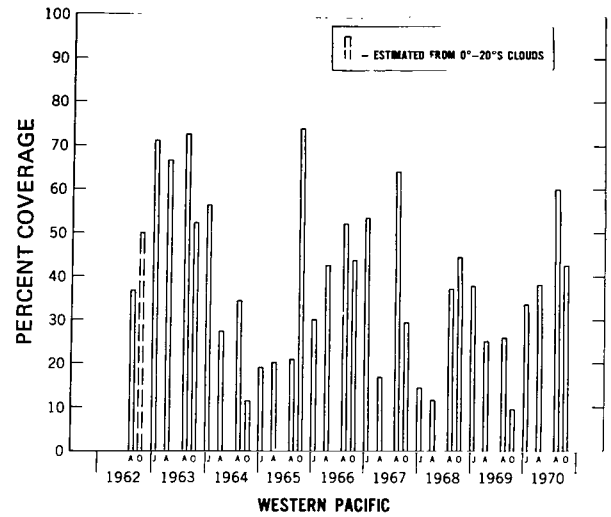

WESTERN PACIFIC
% OF AREA COVERED BY ≥ 6/10 CLOUD COVER
0°–30°N 180°–130°E

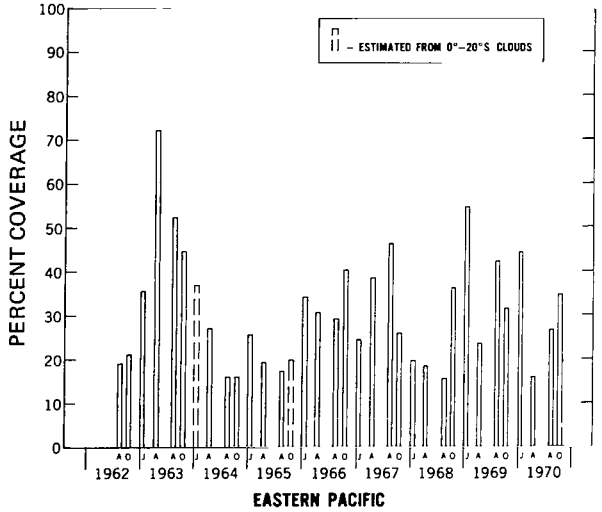

EASTERN PACIFIC
% OF AREA COVERED BY ≥ 6/10 CLOUD COVER
0°–25°S 100°W–180°

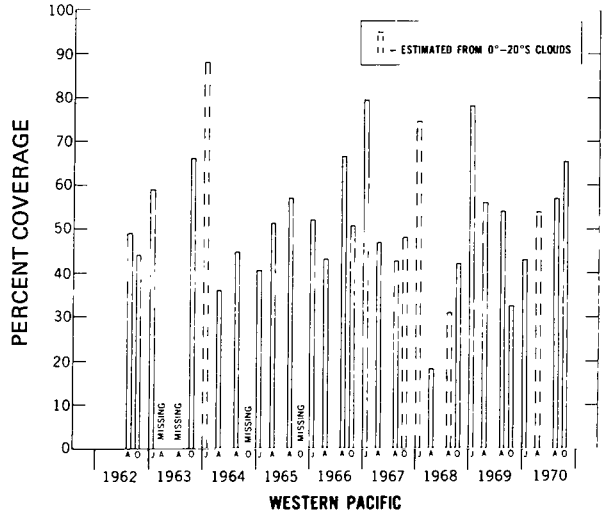

WESTERN PACIFIC
% OF AREA COVERED BY ≥ 6/10 CLOUD COVER
0°–25°S 180°–130°E

Appendix C

Statistical Techniques

The use of 12-month equally weighted running means (EWRM) as a smoothing technique is commonplace in climatological research; however, their use introduces one unfortunate property. As can be seen in Figure C1, there is a polarity reversal at point *A*, which can produce erroneous frequencies in a spectral analysis. A solution to this problem would be to place all the data to be studied in an anomaly format by using long-term means from the data. The monthly mean represents the annual cycle, and its subtraction from the long-term mean should eliminate this regular cycle. A plot of the monthly anomaly data proved too noisy, so the EWRM technique was utilized.

Another smoothing technique was tested to see if the polarity reversal effect was indeed damaging to the data analysis. Two parameters, Darwin monthly surface pressure and tropical island monthly rainfall for 30 years of record, were put into anomaly form by using long-term means from the data. Then a normal curve-smoothing technique was applied. This technique does not introduce the polarity reversals or phase shifts found with exponential techniques. It makes use of unequal weighting factors *f*

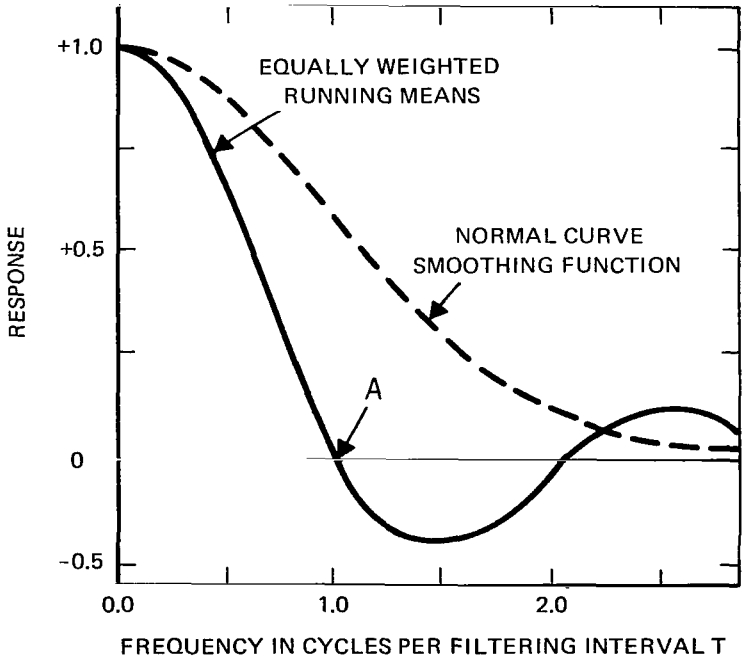

Figure C1—A comparison of the EWRM and normal curve-smoothing techniques. Polarity reversal is known at point *A*.

which are computed by

$$f = \frac{N!}{m!\,(N-m)} \Big| 2^n,$$

where $N = 12$ and $m = 0, 1, 2, \ldots, 12$. After smoothing in this manner was completed, the results proved highly comparable with the data processed by the EWRM technique (Table C1).

As can be seen, there was only a small reduction in the correlation values when the normal curve-smoothing technique was used. Similarly, the lag value for both cases was the same. Given the long length of record used, it now appears that the polarity reversal was of such a minor nature as not to be of any significance. The EWRM technique was then accepted as valid for this research study. Figure C2 shows an example of the monthly and 3-month formats for SST anomalies (0° to 10°N) and the final EWRM format that was used in the APSA program.

One of the useful features of the APSA program was the calculation of the autocovariance of each data set from zero to some stated number of lags in both a positive and negative direction. Normally, 10 percent of the total number of data points were used to establish the lag limit. Examination of the autocorrelation versus the lag curve then gave a good indication as to the success of efforts to remove regular trends such as the annual cycle. If everything appeared to be in order, the square root of the autocovariance at zero lag was taken to give the standard deviation for the individual series. A second feature of the program then crossed the designated base series (1) with another series (2) in both a positive and negative direction out to the number of lags used for the autocovariance calculations.

Crosscovariance values were then calculated at each lag point for the two series being crossed. Examination of plots of crosscovariance values versus lag values for any two series allowed selection of the most significant lag point. The final step was the hand calculation of the correlation coefficient. In this paper, the correlation values shown in Tables 7 to 13 represent crosscovariance values for two series at a selected lag, divided by the multiple of the standard deviation of both series.

Figures C3 and C4 present the printout of the APSA program to illustrate how the correlation coefficients and lags in Table 10 are determined for satellite-derived cloudiness and SST anomalies,

Table C1—A comparison of Darwin monthly surface pressure versus monthly tropical rainfall anomalies as computed by two statistical techniques.

Technique	Correlation Coefficient (r)	Lag (months)
12-month equally weighted running means	+0.80	0
Normal curve smoothing of anomalies	+0.74	0

using the relationship

$$r_{1,2} = \frac{\text{crosscovariance}}{S_1 S_2},$$

where

$r_{1,2}$ = correlation coefficient for the two series,

S_1 = standard deviation for series 1,

and

S_2 = standard deviation for series 2.

A number of squares in Tables 10 and 11 list two correlation values instead of one. When two series that follow a sine function are correlated, it is expected that two points of greater correlation will be seen. The true relationship of the two series is often marked by the greater degree of correlation, such as that shown in the lower right-hand quadrant of Figure C3 ($r_{1,2} = -0.92$). However, in some cases, two weak correlations can occur ($r = +0.42, -0.49$ in Table 10). Without prior knowledge of the situation, it is difficult to separate the true relationship from its mirror image on the basis of two correlations only. In these cases, both correlations have been presented to allow the reader to examine both possible relationships.

Statistical confidence in the worth of any correlation value depends on the number of independent observations that make up the data sets. Since a wide range of record lengths was used in this study, no special set of confidence limits was established. However, the shortest record contained 34 observations, and, therefore, these data can be used to establish a tentative acceptance level. If the value of 34 is used and independence is assumed, it can be shown that a correlation that explains 50 percent of the variance between two series would definitely be statistically significant. Therefore, correlation values of about 0.7 or better are used as a guide to the more important relationships.

The use of smoothing and extrapolation techniques that were used before the statistical analysis of the data raise some question as to the absolute validity of the correlation and lag values. One example that is readily apparent is that the beginning and end of trends can be easily smeared in a EWRM series. The lag values could thus be easily off one to two months in either direction. The correlation coefficients themselves also show a variation due to the EWRM smoothing used and should not be accepted as absolute values. However, since this EWRM smoothing was used throughout this study, all correlation coefficients and lags can be compared in a relative sense.

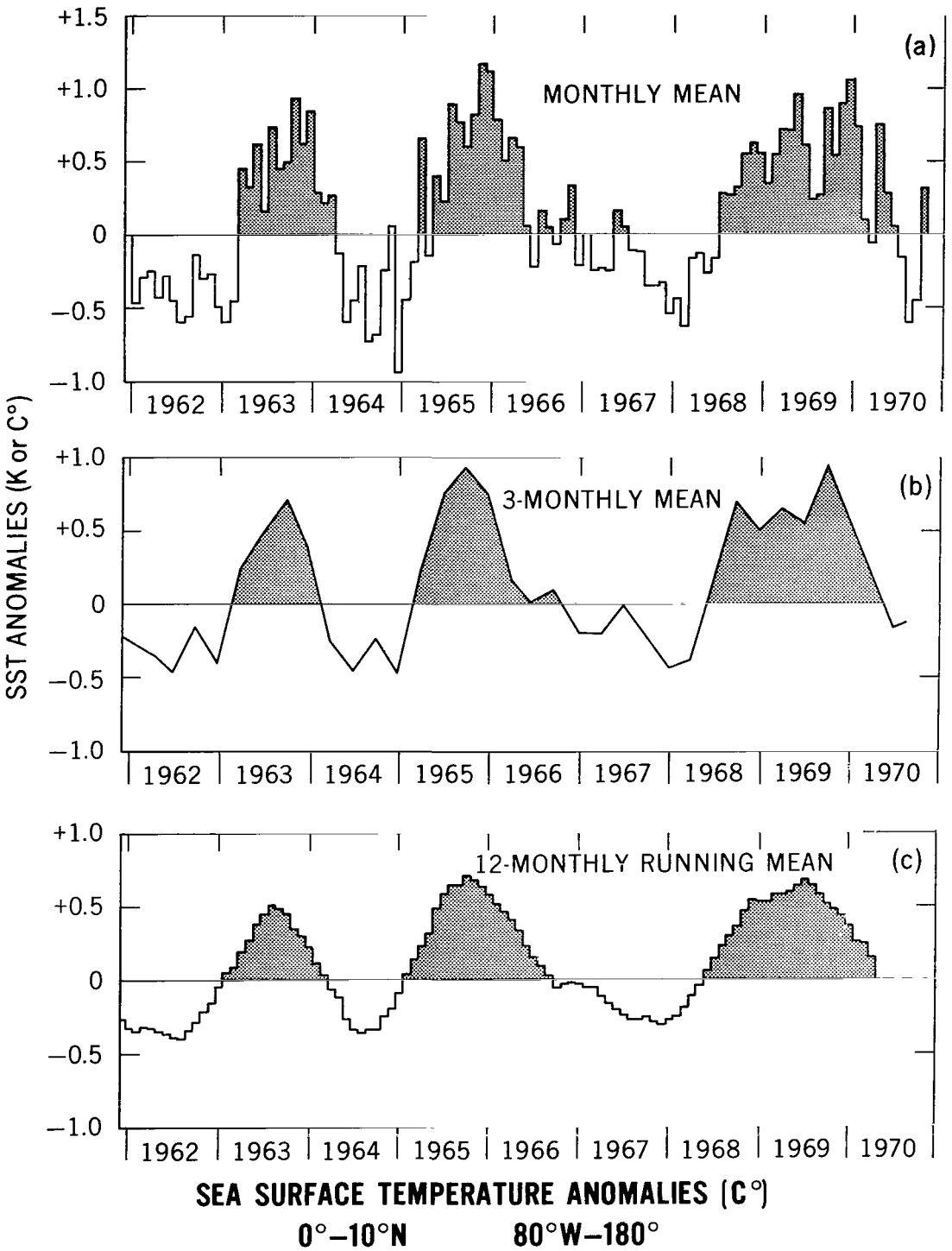

Figure C2—Comparison of (a) the monthly mean, (b) the 3-month mean and (c) the 12-month EWRM of tropical Pacific SST anomalies (0° to 10°N, 80°W to 180°) from 1962 to 1970.

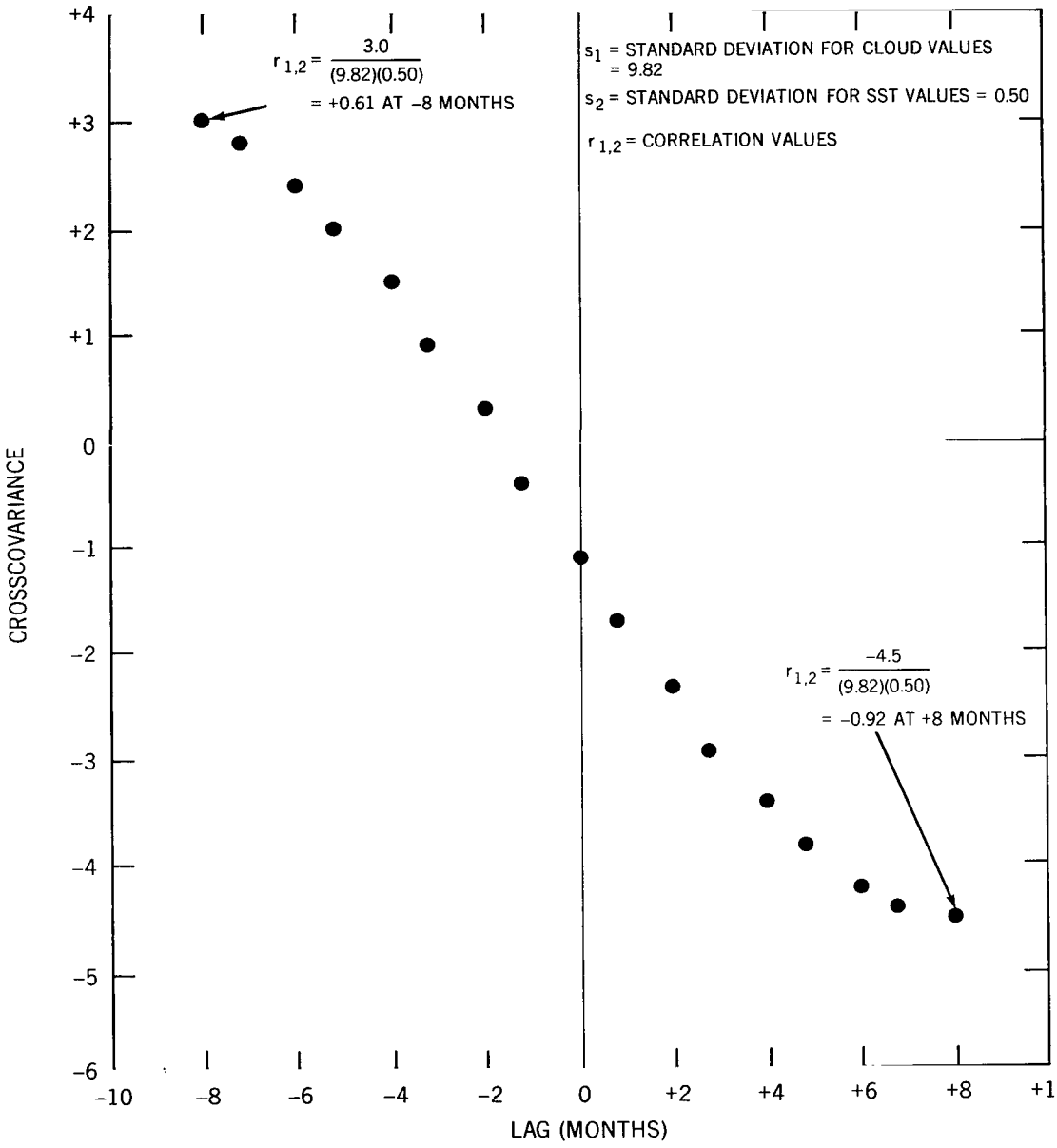

Figure C3—A printout of the APSA program which illustrates how the correlation coefficients (*r*) and lags (months) are determined from crosscovariance and standard deviation for the Northeast Pacific cloudiness (5° to 15°N, 100°W to 180°) and the Southeast Pacific SST anomalies (0° to 10°S, 80°W to 180°) from 1962 to 1970.

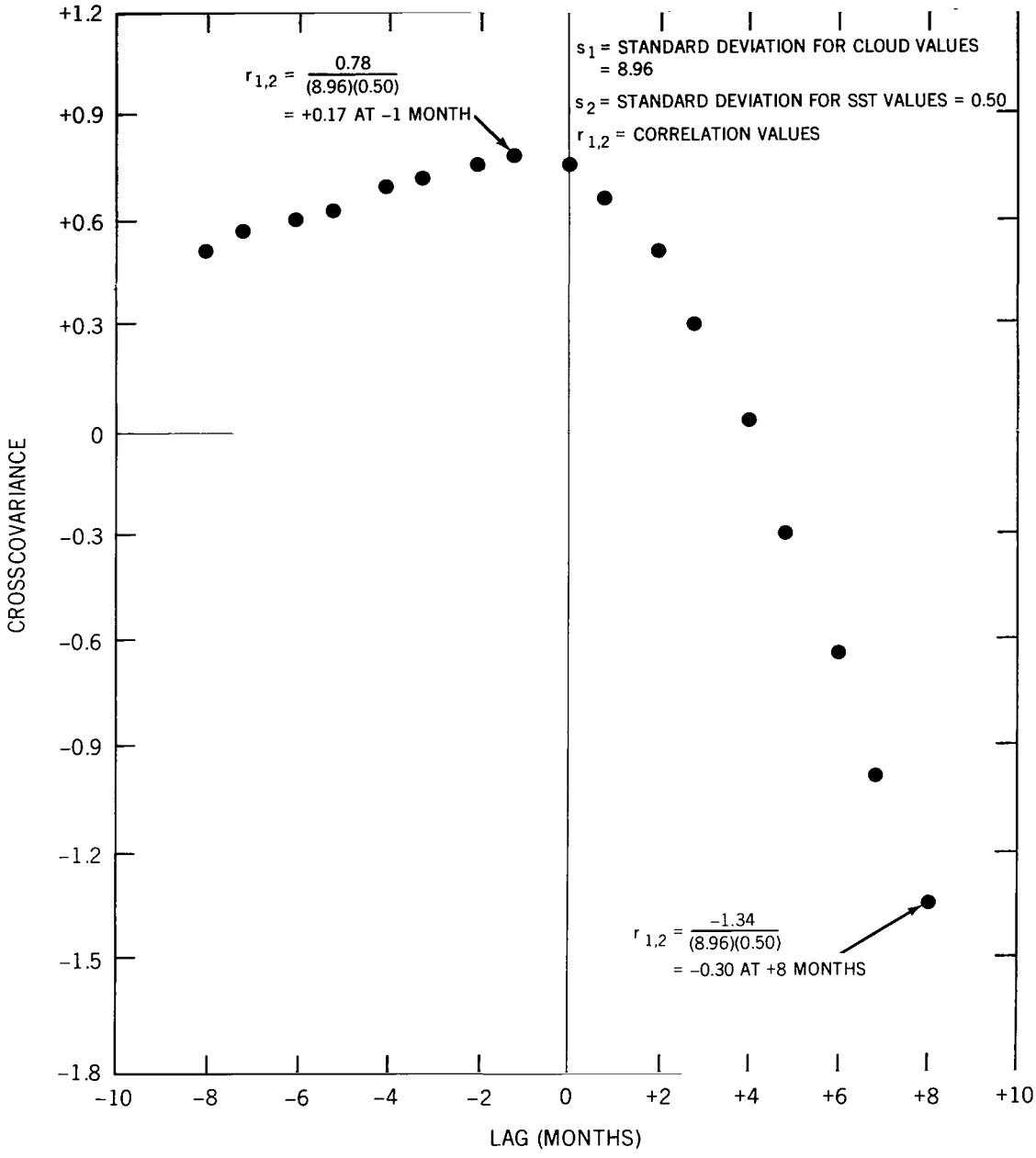

Figure C4—A printout of the APSA program which illustrates how the correlation coefficients (r) and lags (months) are determined from crosscovariance and standard deviation for the Southeast Pacific cloudiness (0° to 10°S, 100°W to 180°) and the Southeast Pacific SST anomalies (0° to 10°S, 80°W to 180°) from 1962 to 1970.

Appendix D

Satellite-Derived Global Tropical Cloudiness Oscillation

With the discovery of an apparent in-phase relationship between the satellite-derived cloudiness variations in the four tropical Pacific quadrants (Figure 19), a brief study of global tropical cloudiness through the use of J. C. Sadler's monthly satellite television nephanalyses* was undertaken. Figure D1a through D1c shows 12-month running means of cloudiness ($\geqslant 4/8$) over the tropical Pacific, Atlantic, and Indian Oceans, 30°N to 30°S, in percent of area covered. A simple monthly count of the total 2.5-degree squares covered by 4/8 cloudiness and greater was made for the period February 1965 to January 1970. A strong maximum cloudiness in early 1966 and 1969 and minimum in early 1968 occurs in all three data sets. Figure D1d shows the 12-month running mean of the 50-mb temperature at Balboa, Canal Zone. Note the strong similarity between this temperature (with 6-month lag) and the above tropical cloudiness. Figure D2 shows a similar relationship between the 12-month running means of global tropical cloudiness (over all three tropical oceans) and the 50-mb Balboa temperature (Biennial Oscillation).

Figure D3 also shows a close relationship between 12-month running means of tropical Pacific and Atlantic SST anomalies and cloudiness from J. C. Sadler's monthly satellite television nephanalyses. Apparently, from this limited study, the tropical Pacific and Atlantic SST's and cloudiness are oscillating in phase, with a 4- to 6-month lag in cloudiness. A study of the tropical Indian Ocean SST's and cloudiness will be the subject of future research.

Definite evidence of television system degradation has been noted in the TIROS and ESSA series of meteorological satellites.** This knowledge has prompted, in part, the switch from vidicon systems to scanning-radiometer techniques in the visible spectrum for future satellites in the ITOS D and SMS series. The variable response of the vidicon system in producing the daily television pictures may have induced an error in the monthly satellite cloudiness data that are described in the main body of the report and in this appendix.

*J. C. Sadler, University of Hawaii, Honolulu, unpublished data.
**T. I. Gray, NESS, and A. Schwalb, NOAA, private correspondence.

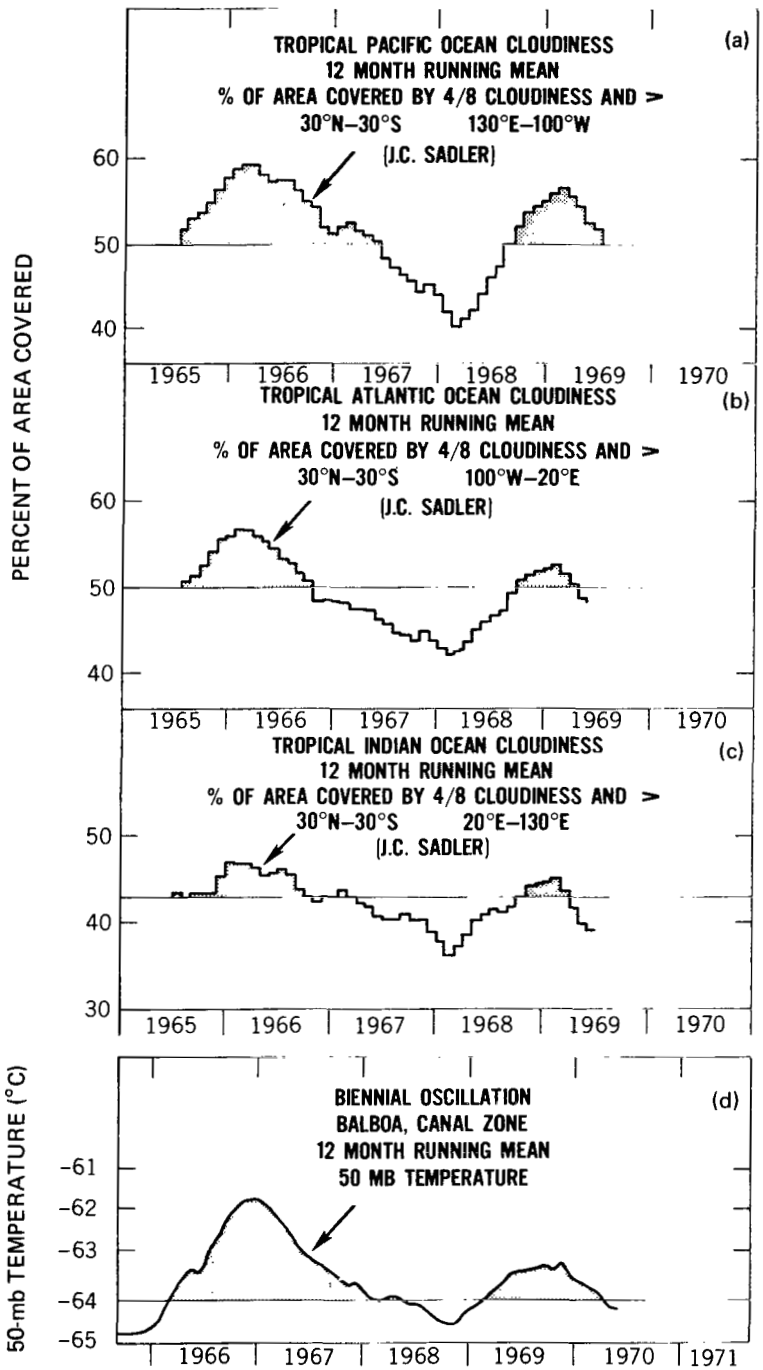

Figure D1—A comparison of 12-month running means of satellite-derived cloudiness in percent of area covered by $\geq 4/8$ cloudiness over (a) the tropical Pacific Ocean (30°N to 30°S, 130°E to 100°W), (b) the tropical Atlantic Ocean (30°N to 30°S, 100°W to 20°E), and (c) the tropical Indian Indian Ocean (30°N to 30°S, 20°E to 130°E); (d) 12-month running mean of 50-mb temperature at Balboa, Canal Zone (Biennial Oscillation).

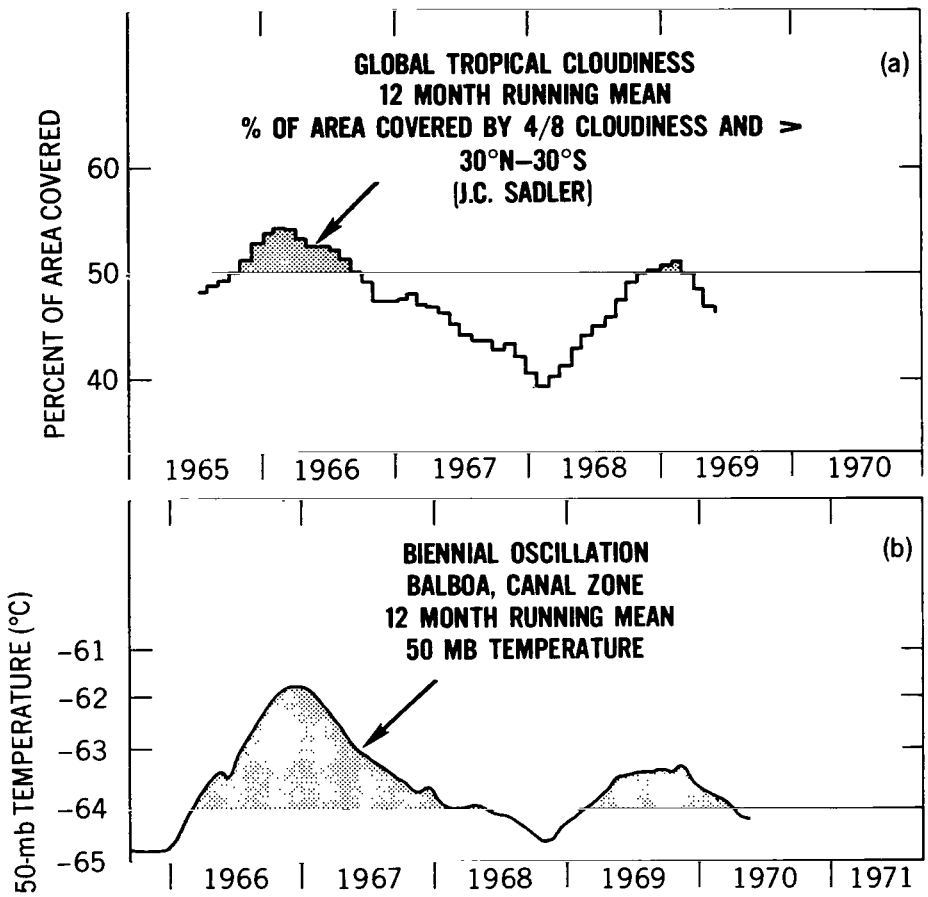

Figure D2—(a) 12-month running mean of satellite-derived global tropical cloudiness in percent of area covered by $\geq$ 4/8 cloudiness, 30°N to 30°S; (b) 12-month running mean of 50-mb temperature at Balboa, Canal Zone (Biennial Oscillation).

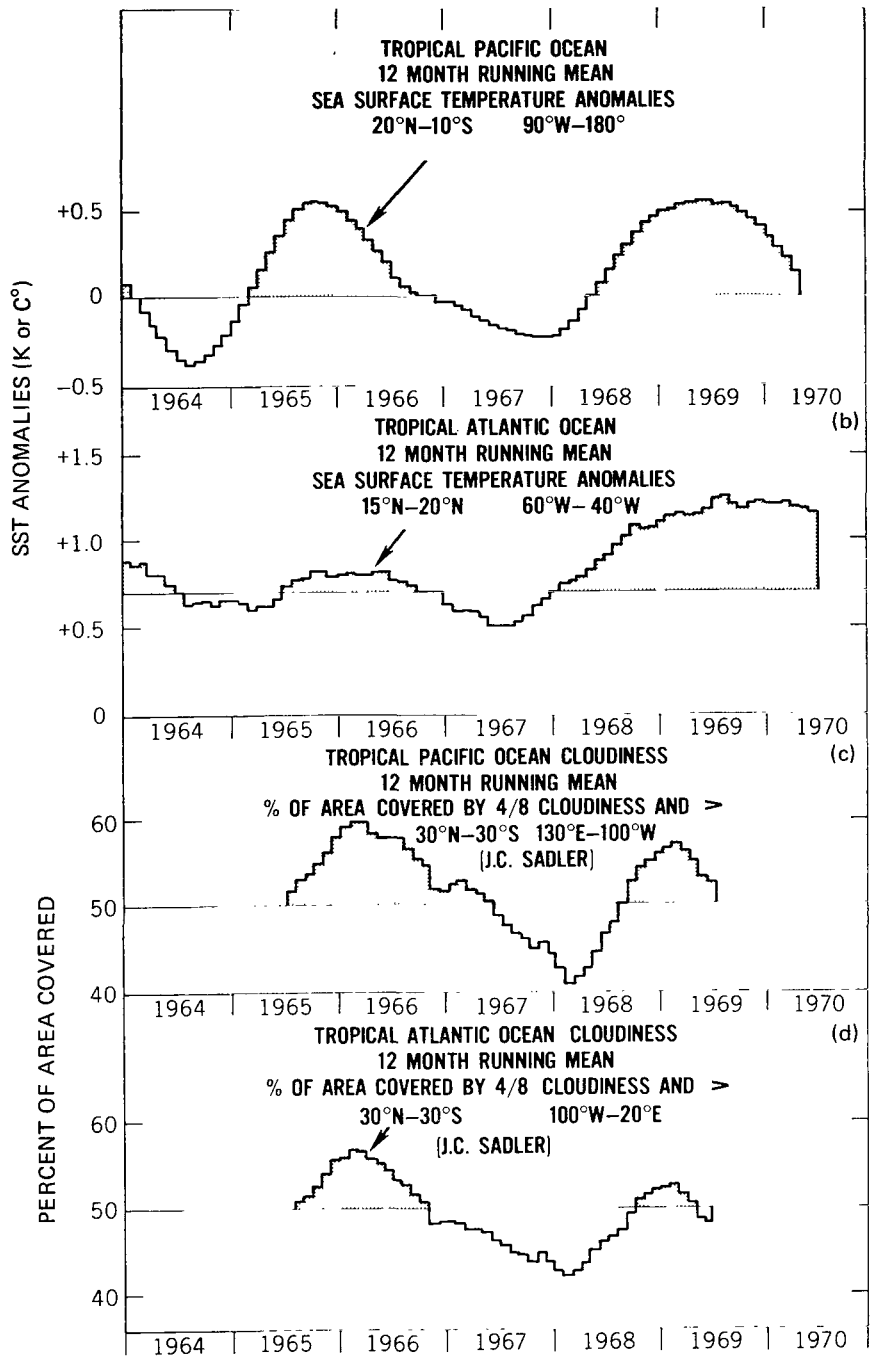

Figure D3–A comparison of 12-month running means of SST anomalies over (a) the tropical Pacific Ocean (20°N to 10°S, 90°W to 180°) and (b) the tropical Atlantic Ocean (15°N to 20°N, 60°W to 40°W); a comparison of 12-month running means of satellite-derived cloudiness in percent of area covered by $\geq$ 4/8 cloudiness over (c) the tropical Pacific Ocean (30°N to 30°S, 130°E to 100°W) and (d) the tropical Atlantic Ocean (30°N to 30°S, 100°W to 20°E).

017 001 C1 U 20 720505 S00903DS
DEPT OF THE AIR FORCE
AF WEAPONS LAB (AFSC)
TECH LIBRARY/WLOL/
ATTN: E LOU BOWMAN, CHIEF
KIRTLAND AFB NM 87117

"The aeronautical and space activities of the United States shall be conducted so as to contribute . . . to the expansion of human knowledge of phenomena in the atmosphere and space. The Administration shall provide for the widest practicable and appropriate dissemination of information concerning its activities and the results thereof."

— NATIONAL AERONAUTICS AND SPACE ACT OF 1958

NASA SCIENTIFIC AND TECHNICAL PUBLICATIONS

TECHNICAL REPORTS: Scientific and technical information considered important, complete, and a lasting contribution to existing knowledge.

TECHNICAL NOTES: Information less broad in scope but nevertheless of importance as a contribution to existing knowledge.

TECHNICAL MEMORANDUMS: Information receiving limited distribution because of preliminary data, security classification, or other reasons.

CONTRACTOR REPORTS: Scientific and technical information generated under a NASA contract or grant and considered an important contribution to existing knowledge.

TECHNICAL TRANSLATIONS: Information published in a foreign language considered to merit NASA distribution in English.

SPECIAL PUBLICATIONS: Information derived from or of value to NASA activities. Publications include conference proceedings, monographs, data compilations, handbooks, sourcebooks, and special bibliographies.

TECHNOLOGY UTILIZATION PUBLICATIONS: Information on technology used by NASA that may be of particular interest in commercial and other non-aerospace applications. Publications include Tech Briefs, Technology Utilization Reports and Technology Surveys.

Details on the availability of these publications may be obtained from:

SCIENTIFIC AND TECHNICAL INFORMATION OFFICE

NATIONAL AERONAUTICS AND SPACE ADMINISTRATION

Washington, D.C. 20546